Doctoral thesis

# Spatial and Conceptual navigation in Early Blind people:

## Testing the scaffolding hypothesis of cognitive maps

Ph.D. Candidate: Sigismondi Federica

Supervisor: Prof. Roberto Bottini

Doctoral program in Cognitive and Brain sciences

CiMeC – Center for Mind/Brain Sciences

University of Trento

**XXXV Cycle**

2019-2024

Center for Mind/Brain Sciences

European Research Council

# ABSTRACT:

Interaction with the environment is a crucial feature that characterizes intelligent biological systems. To do so the information acquired by the surroundings needs to be organized in flexible and generalizable structure, namely cognitive maps, which encode relational information, store it, and make it easily accessible and reusable. The hippocampal-entorhinal system plays a crucial role in the creation of cognitive maps, and, particularly, grid cells have been targeted as the main neural correlate. In humans, grid-like activity has been associated with the encoding of both spatial and abstract knowledge. However, in the field of cognitive maps, the precise relationship between spatial and conceptual knowledge remains unclear. Here, we take blindness as a model to test whether the mechanisms ontogenetically evolved to navigate in space scaffold the navigation through concepts or, on the contrary, if spatial and abstract knowledge develop independently. In this thesis, I provide, for the first time, evidence in favor of the scaffolding hypothesis by observing a reduction of the grid-like coding in the early blind individuals' entorhinal cortex both during a spatial and a conceptual navigation task. Crucially, lack of visual experience seems to influence specifically the grid system, as, instead, the typical cortical networks that support spatial and conceptual navigation show a high resiliency to early visual deprivation. These findings will deepen significantly our understanding of the relationship between spatial and nonspatial concepts, opening the path to novel questions related to the development of the grid system and, more in general of the cognitive maps.

# ACKNOWLEDGMENT

First of all, I would like to deeply thank my supervisor, professor Roberto Bottini, your dedication to work together with your insatiable curiosity inspired me and spurred me to try to do my best every day.

A deep thanks goes to my Oversight Committee members professor Manuela Piazza and Marco Tettamanti. Throughout these years you provide me with insightful comments and inspiring ideas.

Thanks also to my past and presents lab mates which patiently support my moods and tried to cheer me up during bad days (ok, they also give me super insightful advices about my projects, but that goes by the wayside). Two particular mentions need to be done, the first to Yangwen Xu, shared first co-author in the paper presented as chapter 2 of this thesis, you are among the few people that patiently wait me understanding all the math behind our analyses, I own you a lot. The second to Giuliano Giari, for all the laughs and all the tears (mine of course) and all the mountains and the goats' songs, this experience would have not been the same without you by my side, thank you.

Elena and Greta, and in general all my friends and family, that support and always believed in me

Finally, thanks to Flavio and Giorgia.

The idealists argue that the hexagonal rooms are a necessary form of absolute space or, at least, of our intuition of space. They reason that a triangular or pentagonal room is inconceivable. (The mystics claim that their ecstasy reveals to them a circular chamber containing a great circular book, whose spine is continuous and which follows the complete circle of the walls; but their testimony is suspect; their words, obscure. This cyclical book is God.) Let it suffice now for me to repeat the classic dictum: The Library is a sphere whose exact center is any one of its hexagons and whose circumference is inaccessible.

Jorge Louis Borges (1941), The Library of Babel, in The Anatomy of Melancholy (part 2, sect. II, mem. IV)

*Christian,*

*Eventually we've made it.*

*See you later,*

*Fé*

# Table of Contents

# I

# GENERAL INTRODUCTION

Complexity characterizes our world. The amount of sensory and spatial information humans receive from the environment at every moment is uncountable. Crucially, humans do not passively absorb this information as sponges immerse in a bowl full of water, rather, they store and re-elaborate them, to be able to act upon the world to achieve various goals. For all this information to be digested and successfully reused, it needs to be stored in easily accessible, generalizable, and flexible structures named cognitive maps. Consider, for example, how easy it is to arrive at work from your apartment or retrieve the right information during an exam. How can this be possible? Cognitive maps are internal representations in which patterns of regularities, extracted from the external world, are stored in connected clusters. Since their discovery in animals, the construction, development, and functioning of cognitive maps elicited major interest throughout the scientific community. Pioneering research targeted the hippocampal-entorhinal system as a critical region for the creation of cognitive maps. Crucially, it has been shown that, in both humans and animals, cognitive maps subtend the encoding and the organization of both spatial and abstract knowledge. However, the origin of this cross-domain similarity remains unclear. One possibility is that the way we experience and navigate in space influences how we organize and navigate through our memories, thoughts, and conceptual knowledge in general. On the other hand, it could be that the neural mechanism developed to navigate in space and those to navigate in concepts develop independently, thus, abstract knowledge organization and navigation are not influenced at all by individuals' experience and perception of space. Comparing populations that experience space differently such as sighted people to individuals that never experience vision, like congenitally blind individuals, could be a starting point to try to unveil the relation between spatial and abstract knowledge.

The current work aims to provide a first insight into the influence of early visual deprivation on the development of spatial and conceptual cognitive maps through studies that compared sighted and early blind individuals in spatial navigation and conceptual navigation tasks. This thesis is divided into 4 chapters. Chapter 1 aims to provide a general overview of the theoretical background

that inspired the main theoretical question of this work, as well as the experiments constructed to try to address it. Particularly, this first chapter will revolve around two main themes (I) the use of cognitive maps for both spatial and abstract knowledge with a specific focus on the type of neurons that had been targeted as critical for the creation of cognitive maps, such as grid cells, and (II) the influence of endogenous and exogenous factors on the development of grid-like coding in both humans and animals, with particular interest the role played by vision. This chapter aims to provide the reader with all the necessary literature background to understand, and appreciate, the importance of unveiling the relationship between spatial and conceptual knowledge by addressing what I think is still one of the main unsolved, yet intriguing, questions: is the way we navigate in space shaping how we organize abstract knowledge? The two different ways in which we can answer this question could be operationalized in two different hypotheses. The scaffolding hypothesis assumes that the neural machinery ontogenetically developed to navigate in space, has been re-used to also navigate conceptual spaces. According to this hypothesis, differences in the way spatial information is processed and navigated will be reflected also in how abstract knowledge is navigated. On the contrary, the independence hypothesis assumes that the way humans have learned to navigate in space through experience did not influence the way they move in their conceptual spaces. Under this scenario, possible variations in the encoding of spatial information given by experience will not be reflected in the encoding of conceptual information.
In chapters 2 and 3 I will describe two fMRI experiments conducted on sighted individuals and individuals who lost their sight in the first years of life and never use it functionally to explore the surrounding environments. Chapter 2 will be dedicated to the first project of my PhD, which has been recently published, and aimed to investigate the influence of visual experience on grid-like coding in the entorhinal cortex during an imagined navigation task. In this study, we asked participants to imagine navigating a clock-like environment while undergoing an fMRI session. In Chapter 3 I will describe the second experiment of my PhD, which at the moment of writing is still ongoing, in which through the use of a sound analogy task we aimed to study if the classical 60˚sinusoidal modulation of the BOLD signal, commonly associated to grid-like activity, and detected in conceptual navigation tasks in sighted individuals, is detectable in the same measure in early blind individuals' entorhinal cortex. This thesis will be concluded with a general discussion (Chapter 4) in which the results of the two experiments will be taken and interpreted

together aiming to provide the first evidence in support of either the scaffolding or the independence hypothesis.

## 1. Getting oriented: cognitive maps for spaces and concepts

If we think about the amount of knowledge acquired during a lifetime, it is evident that storing every single piece of information independently can become an overwhelming, as well as computationally demanding task. Intelligent biological systems develop a rather clever way to deal with this. Instead of throwing away the information acquired each time, the brain stores and generalizes them in flexible, in-mind representations of the world [1–4]. These representations, which are everything but static, can be updated through experience and used to successfully interact with the environment allowing the development of adapting behaviors and problem-solving [5]. How these representations are constructed and developed, and which are their neural correlates, is a question that intrigued the field of cognitive neuroscience for ages. The first observation of adaptive behavior came from the animal cognition field. Indeed, during a maze completion task in rodents, Tolman[6] observed that the rats were able to easily find a way out from the maze, after having familiarized with it, even when the maze structure was changed. The conclusion to which Tolman and colleagues arrived was that the rats were able to construct an internal representation of the world, namely a cognitive map[6], which kept into account the relations between events, in the same way, a physical map would represent the connection between two places, so that the consequences of the actions became more predictable [1,2,7]. Several studies on rodents [8] and, later, on humans [7,9] targeted the hippocampal formation, and entorhinal cortex located within it, as the main brain correlate of cognitive maps[1,2,10,11,6]. The importance of the Hippocampal-Entorhinal system in supporting the creation and the use of cognitive maps seems to be deputy to the presence of a peculiar set of spatially tuned neurons, [13,14], among which place [15], head-direction [16], and grid cells [17]. Place [15] and head direction cells [16] provide a one-to-one relationship with spatial features, which are the location and the heading directions of the agent within an environment, respectively. Grid cells, on the contrary, with their multiple firing fields, encode more complex spatial information, such as the relations between different landmarks within the environment, providing

an explicit representation of the space [17–19]. First observed in rats' entorhinal cortex during a classic foraging task[17,20,21], these cells have been observed in different animal species' entorhinal cortex (EC), such as mice [22], bats[23,24], and monkeys [25] during different navigation-related tasks with the use of invasive techniques. In humans, the direct recording of neuronal activity is rarely possible, however, it has been observed that a proxy of grid cells' activity, grid-like coding, can be detected in humans' EC with non-invasive neuroimaging techniques such as functional magnetic resonance (fMRI) and magnetoencephalography (MEG). Indeed, given the peculiar hexagonal-like organization of grid cells firing field, it is, in principle, possible to detect a 60° sinusoidal modulation of the Blood Oxygenation Level Dependent (BOLD) signal (6-fold symmetry) as a function of moving directions in both spatial and abstract environments [34,35][26–34]. Moreover, in recent years the presence of a grid-like type of neurons in humans' entorhinal cortex has also been confirmed by electrophysiology experiments conducted on epileptic patients implanted with electrodes in medial temporal lobe regions[35].

In the following sections, I will more deeply discuss the role of cognitive maps related to the navigation and organization of spatial and abstract knowledge, focusing mainly on the role of grid cells.

## 1.1 Where I am and where I should go: the role of grid-like coding in spatial navigation

A wide set of highly interconnected brain areas, such as the parietal, temporal, and medial prefrontal cortex, contribute to humans' ability to move and orient in space and constitute the so-called Human Navigation Network [7,36–41]. Among this network, the hippocampal formation plays a very important role in navigation-related abilities such as, for example, spatial processing of novel environments, wayfinding [42,43], and, most importantly, cognitive map creation [14]. As mentioned above, grid cells have been largely correlated to the creation and use of cognitive maps and were first discovered in rats' EC [17]. Given the difference in species, however, results that emerged from animal studies are complicated to interpret and generalize to humans. Indeed, notwithstanding in literature, it has been shown that some anatomical structures, like the Hippocampal Formation, are preserved across mammals [8], one of the most important questions

that needed to be addressed was whether a similar population of cells, could also be detected in human's Entorhinal cortex. In humans, rather than animals, single-cell recording of brain activity is rarely possible, therefore, usually, studies rely on indirect measures of neuronal activity through non-invasive neuroimaging techniques such as fMRI, MEG, and electroencephalography (EEG). Studying the entorhinal cortex with non-invasive techniques, however, can be challenging, due to its proximity to air cavities which enhance distortions artifacts and its deep position in the brain [44]. The first attempt to investigate the presence of a Grid-like coding in humans, using fMRI, was made by Doeller in 2010 [29] which assumed that the particular geometrical arrangement of grid-cells firing fields will modulate the peak of the BOLD signal at regular intervals of 60˚, where movements aligned with one of the three main axes of the hexagonal grid will elicit higher activation compared to those misaligned. Doeller and colleagues [29] tested the presence of grid-like coding in healthy-sighted individuals by asking them to walk inside a circular arena, mimicking the foraging task performed by rodents, and reaching different objects situated in specific positions in the environment. The circular arena was surrounded by mountains, that were used as landmarks to give participants the possibility to orient themselves in the space. To analyze fMRI data, the authors, implemented an innovative technique called Quadrature Filter analysis. This technique is grounded on the assumption that the main orientation of the Hexadirectional grid in each individual's entorhinal cortex is different. Therefore, to maximize the detection of a grid-like signal, the first thing to do would be to compute the orientation of the grid. Briefly, quadrature filter analysis can be seen as a 2-way crossvalidation in which half of the collected data would be used to estimate the mean grid orientation, and the remaining half of the data would be used to test this orientation. If a grid-like signal is detected in the EC a six-peak sinusoidal modulation of the BOLD signal should be observed. A significant 6-fold symmetry was found in the right Entorhinal Cortex of the participants while performing the spatial navigation task. This signal, furthermore, correlates with participants' spatial memory performance [29]. These findings provide the first evidence not only that a grid-like code emerges, and is detectable in humans, but also that this signal might usefully guide the behavior. Later on, in 2013 Jacobs and colleagues provided the first direct evidence of grid-like cells in humans by recording the activity of neurons in the medial temporal lobe in implanted epileptic patients while they were performing a spatial navigation task similar to the one described above [35].

Spatial navigation abilities are not restricted to the actual physical navigation Indeed, individuals can easily recreate a map of a known environment in their mind and navigate it there, in their imagination. This spurred the scientific community to investigate whether grid-like coding in humans' entorhinal cortex could be detected also in those cases in which the agent did not move (or have the perception to move, like in virtual reality situations) its body. Horner and colleagues 2016 [31] recycled the same spatial navigation task used by Doeller first, and Jacobs later [29,35], first asking participants to imagine reaching a target object in the arena, and only later to move through it. Results showed the emergence of a grid-like coding in bilateral entorhinal cortex: on the left during the movement period, and on the right during the imagined period. These findings provided the first evidence that individuals' ability to mentally transverse the space is also supported by entorhinal-based cognitive maps.

Planning is another fundamental aspect that characterizes spatial navigation, which allows people to plan the next steps, simulating in their minds hypothetical scenarios. Animal single-cell recording experiments, for instance, detected place cell activity in rodents' hippocampus, during rest periods, associated with the representation of upcoming trajectories. This phenomenon, known as 'pre-play', was observed to be stronger if the path to which the animal was thinking would have led to a rewarded location [45,46]. Future thinking abilities, in humans, rely on a wide set of brain regions crucial for episodic memory, navigation, and predictions [47–50]. In 2016, Bellmund and colleagues showed, for the first time, that grid-like coding could be also elicited when participants planned movements to perform to reach a point 'B' starting from a point 'A' confirming the enrolment of the entorhinal cognitive maps in mental simulations [27].

The main sense on which humans and animals rely to extract information from space is vision [51,52]. One of the main roles of the grid system is to support the extraction and organization of spatial relations. Therefore, one could predict that grid-like coding will be detected also during visuospatial searching tasks. The first evidence in favor of this possibility came from non-human primate studies in which animals were engaged in a visual tracking task [25,53]. Later on, a signature of grid-like coding during visual searching tasks was detected also in humans' EC [32,54] Further studies confirmed this pattern of results [55], some of which indicated that rather than eye movements themselves, covert attention mechanisms might influence the emergence of grid-like coding in EC during these kind of tasks[56], [30].

Grid-like coding seems to process more than the mere spatial relationships of an environment to create a map of it. Indeed, a growing set of evidence suggests that this signal could be influenced by salient environmental features. First of all, recordings of neuronal activity in the EC of rodents, engaged in exploring new environments revealed that the size of grid cells' firing fields, at the beginning of the exploration, was bigger compared to the standard observed one, and reduced as a function of the familiarization with the environment[57]. Potentially, this biological response to new spatial layouts might reflect the need to have, quickly, a complete, albeit rough, representation of new spaces, to get oriented (bigger firing fields to cover the entire space with low resolution). The representation then became more and more detailed as a function of the time spent within that environment (firing field size return to the standard to provide more fine-grained spatial representations). Moreover, it has been observed that, during navigation, the size and arrangement of grid cell firing fields in animals change as they approach a goal, such as food or the exit of the experimental maze[58–60]. Finally, another interesting piece of evidence is the grid cells phase anchoring phenomena. Animals' studies first and humans' studies later, observed that in polarized environments, such as square arenas, grid cells' firing phases (in animals)[19] or mean grid orientations (in humans)[54], tend to cluster along the main axes of the environment mimicking an anchoring behavior that might be used to get more easily oriented. Interestingly, in humans has also been shown that tilting the experimental arena that participants were navigating, produces also a correlated tilt of their mean grid orientations [54].

## 1.2 A map for humans' thoughts: the role of grid-like coding in conceptual navigation

Grid cell detection in humans' Entorhinal cortex has led to a series of fascinating findings that helped the scientific community disentangle the mechanisms underlying people's ability to rely on cognitive maps to navigate the surrounding environments leaning on a 'high performance - low cost' system [2,4]. Crucially, however, several studies observed that the involvement of the hippocampal formation goes well beyond the computation of spatial-related information. Indeed, activation in this area has been correlated to perception and memory formation and retrieval [61–63,63–67]. How do human beings organize and access their thoughts, memory, and all the different types

of abstract knowledge that they acquire during their lifetimes? A fascinating possibility is that humans construct low-dimensional, navigable, and manipulable spaces where to store their thoughts and memories and retrieve them at the right moment, exactly as they construct maps of physical spaces. If conceptual knowledge would be truly organized in a map-like structure it would be realistic to theorize that information would be organized according to their most salient characteristics in a 2-dimensional space, where, on each axis, one feature would be represented. In this way, similar concepts will be positioned closer to each other with the distance increasing as a function of dissimilarity [1,2,4]. If this hypothesis is correct, we could plausibly predict the recruitment of entorhinal cognitive maps in which concepts can be navigated similarly compared to how spatial information is navigated. In humans, the first attempt to investigate whether abstract stimuli were organized in a map-like fashion, and elicited the same 6-fold sinusoidal modulation observed in spatial tasks, was made by Constantinescu and colleagues (2016)[28]. The authors created a 2-dimensional 'bird space' defined by two continuous variables that were the neck and the leg length of a bird silhouette. To each different bird silhouette, a Christmas symbol was assigned. After having learned the association between each bird with each symbol, participants underwent an fMRI session, where they were asked to watch a video of birds morphing according to a predefined neck-leg ratio and imagine what would have been the final shape of the bird if the morph would have continued with the same ratio. At the end of the imagination period, participants were asked which symbol, between two choices, the bird they had imagined was associated with. The authors observed a grid-like signal in most of the areas found during spatial navigation tasks, including the right Entorhinal cortex[28]. These results were further supported by an animal study in which hippocampal-entorhinal neurons were recorded as rodents navigated a unidimensional sound space, defined by different sound frequencies, using a joystick. The authors reported that the firing properties of the hippocampal-entorhinal cells active during this task were similar to those of place and grid cells observed during standard spatial navigation tasks. This finding suggests the existence of a common mechanism in the brain that supports the encoding of various types of information, not only spatial information[68]. Further, human studies confirm the results obtained by Constantinescu [28], detecting a grid-like signal in humans' EC during the navigation of 'odors', 'socials', and 'words' spaces [26,69,70]. In more recent years grid-like coding has been associated also with higher-function cognitive processes such as decision-making and goal-directed navigation [33,71–74]. However, it is worth noticing that, the grid-like coding detected in the above-cited

conceptual navigation studies reflects the navigation of a space constructed ad-hoc in laboratories and that required extensive training of the participants to be learned and properly navigated. Therefore, it is difficult to conclude that the grid system supports conceptual navigation in everyday life contexts. Recently, Qasim and colleagues [75] developed a highly ecological and innovative paradigm to investigate the role of grid-like coding in conceptual navigation. Indeed, they recorded neuronal activity in neurosurgical patients, in the medial temporal lobe, while undergoing the navigation of a 2-dimensional emotions space defined by arousal and valence. The main innovation provided by this study is that participants did not need to undergo any training prior performing the experiment. As a matter of fact, they were asked to perform what could be described as a standard memory task in which they saw sets of 12 different pictures representing various subjects (animals, humans, landscapes, and so on) and were required to keep them in mind. After a brief distraction phase in which participants saw dots appearing on the screen, they were required to recall the 12 previously seen images. Unbeknown to the participants the presented images occupy a specific position in the 2-dimensional emotion space, defined by their valence and arousal ratings. Authors characterize the presence of grid-like neurons by first creating a firing map of the emotions space, and isolating neurons that showed multiple firing peaks, then, for those neurons, a gridness score was computed. Results showed that a significant percentage of neurons, among the ones recorded, showed a grid-like firing pattern during the task, which cannot be explained by arousal and valence per se, not by any of the alternative arrangements tested. This study showed, for the first time, direct evidence, in humans, that grid-like neurons subtend navigation of conceptual spaces in a highly ecological task, providing support to the hypothesis that this mechanism can effectively support the organization of abstract knowledge in individuals' everyday life.

In this first part of Chapter 1, I've tried to give an exhaustive overview of the knowledge we have about the development and the reliance on entorhinal cortex cognitive maps, under typical conditions, by discussing the main results in the field. In the second part, I will focus on the different cases in which the grid-like signal, in humans and animals, has been found to be altered or simply lose its stability.

1.3. The influence of endogenous and exogenous factors on the development of cognitive maps neural geometry

In the previous paragraphs, I've reported evidence that seems to suggest that both spatial and abstract knowledge rely upon cognitive maps and elicit the same neural correlate: grid-like coding. However, the ontogenetic development (during lifetime) of grid-coding in the human entorhinal cortex is virtually unexplored, and we know very little about the emergence and maintenance of grid-cell mediated allocentric cognitive maps in humans. For instance, the typical functioning of grid-coding in humans is impaired by some genetic factors. Animal studies observed a correlation between high concentrations of microtubule-associated protein tau (MAPT) in the hippocampal formation and grid cell firing stability [76]. Indeed, comparing grid cell activity in mice in which the MAPT concentrations were experimentally manipulated, to control mice, while performing a maze completion task, it was possible to observe a reduced grid cells' firing as well as grid score [76]. Similar results have been found in humans by conducting experiments on APOE-ε4 carriers individuals [77,78]. Briefly, the ε4 allele of the APOE gene is associated with a higher risk of developing Alzheimer's Dementia (AD) a pathology that is well-known to affect, among others, individuals' ability to orient in space. Crucially, one of the first brain regions affected by this dementia in the early stages is the Entorhinal cortex. Recycling one of the most used spatial navigation paradigms, which consists of an object-location memory task while navigating a virtual arena, it has been possible to demonstrate a reduced grid-like coding in the Entorhinal Cortex of APOE- ε4 carrier participants compared to controls. Healthy aging might be another factor influencing the stability of the grid-like coding in humans. It has, indeed, been shown that during an object location memory task, the grid-like signal detected in old participants was significantly lower compared to the one detected in young participants [79]. This reduction correlates with the same participant's path integration performance, a behavioral correlate associated with entorhinal cortex cognitive maps, with a lower gridness score associated with higher path integration errors. The presence of higher levels of tau protein, a specific allele associated with the APOE gene, or aging, are not the only factors that influence the expression of a grid-like coding in humans' and animals' EC. Indeed, there is evidence reporting variation in grid-coding both in animals and

humans correlated to environmental features or the reliance on a more egocentric, rather than allocentric, frame of reference to encode spatial relations. In 2015 Krupic [80], recorded the activity of medial temporal neurons in rodents that explore environments that have different geometries (circles, squares, or trapezoids). Results from this experiment revealed that whether in a circular or squared environment the neural geometry of grid cells' firing fields was preserved, even though in squares the firing pattern of grid cells tended to align to the walls, in highly polarized environments such as trapezoidal arenas, the hexagonal organization was completely disrupted. Crucially, Derdikman [81] and colleagues, investigating if and how compartmentalized environments could affect grid cell organization, showed, for the first time, that, under specific environmental conditions the disruption of grid representation is not casual, rather it reorganizes in sub-maps which encode locations in each portion of the space separately. In his study, animals were asked to navigate an empty squared arena and a hairpin maze. Interestingly, the hairpin-maze condition was performed both by introducing walls in the environment and by forcing the animal to navigate an empty arena in a zig-zag fashion. Direct neural recording of entorhinal cortex neuronal activity, revealed that in the hairpin maze environment with walls, grid cells firing fields organization gives rise to a 90° rotational periodicity in which, grid cells seemed to map each corridor of the hairpin maze separately rather than encode spatial relation of all the environment together. Interestingly, in the condition in which rodents were only forced to mimic navigation in the hairpin maze (zig-zag movements), the hexagonal organization of gird cells firing fields was restored [81]. In humans' similar patterns of results were detected in spatial navigation tasks using fMRI. The first evidence of the emergence of a variation of the typically detected 6-fold symmetry was provided by He and colleagues [82]. In their experiment, they asked participants to navigate a square arena and a hairpin maze. In the hairpin maze, participants to get a better sense of their position in the space, saw the location of the target object they had to reach poking out of the wall. What they observed was the emergence of a 4-fold sinusoidal modulation of the BOLD signal in humans' EC during the hairpin maze navigation, contrasting, with the detection of 6-fold sinusoidal BOLD modulation emerging during the navigation of the open arena. To characterize the emergence of these alternative periodicities, the authors investigate the distributions of the orientation of the grid across participants. Interestingly what they noticed was that 4-fold main grid orientations across participants were not uniformly distributed in space, rather they clustered around the two main cardinal axes (north-south and east-west). This anchoring phenomenon could reflect a similar

mechanism compared to the one observed in rodents, in which the introduction of barriers influenced the global encoding of spatial information, in favor of a more local encoding of the spatial relation of that delimited area of the space [82]. However, the introduction of barriers in the environment is not the only evidence of 4-fold BOLD modulation in humans' entorhinal cortex. Wagner and colleagues [83], observed the emergence of the same variation of cognitive maps neural geometry (4-fold symmetry) when participants were asked to exactly retrace a previously seen path. Differently from the study mentioned above, in this experiment participants navigate an open field arena with no obstacles or barriers. First participants were asked to simply observe an avatar moving with the arena. Here, authors detected the typically reported 6-fold symmetry in participants' entorhinal cortex. Secondly, participants were required to navigate the arena from a first view perspective, performing as accurately as possible the path they have previously observed. Crucially, quadrature filter analyses performed during the navigation period, revealed the emergence of the 4-fold symmetry[83]. The results reported by the aforementioned study raised the possibility that, at least in humans, the reduction of the 6-fold symmetry and the emergence of a variation in the typical periodicity, could be related not only to the presence of barriers that do not allow a complete understanding of the environmental layout at first sight, but rather to the reliance on a different frame of reference, the egocentric one, that in specific situations, could better serve the purpose of orienting in the space. In both experiments [82,83], indeed, it could be hypothesized that reliance on the two main cardinal axes (north-south, east-west) facilitates participants' movements in the space through a comparison of the to-be performed trajectory with those two axes. Supporting this hypothesis, a recent study by Moon and colleagues [84] reported how reliance on an egocentric frame of reference during navigation, is reflected in a reduced grid-like signal in the entorhinal cortex. In this fMRI experiment participants were asked to navigate a circular arena under two conditions, the first condition was similar to the one reported in classical spatial navigation studies [29,85] in which participants navigate the arena in a first-person perspective (no-body condition). In the second condition, the authors aimed to enhance participants' self-perception with the introduction of an avatar that mimicked their position (supine) within the fMRI scanner (body condition). Grid analyses conducted on the body condition revealed a reduction of the grid-like coding in the EC correlated with higher activity in the parietal cortex, which is usually associated with egocentric representations [61,86].

The influence of egocentric processing of spatial information, on the 6-fold symmetry, might be attributed to the fact that typically cognitive maps encode spatial relations relying on allocentric representations. Therefore, it might be that when particular situations make participants relying more onto an egocentric reference frame, grid coding could be disrupted or modified.

**2. (In)dependence: Uncovering the relation between space and concepts**

In previous paragraphs I've extensively described experiments that show that the navigation of spatial and abstract knowledge rely on the same neural correlated, grid-like coding, supporting the hypothesis that both domains ground on cognitive maps. However, the aforementioned studies investigated the emergence of grid-like coding in the entorhinal cortex always considering individuals who have similar experience of the space. Therefore, one main and intriguing question remains unanswered: What is the relation between spatial and conceptual knowledge? Two hypotheses can be formulated: the **scaffolding hypothesis** postulates that the mechanisms to navigate in space, ontogenetically evolved from animals to humans are, by these last, recycled and adapted also to organize and navigate the mind space. Thus, differences in the way space is navigated will be reflected also in the way concepts will be navigated. According to this hypothesis, an alteration in grid-like coding in the entorhinal cortex during spatial navigation will be reflected in a similar alteration of this neural correlate also in conceptual navigation. On the other hand, the **independence hypothesis** states that cognitive maps for space and concepts develop independently, and variation that might be found in grid-coding in spatial navigation as a consequence of a different intake of spatial information, will not be necessarily reflected in conceptual navigation.

The scaffolding hypothesis is something that has already been observed in several different cognitive domains spanning from time [87–90] and numbers perception [91,92] to emotions [93] and valence [94], and to the organization of serial information in working memory [95]. However, such influence has never been tested in the field of cognitive maps. Time is one of the clearest examples of this phenomenon. Time is a concept that, per se, does not have anything that would recall space, yet, people referring to it use spatial metaphors, such as: 'You have a bright future in *front of you'* [96]. The association between space and time has been empirically tested, with behavioral experiments,

that proved the existence of a mental timeline (MTL [97–100]), that is, the mechanism by which, when individuals are asked to recall past or imagine future events, they tend to position past events behind or, at their left, and future events in front, or, at their right. It has been demonstrated that the typical MTL can be altered both by reading experience[87]. Specifically, when participants were asked to judge the temporality of events included in a mirror-reverse sentence the standard rightward directionality of the MTL was reversed, making it so that, contrary to what is typically observed, they associate past events with the right side of the space and future event with the left side of the space. Moreover, when the target sentence was rotated by 90° the MTL rotated accordingly [87]. Similarly, this space-concepts association has been observed also in number organization. Indeed there is evidence that individuals organize numbers in a Mental Number Line (MNL) in which the magnitude of the numbers increases by moving rightward on it (small numbers are located on the left and large number on the right, [101,102]). The existence of the MNL has been empirically proven by behavioral experiments in which it has been demonstrated that participants were faster responding to small numbers with their left hand, and to bigger numbers with their right hand, a phenomenon that take the name of Spatial-Numerical Association of Response Code (SNARC) effect [103–107]. Once again, supporting the hypothesis that the experience individuals have of the space, has an influence on number organization, it has been shown that MNL organization can be altered both by reading experience and culture [87–89,92]. Evidence in literature indicates that when asked to judge whether a number appearing on a screen was odd or even, people belonging to Western cultures (reading preference from right to left) were faster in responding with their left hand for small and right hand for big numbers (SNARC effect), on the contrary people belonging to Arabic cultures (reading preference from left to right) showed the opposite pattern, classifying faster small number with the right hand and big numbers with the left hand [92]. Moreover, also finger counting influence the emergence of the standard rightward directionality of the MNL [108]. Pitt and colleagues[108] conducted and experiment in which half of the participants tested were required to count on their finger from 1 to 10 leftward and the other half were required to do the same but counting rightward on their finger. After this phase, a standard parity-judgement task to test the SNARC effect was performed. Results showed that participants that were exposed to the rightward directionality of finger counting, showed a reverse SNARC effect, associating more often, big numbers to the left side of the MNL, and small numbers to the right side of the MNL [108]. Visual experience also seems to play a role in the creation of the above-mentioned space-concepts

association. It has indeed been reported that when early blind individuals were required to make a temporal judgment on words by moving their hands forward or backward, they did not show any specific spatial-temporal preference, contrary to sighted individuals which, instead, show a clear spatial-temporal preference by consistently moving their hand forward if the word referred to a future concept, and backward if the word referred to a past concept. This result suggests an influence of visual experience, possibly related to how early blind process spatial information on the development of typical MTL [90]. Similarly, lack of visual experience seemed to play a role in the development of space-number association [91]. Indeed, Crollen and colleagues in 2013 [91] performed a numerical comparison task to investigate the influence of hand position on the expression of the MNL, asking participants to judge whether a number presented orally (range from 1 to 9), was greater or smaller compared to 5, with their hand crossed or perpendicular to the table. Results indicate that whether in sighted individuals the organization of the MNL was not affected by hands' position, in early blind participants, during the 'crossed-hand' condition the MNL was reversed, revealing a hands position-number association [91]. Not only time perception and number organization are influenced by space but also more abstract concepts such as emotions and valence. The body specificity hypothesis [94] offers a good example of this phenomenon. Casasanto in 2009 [94] performed a series of experiments aimed to investigate whether the way humans interact with the external world would also influence how thoughts are organized. In his experiments, he investigates whether the classic association between 'good' and the right side of the space, and 'bad' and the left side of the space [109] was influenced by individuals' manual preferences. Particularly, left-handed and right-handed participants performed a behavioral paper and pencil task in which they had to choose which among two boxes, one on the left and one on the right in the horizontal condition, and one on the top and the other on the bottom in the vertical condition, two animals should be placed. Results demonstrated that in the horizontal condition, right-handed individuals associate 'good' with the right side and 'bad' with the left side, whereas left-handed participants did the opposite ('good' on the left and 'bad' on the right). Interestingly the same valence-space association was found also when, instead of drawing the animal in the corresponding box, individuals were just asked to indicate orally where the animal should go, excluding potential biases derived from the movement of the hand [94]. Crucially, these patterns of results can be reversed in right and left-handed if the use of the dominant hand was precluded also for a short time window [110], providing evidence supporting the hypothesis that the way humans act

on the word influences how they organize valence space. Further support for this hypothesis came from a study investigating whether motor actions influence emotional memories [93]. In this study participants were asked to move marbles from a bottom shelf to an upper shelf and vice-versa. When participants were asked to move marbles from a bottom shelf to an upper one, they were subsequently more eagled to share positive autobiographical memories compared to when the marbles were moved from the top to the bottom. In this latter case, participants reported a higher number of negative autobiographical memories [93]. Finally, it has been observed that efficient retrieval of serial information in working memory, ground on the use of spatial configurations and attention, to organize the information, as if individuals marked down on their in-mind whiteboard the things to keep in mind and then, to retrieve the object needed in a specific moment, scan the stored list from left to right as they were actually reading it (Mental Whiteboard Hypothesis, [111]). Empirical evidence for this hypothesis has been observed when participants were required to memorize a list of items, and then to categorize them among a list of distractors. In these experiments, it has been observed that participants tended to respond faster with their right hand for items at the beginning of the list (i.e., the first presented during the encoding phase) rather than to those toward the end of the list (i.e., the lasts presented during the encoding phase). This phenomenon has been referred to as the Ordinal Position Effect (OPE, [95,112,113]). Similarly to what observed in the time, number and emotion cognitive domains, also the OPE is influence by differences in the way individuals encode spatial relation. Indeed, testing early blind individuals in a task, in which they had first to memorize a list of 5 fruits and vegetables, and then categorize them correctly, the usually detected effect in sighted (i.e., faster response for item at the beginning of a list and slower for item at the end of the list with the right hand, see above) was not detected in early blind individuals [95]. In this latter case, the absence of an OPE effect in early blind individuals might be related to the way this population acquire information from space. Indeed, differently from other senses, vision allows a global computation of multiple information at a glance, whereas it has been demonstrated that early blind rely on a more sequential encoding of spatial information [114,115]. Thus, it could be, that a vision-based experience of the world, which allows simultaneous encoding of spatial relation, is required for the emergence of the OPE [95].

Recently, it has been demonstrated that the influence of spatial organization on concepts can also be detected in patterns of eye gaze. Indeed, using a looking-to-nothing paradigm associated with a verbal fluency task, it has been possible to observe in the pattern of eye movements, recorded

through the eye-tracker, the reliance on the MNL when participants were asked to say random numbers (i.e., the direction of the gaze toward left for small number and toward right for large numbers) and reconstruct the typically reported color wheel when participants were asked to randomly name different colors [116].

We tested the scaffolding hypothesis by using early blind as a model system. In these terms, early blind individuals who learn to navigate space differently will also navigate concepts in a different way compared to sighted control individuals. Given that our interest relies on entorhinal cognitive maps we therefore predict: first that grid-like coding will be altered in early blind compared to sighted controls individuals in spatial navigation and, second, that the same or similar alterations will be observed also when early blind navigate through concepts.

To test this hypothesis, we first need to know whether grid-like coding is altered in early-blind people during spatial navigation. This is the objective of the second chapter of this thesis.

### 3. Introduction to the experimental work

In the following two chapters, I will describe two works (one of which has already been published) in which I'll target two crucial questions in the field of cognitive maps and spatial and abstract knowledge:

1. Does visual experience influence the emergence of grid-like coding during imagined spatial navigation?

2. Does visual experience influence the emergence of grid-like coding during conceptual navigation?

I addressed these two questions through separate fMRI experiments involving both sighted and early blind individuals, to which I dedicated the five years of this Ph.D. Working with special populations, such as blind individuals, presents several challenges in terms of both experimental

design and participant recruitment. The first challenge lies in designing an experiment with limited alternatives, as visual stimuli cannot be used. The second challenge is recruiting early blind participants, who come from all over Italy and occasionally from other European countries. The early blind participants who agree to participate in our experiments typically stay in Rovereto for 2 or 3 days, depending on the number of experiments in which they participate. This process requires extensive logistical planning and full-time availability from our team during their visits to the lab.

**References:**


1. Behrens TEJ, Muller TH, Whittington JCR, et al. What Is a Cognitive Map? Organizing Knowledge for Flexible Behavior. *Neuron*. 2018;100(2):490-509. doi:10.1016/j.neuron.2018.10.002

2. Bellmund JLS, Gärdenfors P, Moser EI, Doeller CF. Navigating cognition: Spatial codes for human thinking. *Science*. 2018;362(6415):eaat6766. doi:10.1126/science.aat6766

3. Buzsáki G, Moser EI. Memory, navigation and theta rhythm in the hippocampal-entorhinal system. *Nat Neurosci*. 2013;16(2):130-138. doi:10.1038/nn.3304

4. Whittington JCR, Muller TH, Mark S, et al. The Tolman-Eichenbaum Machine: Unifying Space and Relational Memory through Generalization in the Hippocampal Formation. *Cell*. 2020;183(5):1249-1263.e23. doi:10.1016/j.cell.2020.10.024

5. Courellis HS, Minxha J, Cardenas AR, et al. Abstract representations emerge in human hippocampal neurons during inference. *Nature*. 2024;632(8026):841-849. doi:10.1038/s41586-024-07799-x

6. Tolman EC. Cognitive maps in rats and men. *Psychological Review*. 1948;55(4):189-208. doi:10.1037/h0061626

7. Epstein RA, Patai EZ, Julian JB, Spiers HJ. The cognitive map in humans: Spatial navigation and beyond. *Nature Neuroscience*. 2017;20(11):1504-1513. doi:10.1038/nn.4656

8. Clark RE, Squire LR. Similarity in form and function of the hippocampus in rodents, monkeys, and humans. *Proc Natl Acad Sci USA*. 2013;110(supplement_2):10365-10370. doi:10.1073/pnas.1301225110

9. Iaria G, Petrides M, Dagher A, Pike B, Bohbot VD. Cognitive strategies dependent on the hippocampus and caudate nucleus in human navigation: variability and change with practice. *J Neurosci*. 2003;23(13):5945-5952. doi:10.1523/JNEUROSCI.23-13-05945.2003

10. Buzsáki G, Christen Y, eds. *Micro-, Meso- and Macro-Dynamics of the Brain*. Springer International Publishing; 2016. doi:10.1007/978-3-319-28802-4

11. Moser EI, Moser MB, McNaughton BL. Spatial representation in the hippocampal formation: a history. *Nat Neurosci*. 2017;20(11):1448-1464. doi:10.1038/nn.4653

12. Tolman EC. COGNITIVE MAPS IN RATS AND MEN.

13. Moser EI, Kropff E, Moser MB. Place Cells, Grid Cells, and the Brain's Spatial Representation System. *Annu Rev Neurosci*. 2008;31(1):69-89. doi:10.1146/annurev.neuro.31.061307.090723

14. Rowland DC, Roudi Y, Moser MB, Moser EI. Ten Years of Grid Cells. *Annu Rev Neurosci*. 2016;39(1):19-40. doi:10.1146/annurev-neuro-070815-013824

15. O'Keefe J, Dostrovsky J. The hippocampus as a spatial map. Preliminary evidence from unit activity in the freely-moving rat. *Brain Research*. 1971;34(1):171-175. doi:10.1016/0006-8993(71)90358-1

16. Taube JS, Muller RU, Ranck JB. Head-direction cells recorded from the postsubiculum in freely moving rats. I. Description and quantitative analysis. *J Neurosci*. 1990;10(2):420-435. doi:10.1523/JNEUROSCI.10-02-00420.1990

17. Hafting T, Fyhn M, Molden S, Moser MB, Moser EI. Microstructure of a spatial map in the entorhinal cortex. *Nature*. 2005;436(7052):801-806. doi:10.1038/nature03721

18. Bush D, Barry C, Manson D, Burgess N. Using Grid Cells for Navigation. *Neuron*. 2015;87(3):507-520. doi:10.1016/j.neuron.2015.07.006

19. Stensola H, Stensola T, Solstad T, Frøland K, Moser MB, Moser EI. The entorhinal grid map is discretized. *Nature*. 2012;492(7427):72-78. doi:10.1038/nature11649

20. Jeewajee A, Barry C, O'Keefe J, Burgess N. Grid cells and theta as oscillatory interference: Electrophysiological data from freely moving rats. *Hippocampus*. 2008;18(12):1175-1185. doi:10.1002/hipo.20510

21. Reifenstein ET, Kempter R, Schreiber S, Stemmler MB, Herz AVM. Grid cells in rat entorhinal cortex encode physical space with independent firing fields and phase precession at the single-trial level. *Proceedings of the National Academy of Sciences*. 2012;109(16):6301-6306. doi:10.1073/pnas.1109599109

22. Fyhn M, Hafting T, Witter MP, Moser EI, Moser MB. Grid cells in mice. *Hippocampus*. 2008;18(12):1230-1238. doi:10.1002/hipo.20472

23. Yartsev MM, Ulanovsky N. Representation of Three-Dimensional Space in the Hippocampus of Flying Bats. *Science*. 2013;340(6130):367-372. doi:10.1126/science.1235338

24. Yartsev MM, Witter MP, Ulanovsky N. Grid cells without theta oscillations in the entorhinal cortex of bats. *Nature*. 2011;479(7371):103-107. doi:10.1038/nature10583

25. Killian NJ, Jutras MJ, Buffalo EA. A map of visual space in the primate entorhinal cortex. *Nature*. 2012;491(7426):761-764. doi:10.1038/nature11587

26. Bao X, Gjorgieva E, Shanahan LK, Howard JD, Kahnt T, Gottfried JA. Grid-like Neural Representations Support Olfactory Navigation of a Two-Dimensional Odor Space. *Neuron*. 2019;102(5):1066-1075.e5. doi:10.1016/j.neuron.2019.03.034

27. Bellmund JL, Deuker L, Navarro Schröder T, Doeller CF. Grid-cell representations in mental simulation. *eLife*. 2016;5:e17089. doi:10.7554/eLife.17089

28. Constantinescu AO, OReilly JX, Behrens TEJ. Organizing conceptual knowledge in humans with a gridlike code. *Science*. 2016;352(6292):1464-1468. doi:10.1126/science.aaf0941

29. Doeller CF, Barry C, Burgess N. Evidence for grid cells in a human memory network. *Nature*. 2010;463(7281):657-661. doi:10.1038/nature08704

30. Giari G, Vignali L, Xu Y, Bottini R. MEG frequency tagging reveals a grid-like code during attentional movements. *Cell Reports*. 2023;42(10):113209. doi:10.1016/j.celrep.2023.113209

31. Horner AJ, Bisby JA, Zotow E, Bush D, Burgess N. Grid-like Processing of Imagined Navigation. *Current Biology*. 2016;26(6):842-847. doi:10.1016/j.cub.2016.01.042

32. Nau M, Navarro Schröder T, Bellmund JLS, Doeller CF. Hexadirectional coding of visual space in human entorhinal cortex. *Nat Neurosci*. 2018;21(2):188-190. doi:10.1038/s41593-017-0050-8

33. Park SA, Miller DS, Boorman ED. Inferences on a multidimensional social hierarchy use a grid-like code. *Nat Neurosci*. 2021;24(9):1292-1301. doi:10.1038/s41593-021-00916-3

34. Viganò S, Bayramova R, Doeller CF, Bottini R. *Mental Search of Concepts Is Supported by Egocentric Vector Representations and Restructured Grid Maps*. Neuroscience; 2023. doi:10.1101/2023.01.19.524704

35. Jacobs J, Weidemann CT, Miller JF, et al. Direct recordings of grid-like neuronal activity in human spatial navigation. *Nat Neurosci*. 2013;16(9):1188-1190. doi:10.1038/nn.3466

36. Bird CM, Burgess N. The hippocampus and memory: insights from spatial processing. *Nat Rev Neurosci*. 2008;9(3):182-194. doi:10.1038/nrn2335

37. Chersi F, Burgess N. The Cognitive Architecture of Spatial Navigation: Hippocampal and Striatal Contributions. *Neuron*. 2015;88(1):64-77. doi:10.1016/j.neuron.2015.09.021

38. Clark BJ, Simmons CM, Berkowitz LE, Wilber AA. The retrosplenial-parietal network and reference frame coordination for spatial navigation. *Behavioral Neuroscience*. 2018;132(5):416-429. doi:10.1037/bne0000260

39. Epstein RA. Parahippocampal and retrosplenial contributions to human spatial navigation. *Trends in Cognitive Sciences*. 2008;12(10):388-396. doi:10.1016/j.tics.2008.07.004

40. Julian JB, Keinath AT, Marchette SA, Epstein RA. The Neurocognitive Basis of Spatial Reorientation. *Current Biology*. 2018;28(17):R1059-R1073. doi:10.1016/j.cub.2018.04.057

41. Patai EZ, Spiers HJ. The Versatile Wayfinder: Prefrontal Contributions to Spatial Navigation. *Trends in Cognitive Sciences*. 2021;25(6):520-533. doi:10.1016/j.tics.2021.02.010

42. Kaplan R, Horner AJ, Bandettini PA, Doeller CF, Burgess N. Human hippocampal processing of environmental novelty during spatial navigation. *Hippocampus*. 2014;24(7):740-750. doi:10.1002/hipo.22264

43. McNamara TP, Shelton AL, Shelton AL. Cognitive maps and the hippocampus. *Trends Cogn Sci*. 2003;7(8):333-335. doi:10.1016/s1364-6613(03)00167-0

44. Nau M. Functional imaging of the human medial temporal lobe. Published online August 30, 2022. doi:10.17605/OSF.IO/CQN4Z

45. Dragoi G, Tonegawa S. Preplay of future place cell sequences by hippocampal cellular assemblies. *Nature*. 2011;469(7330):397-401. doi:10.1038/nature09633

46. Ólafsdóttir HF, Barry C, Saleem AB, Hassabis D, Spiers HJ. Hippocampal place cells construct reward related sequences through unexplored space. Eichenbaum H, ed. *eLife*. 2015;4:e06063. doi:10.7554/eLife.06063

47. Buckner RL. The role of the hippocampus in prediction and imagination. *Annu Rev Psychol*. 2010;61:27-48, C1-8. doi:10.1146/annurev.psych.60.110707.163508

48. Byrne P, Becker S, Burgess N. Remembering the past and imagining the future. *Psychol Rev*. 2007;114(2):340-375. doi:10.1037/0033-295X.114.2.340

49. Hasselmo ME. A model of episodic memory: Mental time travel along encoded trajectories using grid cells. *Neurobiol Learn Mem*. 2009;92(4):559-573. doi:10.1016/j.nlm.2009.07.005

50. Schacter DL, Addis DR, Hassabis D, Martin VC, Spreng RN, Szpunar KK. The Future of Memory: Remembering, Imagining, and the Brain. *Neuron*. 2012;76(4):10.1016/j.neuron.2012.11.001. doi:10.1016/j.neuron.2012.11.001

51. Nau M, Julian JB, Doeller CF. How the Brain's Navigation System Shapes Our Visual Experience. *Trends in Cognitive Sciences*. 2018;22(9):810-825. doi:10.1016/J.TICS.2018.06.008

52. Piccardi L, De Luca M, Nori R, Palermo L, Iachini F, Guariglia C. Navigational Style Influences Eye Movement Pattern during Exploration and Learning of an Environmental Map. *Front Behav Neurosci*. 2016;10. doi:10.3389/fnbeh.2016.00140

53. Killian NJ, Potter SM, Buffalo EA. Saccade direction encoding in the primate entorhinal cortex during visual exploration. *Proceedings of the National Academy of Sciences*. 2015;112(51):15743-15748. doi:10.1073/pnas.1417059112

54. Julian JB, Keinath AT, Frazzetta G, Epstein RA. Human entorhinal cortex represents visual space using a boundary-anchored grid. *Nat Neurosci*. 2018;21(2):191-194. doi:10.1038/s41593-017-0049-1

55. Staudigl T, Leszczynski M, Jacobs J, et al. Hexadirectional Modulation of High-Frequency Electrophysiological Activity in the Human Anterior Medial Temporal Lobe Maps Visual Space. *Current Biology*. 2018;28(20):3325-3329.e4. doi:10.1016/j.cub.2018.09.035

56. Wilming N, König P, König S, Buffalo EA. Entorhinal cortex receptive fields are modulated by spatial attention, even without movement. Turk-Browne N, ed. *eLife*. 2018;7:e31745. doi:10.7554/eLife.31745

57. Barry C, Ginzberg LL, O'Keefe J, Burgess N. Grid cell firing patterns signal environmental novelty by expansion. *Proc Natl Acad Sci U S A*. 2012;109(43):17687-17692. doi:10.1073/pnas.1209918109

58. Boccara CN, Nardin M, Stella F, O'Neill J, Csicsvari J. The entorhinal cognitive map is attracted to goals. *Science*. 2019;363(6434):1443-1447. doi:10.1126/science.aav4837

59. Butler WN, Hardcastle K, Giocomo LM. Remembered reward locations restructure entorhinal spatial maps. *Science*. 2019;363(6434):1447-1452. doi:10.1126/science.aav5297

60. Nyberg N, Duvelle É, Barry C, Spiers HJ. Spatial goal coding in the hippocampal formation. *Neuron*. 2022;110(3):394-422. doi:10.1016/j.neuron.2021.12.012

61. Bottini R, Doeller CF. Knowledge Across Reference Frames: Cognitive Maps and Image Spaces. *Trends in Cognitive Sciences*. 2020;24(8):606-619. doi:10.1016/j.tics.2020.05.008

62. Eichenbaum H. Hippocampus: cognitive processes and neural representations that underlie declarative memory. *Neuron*. 2004;44(1):109-120. doi:10.1016/j.neuron.2004.08.028

63. Eichenbaum H. Time (and space) in the hippocampus. *Current Opinion in Behavioral Sciences*. 2017;17:65-70. doi:10.1016/j.cobeha.2017.06.010

64. McKenzie S, Frank AJ, Kinsky NR, Porter B, Rivière PD, Eichenbaum H. Hippocampal Representation of Related and Opposing Memories Develop within Distinct, Hierarchically Organized Neural Schemas. *Neuron*. 2014;83(1):202-215. doi:10.1016/j.neuron.2014.05.019

65. Nadel L. The hippocampus and space revisited. *Hippocampus*. 1991;1(3):221-229. doi:10.1002/hipo.450010302

66. Schiller D, Eichenbaum H, Buffalo EA, et al. Memory and Space: Towards an Understanding of the Cognitive Map. *J Neurosci*. 2015;35(41):13904-13911. doi:10.1523/JNEUROSCI.2618-15.2015

67. Voss JL, Bridge DJ, Cohen NJ, Walker JA. A Closer Look at the Hippocampus and Memory. *Trends in Cognitive Sciences*. 2017;21(8):577-588. doi:10.1016/j.tics.2017.05.008

68. Aronov D, Nevers R, Tank DW. Mapping of a non-spatial dimension by the hippocampal–entorhinal circuit. *Nature*. 2017;543(7647):719-722. doi:10.1038/nature21692

69. Parkinson C, Liu S, Wheatley T. A Common Cortical Metric for Spatial, Temporal, and Social Distance. *Journal of Neuroscience*. 2014;34(5):1979-1987. doi:10.1523/JNEUROSCI.2159-13.2014

70. Viganò S, Rubino V, Soccio AD, Buiatti M, Piazza M. Grid-like and distance codes for representing word meaning in the human brain. *NeuroImage*. 2021;232:117876. doi:10.1016/j.neuroimage.2021.117876

71. Liang Z, Wu S, Wu J, Wang WX, Qin S, Liu C. Distance and grid-like codes support the navigation of abstract social space in the human brain. *eLife*. 2024;12:RP89025. doi:10.7554/eLife.89025

72. Nitsch A, Garvert MM, Bellmund JLS, Schuck NW, Doeller CF. Grid-like entorhinal representation of an abstract value space during prospective decision making. *Nat Commun*. 2024;15(1):1198. doi:10.1038/s41467-024-45127-z

73. Viganò S, Rubino V, Di Soccio A, Buiatti M, Piazza M. *Multiple Spatial Codes for Navigating 2-D Semantic Spaces*. Neuroscience; 2020. doi:10.1101/2020.07.16.205955

74. Viganò S, Bayramova R, Doeller CF, Bottini R. Mental search of concepts is supported by egocentric vector representations and restructured grid maps. *Nat Commun*. 2023;14(1):8132. doi:10.1038/s41467-023-43831-w

75. Qasim SE, Reinacher PC, Brandt A, Schulze-Bonhage A, Kunz L. Neurons in the human entorhinal cortex map abstract emotion space. Published online August 12, 2023. doi:10.1101/2023.08.10.552884

76. Fu H, Rodriguez GA, Herman M, et al. Tau Pathology Induces Excitatory Neuron Loss, Grid Cell Dysfunction, and Spatial Memory Deficits Reminiscent of Early Alzheimer's Disease. *Neuron*. 2017;93(3):533-541.e5. doi:10.1016/j.neuron.2016.12.023

77. Bierbrauer A, Kunz L, Gomes CA, et al. Unmasking selective path integration deficits in Alzheimer's disease risk carriers. *Sci Adv*. 2020;6(35):eaba1394. doi:10.1126/sciadv.aba1394

78. Kunz L, Schroder TN, Lee H, et al. Reduced grid-cell-like representations in adults at genetic risk for Alzheimer's disease. *Science*. 2015;350(6259):430-433. doi:10.1126/science.aac8128

79. Stangl M, Achtzehn J, Huber K, Dietrich C, Tempelmann C, Wolbers T. Compromised Grid-Cell-like Representations in Old Age as a Key Mechanism to Explain Age-Related Navigational Deficits. *Current Biology*. 2018;28(7):1108-1115.e6. doi:10.1016/j.cub.2018.02.038

80. Krupic J, Bauza M, Burton S, Barry C, O'Keefe J. Grid cell symmetry is shaped by environmental geometry. *Nature*. 2015;518(7538):232-235. doi:10.1038/nature14153

81. Derdikman D, Whitlock JR, Tsao A, et al. Fragmentation of grid cell maps in a multicompartment environment. *Nat Neurosci*. 2009;12(10):1325-1332. doi:10.1038/nn.2396

82. He Q, Brown TI. Environmental Barriers Disrupt Grid-like Representations in Humans during Navigation. *Current Biology*. 2019;29(16):2718-2722.e3. doi:10.1016/j.cub.2019.06.072

83. Wagner IC, Graichen LP, Todorova B, et al. Entorhinal grid-like codes and time-locked network dynamics track others navigating through space. *Nat Commun*. 2023;14(1):231. doi:10.1038/s41467-023-35819-3

84. Moon HJ, Gauthier B, Park HD, Faivre N, Blanke O. Sense of self impacts spatial navigation and hexadirectional coding in human entorhinal cortex. *Commun Biol*. 2022;5(1):1-12. doi:10.1038/s42003-022-03361-5

85. Horner AJ, Bisby JA, Zotow E, Bush D, Burgess N. Grid-like Processing of Imagined Navigation. *Current Biology*. 2016;26(6):842-847. doi:10.1016/j.cub.2016.01.042

86. Schindler A, Bartels A. Parietal Cortex Codes for Egocentric Space beyond the Field of View. *Current Biology*. 2013;23(2):177-182. doi:10.1016/j.cub.2012.11.060

87. Casasanto D, Bottini R. Mirror reading can reverse the flow of time. *J Exp Psychol Gen*. 2014;143(2):473-479. doi:10.1037/a0033297

88. Pitt B, Ferrigno S, Cantlon JF, Casasanto D, Gibson E, Piantadosi ST. Spatial concepts of number, size, and time in an indigenous culture. *Science Advances*. 2021;7(33):eabg4141. doi:10.1126/sciadv.abg4141

89. Pitt B, Casasanto D. The correlations in experience principle: How culture shapes concepts of time and number. *Journal of Experimental Psychology: General*. 2020;149(6):1048-1070. doi:10.1037/xge0000696

90. Rinaldi L, Fantino M, Vecchi T, Merabet LB, Cattaneo Z. The ego-moving metaphor of time relies on visual experience: No representation of time along the sagittal space in the

blind. *Journal of Experimental Psychology: General*. 2017;147(3):444-450. doi:10.1037/xge0000373

91. Crollen V, Dormal G, Seron X, Lepore F, Collignon O. Embodied numbers: The role of vision in the development of number–space interactions. *Cortex*. 2013;49(1):276-283. doi:10.1016/j.cortex.2011.11.006

92. Shaki S, Fischer MH, Petrusic WM. Reading habits for both words and numbers contribute to the SNARC effect. *Psychonomic Bulletin & Review*. 2009;16(2):328-331. doi:10.3758/PBR.16.2.328

93. Casasanto D, Dijkstra K. Motor action and emotional memory. *Cognition*. 2010;115(1):179-185. doi:10.1016/j.cognition.2009.11.002

94. Casasanto D. Embodiment of abstract concepts: good and bad in right- and left-handers. *J Exp Psychol Gen*. 2009;138(3):351-367. doi:10.1037/a0015854

95. Bottini R, Mattioni S, Collignon O. Early blindness alters the spatial organization of verbal working memory. *Cortex*. 2016;83:271-279. doi:10.1016/j.cortex.2016.08.007

96. Casasanto D, Bottini R. Spatial language and abstract concepts. *WIRES Cognitive Science*. 2014;5(2):139-149. doi:10.1002/wcs.1271

97. Bonato M, Zorzi M, Umiltà C. When time is space: evidence for a mental time line. *Neurosci Biobehav Rev*. 2012;36(10):2257-2273. doi:10.1016/j.neubiorev.2012.08.007

98. Vallesi A, Binns MA, Shallice T. An effect of spatial–temporal association of response codes: Understanding the cognitive representations of time. *Cognition*. 2008;107(2):501-527. doi:10.1016/j.cognition.2007.10.011

99. Vallesi A, McIntosh AR, Stuss DT. How time modulates spatial responses. *Cortex*. 2011;47(2):148-156. doi:10.1016/j.cortex.2009.09.005

100. Weger UW, Pratt J. Time flies like an arrow: Space-time compatibility effects suggest the use of a mental timeline. *Psychonomic Bulletin & Review*. 2008;15(2):426-430. doi:10.3758/PBR.15.2.426

101. Fias W, Bonato M. Chapter 12 - Which Space for Numbers? In: Henik A, Fias W, eds. *Heterogeneity of Function in Numerical Cognition*. Academic Press; 2018:233-242. doi:10.1016/B978-0-12-811529-9.00012-1

102. Zorzi M, Priftis K, Umiltà C. Neglect disrupts the mental number line. *Nature*. 2002;417(6885):138-139. doi:10.1038/417138a

103. Cristoforetti G, Majerus S, Sahan MI, van Dijck JP, Fias W. Neural Patterns in Parietal Cortex and Hippocampus Distinguish Retrieval of Start versus End Positions in Working Memory. *Journal of Cognitive Neuroscience*. 2022;34(7):1230-1245. doi:10.1162/jocn_a_01860

104. Dehaene S, Bossini S, Giraux P. The mental representation of parity and number magnitude. *Journal of Experimental Psychology: General*. 1993;122(3):371-396. doi:10.1037/0096-3445.122.3.371

105. Fias W. The Importance of Magnitude Information in Numerical Processing: Evidence from the SNARC Effect. *Mathematical Cognition*. 1996;2(1):95-110. doi:10.1080/135467996387552

106. Gevers W, Verguts T, Reynvoet B, Caessens B, Fias W. Numbers and space: a computational model of the SNARC effect. *J Exp Psychol Hum Percept Perform*. 2006;32(1):32-44. doi:10.1037/0096-1523.32.1.32

107. Viarouge A, Hubbard EM, Dehaene S. The organization of spatial reference frames involved in the SNARC effect. *Quarterly Journal of Experimental Psychology*. 2014;67(8):1484-1499. doi:10.1080/17470218.2014.897358

108. Casasanto D. Experiential Origins of the Mental Number Line. Published online January 1, 2014. Accessed September 15, 2024. https://www.academia.edu/70687805/Experiential_Origins_of_the_Mental_Number_Line

109. McManus IC. *Right Hand, Left Hand: The Origins of Asymmetry in Brains, Bodies, Atoms, and Cultures*. Harvard University Press; 2002.

110. de la Fuente J, Casasanto D, Martínez-Cascales JI, Santiago J. Motor Imagery Shapes Abstract Concepts. *Cognitive Science*. 2017;41(5):1350-1360. doi:10.1111/cogs.12406

111. Abrahamse E, van Dijck JP, Majerus S, Fias W. Finding the answer in space: the mental whiteboard hypothesis on serial order in working memory. *Front Hum Neurosci*. 2014;8:932. doi:10.3389/fnhum.2014.00932

112. Becker SL. The ordinal position effect. *Quarterly Journal of Speech*. Published online April 1, 1953. doi:10.1080/00335635309381862

113. van Dijck JP, Abrahamse EL, Majerus S, Fias W. Spatial Attention Interacts With Serial-Order Retrieval From Verbal Working Memory. *Psychol Sci*. 2013;24(9):1854-1859. doi:10.1177/0956797613479610

114. Cornoldi C, Beni RD, Roncari S, Romano S. The effects of imagery instructions on total congenital blind recall. *European Journal of Cognitive Psychology*. 1989;1(4):321-331. doi:10.1080/09541448908403092

115. Noordzij ML, Zuidhoek S, Postma A. The influence of visual experience on the ability to form spatial mental models based on route and survey descriptions. *Cognition*. 2006;100(2):321-342. doi:10.1016/j.cognition.2005.05.006

116. Viganò S, Bayramova R, Doeller CF, Bottini R. Spontaneous eye movements reflect the representational geometries of conceptual spaces. *Proceedings of the National Academy of Sciences*. 2024;121(17):e2403858121. doi:10.1073/pnas.2403858121

# II

# ALTERED GRID-LIKE CODING IN EARLY BLIND PEOPLE

---

Federica Sigismondi[1,*,†], Yangwen Xu[1,2,†], Mattia Silvestri[1], Roberto Bottini[1,*]

[1]Center for Mind/Brain sciences, University of Trento, Trento, 38122, Italy.

[2]Max Planck Institute for Human Cognitive and Brain sciences, Leipzig, D-04303, Germany.

[†]These authors contribute equally.

[*]Correspondence: federica.sigismondi@unitn.it, roberto.bottini@unitn.it

This chapter contains a modified version (in the formatting) of the following scientific article reproduced with the permission of Springer Nature: Sigismondi, F., Xu, Y., Silvestri, M., & Bottini, R. (2024). Altered grid-like coding in early blind people. *Nature Communications*, *15*(1), 3476. The following materials were used: introduction, methods, results, discussion, figures, and supplementary materials.

**Abstract**

Cognitive maps in the hippocampal-entorhinal system are central for the representation of both spatial and non-spatial relationships. Although this system, especially in humans, heavily relies on vision, the role of visual experience in shaping the development of cognitive maps remains largely unknown. Here, we test sighted and early blind individuals in both imagined navigation in fMRI and real-world navigation. During imagined navigation, the Human Navigation Network, constituted by frontal, medial temporal, and parietal cortices, is reliably activated in both groups, showing resilience to visual deprivation. However, neural geometry analyses highlight crucial

differences between groups. A 60° rotational symmetry, characteristic of a hexagonal grid-like coding, emerges in the entorhinal cortex of sighted but not blind people, who instead show a 90° (4-fold) symmetry, indicative of a square grid. Moreover, higher parietal cortex activity during navigation in blind people correlates with the magnitude of 4-fold symmetry. In sum, early blindness can alter the geometry of entorhinal cognitive maps, possibly as a consequence of higher reliance on parietal egocentric coding during navigation.

## Introduction

Humans heavily rely on vision to navigate the environment and acquire spatial information[1–4]. However, the role of visual experience in the development and functioning of the brain system dedicated to spatial navigation remains largely unknown. In the brain, the human navigation network (HNN) comprises medial temporal, parietal, and occipital regions that support spatial memory and navigation across complementary allocentric and egocentric reference frames[5–11]. Significant breakthroughs in rodent electrophysiology attribute a crucial role in spatial navigation to the hippocampal-entorhinal system through the construction of allocentric cognitive maps[12] based on the activity of highly specialized neurons, such as place cells[13], head direction cells[14], and grid cells[15]. Whereas place cells and head direction cells encode single locations and heading directions, respectively, grid cells in the medial entorhinal cortex (EC) present multiple firing fields and keep track of agent movements within the environment, tiling the navigable surface in a regular hexagonal grid.

Compared to other modalities, vision provides highly precise and global information regarding the location of both proximal and distal landmarks, which are important for the creation of allocentric maps[16–18]. Notably, visual landmarks displaced in the environment as experimental manipulation cause a shift in the firing field orientation of grid, place, and head-direction cells toward the position of the cues, suggesting visual anchoring of cognitive maps[15,19–22]. Consistently, when rodents need to navigate in the dark, after familiarizing themselves with an environment in plain light, both grid and head direction firing fields can be disrupted and navigation impaired[23,24]. However, experiments with congenitally blind rodents have shown that place cell firing fields develop normally in the absence of vision, although with reduced firing rates[25], and head direction

cells maintain their directional selectivity but with lower precision[24]. Nothing is known about the resilience of place and head direction coding in blind humans, and the development of grid cells in the absence of functional vision remains untested across species. Notably, in the lack of vision, rodents can maintain stable allocentric maps of the environment by relying on olfactory cues[24], a sense that, arguably, is not sufficiently developed in humans to serve the same purpose. How does early or congenital visual deprivation affect spatial navigation and its neural underpinnings in humans?

The ability to create mental maps of the environment is maintained in blind people[26,27], though early lack of vision can impair allocentric spatial coding[28], leading to less reliable distance estimation[29] and higher reliance on egocentric coding[27,30]. A few neuroimaging studies have investigated the influence of early visual deprivation on the neural correlates underlying spatial navigation in early blind individuals using various tasks and reporting inconsistent results[31–35] (see discussion). Crucially, none of these experiments has investigated the impact of blindness on the hippocampal-entorhinal spatial codes.

Here, in an fMRI experiment, we asked blindfolded sighted and early blind participants to imagine navigating inside a clock-like space, walking from one number to another in a straight line, to investigate whether early lack of vision influenced the emergence of grid-like representations in early blind individuals' entorhinal cortex. The clock space was sampled at a granularity of 15° to provide a sufficient angle resolution to detect the hexadirectional signal (6-fold symmetry), which some studies[36-40] have indicated as a proxy for the activity of grid cells in fMRI both during visual[36–38-39] and imagined navigation[40,41]. Participants' active navigation during the task was spurred by the introduction of a control question, solvable only by performing spatial inferences on the relationships between the positions of the different numbers inside the clock. Importantly, we've benefitted of the high familiarity of both groups with the clock environment to control for a possible imbalance of task-familiarity. We also ran a shorter, modified version of the experiment, in which clock navigation was compared to an arithmetic task (Nav-Math Experiment) to test possible differences between sighted and early blind individuals in the activation of navigation-specific regions. Finally, we tested how brain activations relate to real-world spatial navigation in both groups.

**Results**

Blind and sighted individuals successfully navigated the clock space

The imagined navigation task was similar across the two experiments (Clock-Navigation and Nav-Math), (See Methods and Fig. 1A-B), and was developed by adapting imagined navigation tasks from previous studies[40,41]. Blindfolded participants received auditory instructions for their starting and target locations (numbers) inside the clock. They were then told to imagine walking directly from one point to the other. After a jittered imagination period (4 – 6 secs), a third number was announced, and participants had to decide whether the number was located to their left or right. The arithmetic task (performed only in the Nav-Math experiment) was structurally similar to the navigation one. Participants heard three numbers, on which they had to perform simple operations (e.g., 8 + 2 - 4) and then compared the results to a target number presented at the beginning of each block (Fig. 1B). Nineteen early blind participants (who lost completely their sight at birth or before 5 y.o., and report no visual memory; Table S1) and 19 matched sighted controls underwent an fMRI session, preceded by behavioral training in both tasks (math and navigation) and experiments (Nav-Math and Clock-Navigation, see Methods). No difference in accuracy was detected between groups and tasks in the Nav-Math experiment (Repeated-measure ANOVA; main effect of group: $F(1,36) = 0.86$, $p = 0.36$, $\eta^2 = 0.018$, 95%CI = [-0.04, 0.03]; main effect of task: $F(1,36) = 0.85$, $p = 0.36$, $\eta^2 = 0.005$, 95%CI = [-0.006, 0.04]; Group × Task interaction: $F(1,36) = 1.42$, $p = 0.24$, $\eta^2 = 0.008$, 95%CI = [-0.06, 0.01], two-tailed; Fig. 2A). Reaction times (RTs) followed a similar pattern with no differences detected in RTs between groups and tasks in the Nav-Math experiment (main effect of group $\chi^2(1) = 1.53$, $p = 0.21$, 95% CI [-0.39, 0.08]; main effect of task: $\chi^2(1) = 3.59$, $p = 0.06$, 95% CI [-0.02, 0.07]; Group × Task interaction: $\chi^2(1) = 0.24$, $p = 0.62$, 95% CI [-0.04, 0.08], two-tailed, Fig. 2B). Collectively, these results suggest that both sighted and blind participants were able to perform the tasks and to perform comparably. Similarly, in the Clock-Navigation experiment, we did not detect differences in accuracy (two-sample t-test; $t(36) = 2.0$, $p = 0.052$, Cohen's $d = 0.62$, 95%CI = [-0.0018, 0.057], two-tailed, Fig. 2C) and RTs (Linear Mixed-Effect Model; $\chi^2(1) = 2.38$, $p = 0.12$, 95%CI = [-0.03, 0.26], two-tailed, Fig. 2D) between groups. However, outlier analysis revealed the presence of one outlier in accuracy in the sighted controls group. Thus, we've performed the analyses excluding the outlier participant. Results on the RTs remain invariant with no differences between groups (Linear Mixed-Effect Model; 18

sighted controls & 19 early blind individuals, $\chi^2(1) = 2.51$, $p = 0.13$, 95%CI = [-0.02, 0.28] two-tailed). On the other hand, analysis on accuracy detected a significant difference between the two groups (18 sighted controls & 19 early blind individuals, $t(35) = 2.87$, $p = 0.007$, Cohen's $d = 0.94$, 95%CI = [0.01, 0.06], two-tailed).

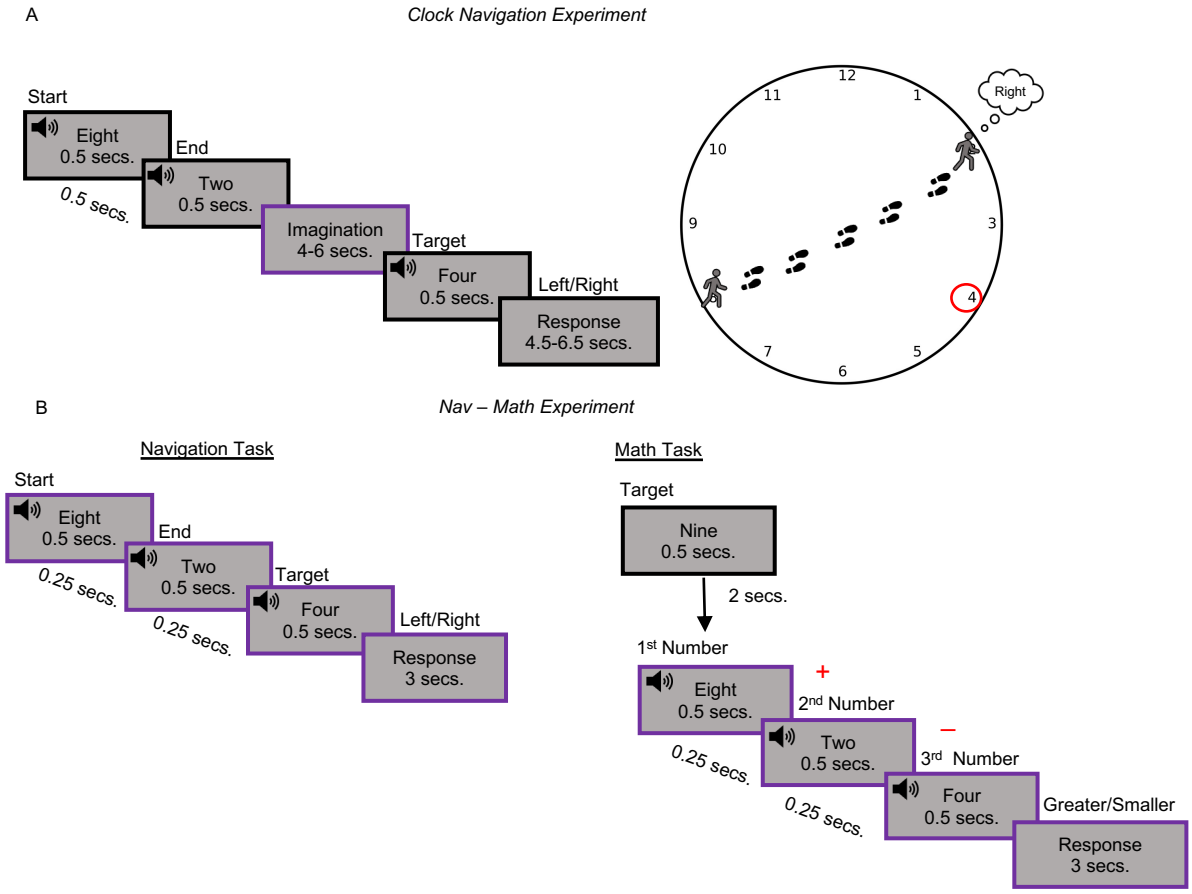


**Fig. 1. Clock-Navigation and Nav-Math experimental timelines**

(A) Timeline of the Clock-Navigation experiment: participants were asked to imagine navigating from one number (Starting point) to another (Ending point) in the clock space, according to auditory instructions. Successful trials were denoted as those in which participants correctly indicated the position (left or right) of a third number (Target number) in the space, compared to their current trajectory, as shown in the graphical representation on the right. The purple box indicates the event of interest for the Quadrature Filter analysis.

(B) Timeline of the Nav-Math experiment: the navigation task structure (left) was similar to that of the Clock Navigation experiment, with timing being the only difference. During the Math task (right), participants heard a number at the beginning of each math block (Target number) and then three more numbers. Participants were asked to sum the first two numbers, subtract the third number from that result,

and then to compare the results with the target number. Importantly, the navigation and mathematic tasks used the exact same numerical stimuli (see Fig. 1B) with different instructions. Purple boxes indicate the periods used for the univariate analysis (participant reaction times were used to determine the duration of the response period).

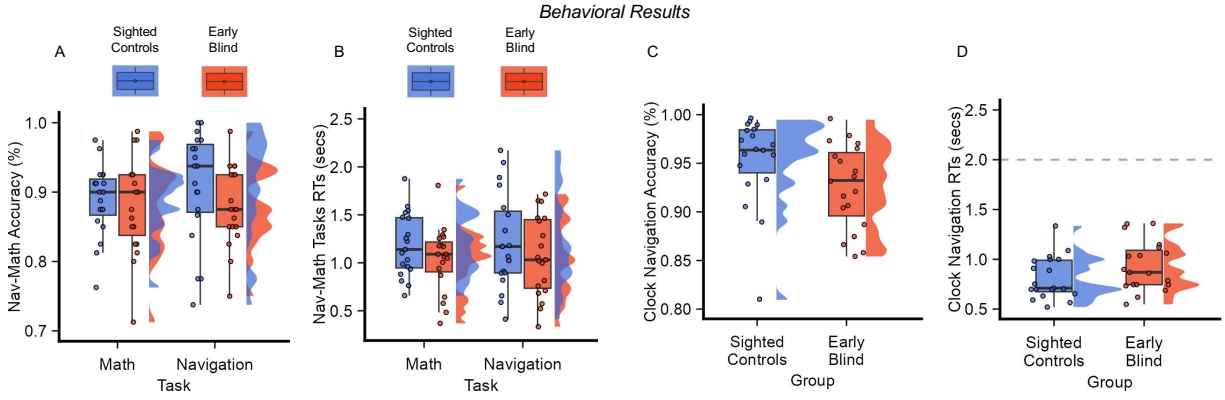


**Fig. 2. Blind and sighted individuals successfully navigated the clock space.**
(A) – (C) Accuracy of the two groups in the Nav-Math (A) and the Clock Navigation (C) experiments. Successful trials were counted as those in which participants correctly responded to the control question (Left/Right or Greater/Smaller). No difference in performance was detected between the two groups in the Clock-Navigation experiment (Two-sample t-test; n = 38, p = 0.052, two-tailed), nor between groups and tasks in the Nav-Math experiment (Repeated-measure ANOVA; n = 38, p = 0.24, two-tailed).
(B) – (D) Reaction Times (RTs) of the two groups (sighted controls in blue and early blind individuals in red). In the Nav-Math experiment, participants were asked to give a response as quickly as possible. No differences were found between groups and tasks (Linear Mixed Effect Model; n = 38, p = 0.61, two-tailed). In the Clock-Navigation experiment all participants answered before the time limit (grey dotted line), with no difference between groups (Linear Mixed Effect Model; n = 38, p = 0.11, two-tailed).
Boxes indicate the interquartile Range (IQR, datapoints included between the first quartile, 25$^{th}$ percentile and the third quartile, 75$^{th}$ percentile), the horizontal black line indicates the median (50$^{th}$ percentile), and the whiskers the distance between the first and third quartile to highest and the lowest value in the sample. The distribution of the data is represented by a density curve beside each box. Significance levels are defined as follow: * $p < 0.05$; ** $p < 0.01$; *** $p < 0.001$. Source data are provided as a Source Data file.

Despite this slight difference in navigation accuracy, it is important to consider that the average accuracy was very high in both groups (19 sighted controls, accuracy % = 95; 19 early blind individuals, accuracy % = 92), therefore we could conclude that both sighted and blind participants were able to successfully navigate the clock environment during the Clock-Navigation experiment.

The human navigation network is resilient to early visual deprivation

We analysed fMRI data from the Nav-Math experiment to investigate whether early blind individuals and sighted controls rely on the same brain network typically involved in navigation (HNN). A brain mask, downloaded from Neurosynth, comprising brain regions in the HNN (Fig. S1, see Methods) was used to detect regions with a greater level of activation during navigation compared to mathematics. The mask included (bilaterally) the middle frontal gyrus (MFG), superior parietal lobe/precuneus (SPL), retrosplenial cortex (RSC), occipital place area (OPA), parahippocampal place area (PPA) and hippocampus (HC).

The univariate contrast (i.e., Navigation > Math) revealed significant activity in all the ROIs, except for the hippocampus, in both sighted and blind people (Fig. 3A-B and Table S1, all results thresholded at $p_{FDR} < 0.05$). No significant cluster of activation emerged when we contrasted the two groups ([Navigation > Math] × [early blind vs. sighted controls]). Highly similar results emerged from unmasked whole-brain analysis (Fig. S2). Given that previous studies have found significant differences between sighted controls and early blind people during navigation tasks using univariate contrasts[31,32], we performed a whole-brain analysis to investigate whether some differences emerged across groups in regions that were not included in our HNN mask. This analysis did not reveal any significant difference between groups when correcting for multiple comparisons ($p_{FDR}< 0.05$). Since previous studies reported that blind individuals tend to rely more on egocentric coding of space compared to sighted individuals[27,28,30], we conducted a Small Volume Correction (SVC) analysis within the inferior parietal cortex (IPC), a region that has been implicated in the egocentric coding of spatial and non-spatial information[42,43]. We used a spherical ROI (Radius = 10mm) centred on Montreal Neurological Institute (MNI) peak coordinates (36/-68/44) obtained from an independent study investigating egocentric spatial representations during imagined navigation in a circular environment, structurally similar to our clock[44]. The analysis revealed a significant difference during imagined navigation between sighted controls and early blind individuals within the inferior parietal cortex ([Navigation > Math] × [early blind > sighted controls]; SVC: Voxel level $p < 0.001$, Cluster-level $p_{FWE} < 0.05$; see Methods and Fig. S3). Supporting the SVC analysis, whole-brain results using a lenient threshold ($p < 0.005$ uncorrected) revealed the emergence of a cluster of activation in the right inferior parietal cortex (IPC, 39/-61/53, Fig. 3C), overlapping with our ROI. We then used this inferior parietal cluster as an

independently localized ROI for analysis in the Clock-Navigation experiment to test for possible parietal-based compensation during navigation in the early blind group.

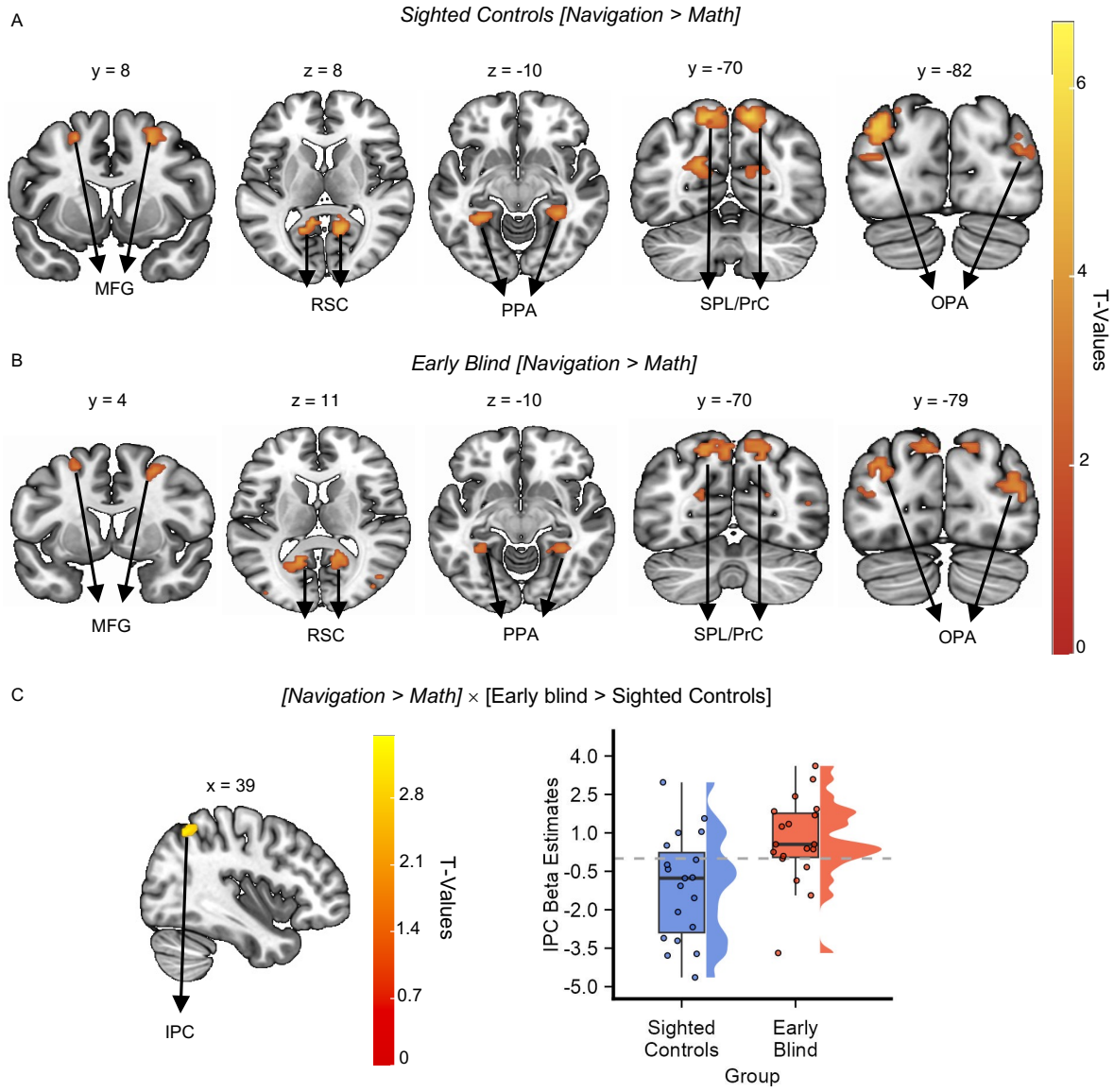


**Fig. 3. The human navigation network is resilient to early visual deprivation.**
(A) – (B) Results of the univariate analysis [Navigation > Math] performed within each group on the Nav-Math experiment data: the results showed activation in both sighted controls (A, n = 19) and early blind (B, n = 19) participants in the HNN mask (the activations were thresholded at $p_{FDR} < 0.05$ and overlapped with the MNI-152 T1 template). Middle frontal gyrus (MFG), superior parietal lobe/precuneus (SPL), retrosplenial cortex (RSC), occipital place area (OPA), parahippocampal place area (PPA).
(C) Whole-brain (left), group-level univariate analysis ([Navigation > Math] × [early blind > sighted controls]) on unmasked data revealed higher activation in the inferior parietal cortex in early blind individuals compared to sighted controls individuals when observed using a lenient threshold (IPC, 39/-61/53, Two sample t-test, n = 38, p < 0.005 uncorrected, activation overlapped with the MNI-152 T1

template). Right: beta estimates extracted within the IPC cluster (Navigation > Math) for each group (for display only) show that the parietal cortex was more involved in the navigation task in the early blind group. Source data are provided as a Source Data file.The boxes indicate the IQR (datapoints included between the first quartile, 25$^{th}$ percentile and the third quartile, 75$^{th}$ percentile), the horizontal black line the median (50$^{th}$ percentile), and the whiskers the distance between the first and third quartile to highest and the lowest value in the sample. The distribution of the data is represented by a density curve beside each box.

Six-fold grid-like coding did not emerge in early blind individuals

Next, we investigated the stability of grid-like coding in the EC of both groups by analyzing the data from the Clock-Navigation Experiment. In fMRI, grid-like coding can be detected as a 60° sinusoidal modulation of the Blood-Oxygen-Level-Dependent (BOLD) signal (6-fold symmetry, 4A-4B), elicited by spatial trajectories aligned with the main axis of the hexagonal grid[36]. We thus applied a four-way cross-validation procedure and implemented quadrature filter analysis in which three partitions (six runs) of the data were used to estimate the subject-specific grid orientation (phase, $\phi$), and the remaining partition (two runs) was used to test the strength of the 60° sinusoidal modulation of the BOLD signal in EC after realigning the trajectories' angles to each participant's specific grid orientation[36,37] (see Methods). Considering the lack of an a priori hypothesis on grid-coding lateralization, we first combined all sighted controls' bilateral ECs into a single ROI, thus estimating a common grid orientation for the left and the right EC[37]. No significant 60° sinusoidal modulation (6-fold symmetry) of the BOLD signal was found in the sighted bilateral EC (One sample t- test; $t(18) = 1.07$, $p = 0.30$, Cohen's $d = 0.24$, 95% CI = [-0.06, 0.2], $\alpha = 0.05$, two-tailed). We then analyzed the two hemispheres separately and found a significant signature of grid-like coding in the sighted controls' left EC (Bonferroni-corrected for multiple comparisons across left, right and bilateral hemispheres; one-sample t-test; $t(18) = 2.71$, $p = 0.007$, Cohen's $d = 0.62$, 95 %CI = [0.05, Inf], one-tailed, $\alpha_{Bonferroni} = 0.016$; Fig. 4C-4D) but not in the right EC (Bonferroni-corrected for multiple comparisons across left, right and bilateral hemispheres; one-sample t-test; $t(18) = -0.04$, $p = 0.5$, Cohen's $d = 0.009$, 95% CI = [-0.15, Inf], one-tailed, $\alpha_{Bonferroni} = 0.016$; Fig. 4C-4D). Interestingly, the left lateralization of the grid-like signal was also reported in the two previous studies on imagined navigation[40,41]. Equal analyses performed on alternative models in the left EC (4-,5-,7-, and 8-fold symmetry) confirmed the specificity of our 6-fold symmetry results (Bonferroni-corrected across left, right and bilateral hemispheres; one-sample t-test; 4-fold: t(18)

= - 1.58, p =0.93, Cohen's d = 0.36, 95% CI = [-0.25, Inf]; 5-fold: t(18) = 0.35, p = 0.37, Cohen's d = 0.08, 95% CI = [-0.18, Inf]; 7-fold: t(18) = 1.38, p = 0.09, Cohen's d = 0.31, 95% CI = [-0.02, Inf], and 8-fold: t(18) = -0.73, p = 0.76 Cohen's d = 0.17, 95% CI = [-0.22, Inf],all results one-tailed, $\alpha_{Bonferroni} = 0.016$; Fig. 4C). Moreover, we did not detect any significant modulation of the BOLD signal when alternative models were tested in the right EC (Bonferroni-corrected across left, right and bilateral hemispheres; 4-fold: t(18) = - 0.86, p = 0.8, Cohen's d = 0.20, 95% CI = [-0.2, Inf]; 5-fold: t(18) = 1.23, p = 0.11, Cohen's d = 0.28, 95%CI = [-0.06, Inf]; 7-fold: t(18) = 1.56, p= 0.07, Cohen's d = 0.35, 95%CI = [-0.05, 0.36], and 8-fold: t(18) = -0.54, p = 0.7, Cohen's d = 0.12, 95%CI = [-0.23, Inf],all results one-tailed, $\alpha_{Bonferroni} = 0.016$). The same analysis was conducted on the early blind population. Accounting for the non-normal distribution of 6-fold symmetry beta estimates in this group (Shapiro-Wilk normality test; Bilateral EC: W = 0.87, p = 0.01; Left EC: W = 0.89, p = 0.03 and Right EC: W = 0.81, p = 0.001, see Methods), we performed a Wilcoxon signed-ranked test (For completeness, if we apply the Wilcoxon test to the sighted controls data mentioned in the previous paragraph, results did not change: Bonferroni-corrected for multiple comparison across left, right and bilateral hemispheres; Left EC: V = 154, z = -2.35, p = 0.0078, r = 0.54, 95%CI = [-0.04, Inf]; Right EC: V = 95, z = 0, p = 0.5, r = 0, 95%CI = [-0.15, Inf],all results one-tailed, $\alpha_{Bonferroni} = 0.016$). We did not find a significant 6-fold symmetry in the early blind participants, neither when considering the bilateral EC ROI (V= 77, z = -0.7 p = 0.76, r = 0.16, 95% CI = [-0.39, Inf], one-tailed, $\alpha = 0.05$) nor the hemispheres separately (Left EC: V= 86, z = 0.34; p = 0.64, r = 0.08, 95% CI = [-0.47, Inf], and Right EC: V= 104, z = -0.34; p = 0.37, r = 0.08, 95% CI = [-0.27, Inf], all results one-tailed, $\alpha = 0.05$, Fig. 4E). Notwithstanding the inconsistent pattern of results found in the two groups, grid-like representation in the early blind individuals' left EC was not significantly lower than the one expressed by sighted controls (Wilcoxon ranked-sum test W = 231, z = -1.06, p = 0.14, r = 0.24, 95%CI = [-0.14, 0.72], two-tailed, $\alpha = 0.05$; Fig. 4F). This non-significant result might be attributed to the higher individual differences observed within the early blind population (Standard deviation from the mean (SD); sighted controls = 0.21; early blind = 0.96; Levene's test for Homogeneity of variance between groups; F(1,36) = 11.69, p = 0.001, two-tailed, $\alpha = 0.05$). However, the lack of hexadirectional coding in early blind individuals was strengthened by Bayesian analysis showing no evidence of six-fold symmetry in this group (Left EC $BF_{10} = 0.23$; error % = 0.016; Right EC: $BF_{10} = 0.24$, error % = 0.016; Bilateral EC: $BF_{10} = 0.27$, error % = 0.017).

Accounting for the possible difference in clock-navigation accuracy between the two groups (see above), we had furthermore investigated whether the reduced grid-like activity in early blind participants' EC was attributable to this putative difference.

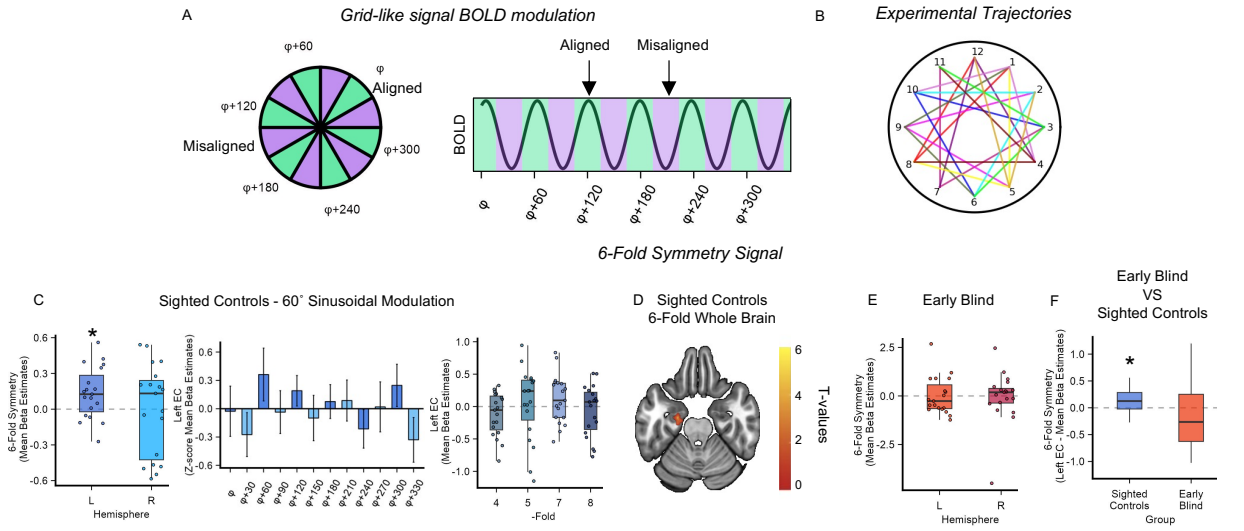


**Fig. 4. Six-fold grid-like coding do not emerge in early blind individuals' EC.**

(A) Left: grid cells fire more when the navigator moves in a direction aligned (green) with the preferred grid orientation (ϕ) and its 60˚ multiples, compared to misaligned directions (purple). Right: grid-like coding can be detected using fMRI as a 60˚ sinusoidal modulation of the BOLD signal (6-fold symmetry), as the conjunctive activation of grid cells produced a higher BOLD modulation for movements aligned rather than misaligned with the main grid orientation.

(B) Participants performed 24 trajectories in each run, sampling the space with a granularity of 15˚. Different colours represent different experimental trajectories, the same colours have been used to identify experimental trajectories with a common starting/ending point.

(C) Quadrature filter analysis revealed the presence of a significant 6-fold symmetry in the sighted controls' left EC (left, one-sample t-test; n = 19, p = 0.007, $\alpha_{Bonferroni} = 0.016$, one-tailed), noticeable also as a 60˚ sinusoidal modulation of the EC BOLD signal (Data are presented as mean value +/- SEM, for display only). No significant BOLD modulations were found in the tested alternative periodicities (right panel). Source data are provided as a Source Data file.

(D) Whole-brain, group-level analyses revealed a cluster of activation in the left EC of sighted participants for the periodicity of interest (60˚; the activation overlaps with the MNI-152 T1 template at an uncorrected threshold of $p < 0.01$ voxel-level, one-sample t-test), for display only.

(E) ). No 6-fold symmetry modulation was detected in the early blind individuals' EC (Wilcoxon signed-rank test; n = 19, Left EC: p = 0.37, and Right EC: p = 0.37, all results one-tailed, $\alpha = 0.05$). Source data are provided as a Source Data file.

(F) No differences between groups were observed (Wilcoxon test; n = 38, p = 0.14, r = 0.24, $\alpha = 0.05$, two-tailed). Source data are provided as a Source Data file.

In box-plots the boxes indicate the IQR (datapoints included between the first quartile, 25$^{th}$ percentile and the third quartile, 75$^{th}$ percentile), the horizontal black line the median (50$^{th}$ percentile), and the whiskers

the distance between the first and third quartile to highest and the lowest value in the sample. Significance levels are defined as follow: * $p < 0.05$; ** $p < 0.01$; *** $p < 0.001$.

We did not detect any significant correlation between accuracy during the Clock-Navigation experiment and the magnitude of 6-Fold symmetry estimates, not when combining the two groups ($r = -0.16$, $p = 0.32$, $r^2 = 0.02$, 95% CI = [-0.46, 0.16]) nor when we considered the two group separately (sighted controls: $r = -0.18$, $p = 0.44$, $r^2 = 0.03$, 95% CI = [-0.59, 0.29]; early blind: $r = -0.30$, $p = 0.2$, $r^2 = 0.09$, 95% CI = [-0.66, 0.17], Fig. S4). If something, the correlation between 6-fold symmetry estimates and accuracy in early blind individuals showed the opposite (negative) trend, letting us conclude that the reduction of grid-like coding in early blind individuals' EC could be unlikely explained by differences in accuracies between the groups.

In sum, a significant six-fold symmetry emerged in sighted controls (as predicted), but not in early blind individuals. Nevertheless, given the lack of a between-groups interaction, we can't conclude that the typical hexadirectional grid code is different across sighted controls and early blind people. However, it might be that the unstable six-fold symmetry in early blind participants' EC is related to an alteration of the typical hexadirectional geometry. We've tested this hypothesis in the following paragraph.

A different neural geometry in the blind individuals' entorhinal cortex

Given the absence of 6-fold symmetry in the EC, we tested whether early blind individuals showed a significant effect in one of the alternative control models. This analysis revealed the emergence of a significant 90° sinusoidal modulation of the BOLD signal (4-fold) in the early blind individuals' bilateral EC (Bonferroni-corrected across five tested periodicities, one-tailed, one-sample t-test; $t(18) = 2.77$, $p = 0.006$, Cohen's $d = 0.64$, 95% CI = [0.11, Inf], $\alpha_{Bonferroni} = 0.01$; Fig. 5A – 5B) and no other significant sinusoidal modulations (Bonferroni-corrected across five tested periodicities, one-tailed, one-sample t-test; 5-fold: $t(18) = 1.72$, $p = 0.05$, Cohen's $d = 0.40$, 95% CI = [-0.0009, Inf]; 7-fold: $t(18) = -1.95$, $p = 0.96$, Cohen's $d = 0.45$, 95%CI = [-0.64, Inf]; 8-fold: $t(18) = -0.89$, $p = 0.8$, Cohen's $d = 0.20$, 95% CI = [-0.5, Inf]. Wilcoxon signed-ranked test: 6-fold, $V = 77$, $z = -0.7$ $p = 0.76$, $r = 0.16$, 95% CI = [-0.39, Inf], one-tailed, $\alpha_{Bonferroni} = 0.01$; Fig. 5A). Crucially, the magnitude of 4-fold symmetry in the early blind group was significantly higher than

sighted controls group (Two-sample t-test; t(36) = -3.18, p = 0.003, Cohen's d = 1.03, two-tailed, $\alpha = 0.05$, 95% CI = [-0.69, -0.15]; Fig. 5C).

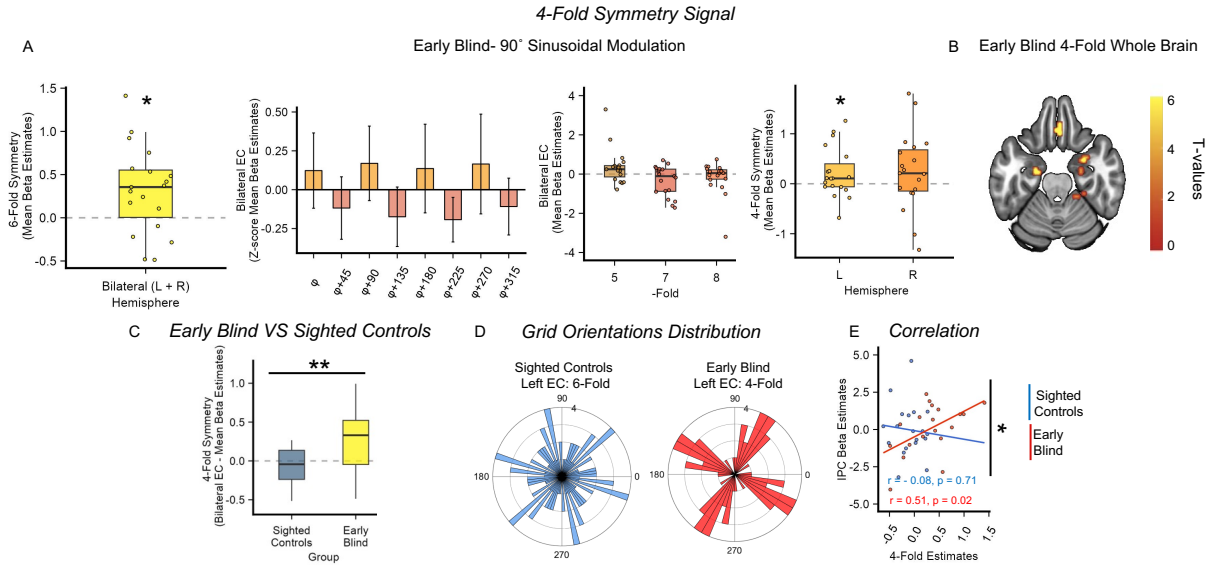


**Fig. 5. Early blind individuals and sighted showed different neural geometries in the entorhinal cortex.**

(A) Quadrature filter analysis performed on alternative periodicities revealed a significant 90˚ sinusoidal modulation of the BOLD signal (A, right) in early blind individuals' Bilateral EC (one-sample t-test; n = 19, p = 0.006, $\alpha_{Bonferroni} = 0.01$, one-tailed) which can be also visualized as a sinusoid with peaks at 90˚ and multiples (Data are presented as mean value +/- SEM, for display only). The effect is also present although weakened in individual hemispheres (right panel, one-sample t-test; n = 19, Left EC: p = 0.038; Right EC: p = 0.095, one-tailed, $\alpha = 0.05$). No other significant modulations of the BOLD signal were detected (middle panel). Source data are provided as a Source Data file.

(B) Whole-brain, group-level analyses revealed a cluster of activation in the bilateral EC of early blind participants for the periodicity of interest (90˚; The activation overlaps with the MNI-152 T1 template at an uncorrected threshold of $p < 0.01$, One-sample t-test), for display only.

(C) The 4-fold symmetry effect was significantly higher in early blind group compared to sighted control group (Two-sample t-test; n = 38, p = 0.003, $\alpha = 0.05$, two-tailed). Source data are provided as a Source Data file.

(D) Sighted control 6-fold symmetry left EC grid orientations were uniformly distributed in space (left, Rayleigh test; n = 19, p = 0.55, $\alpha_{Bonferroni} = 0.01$, two-tailed). Contrarily, the 4-fold symmetry grid orientations in the left EC of early blind individuals were significantly clustered (right, Rayleigh test; n = 19, p = 9.0831e-04, $\alpha_{Bonferroni} = 0.01$, two-tailed). Source data are provided as a Source Data file.

(E) Inferior Parietal Cortex (IPC) activity during navigation in the Clock navigation experiment significantly correlates with the magnitude of the 4-fold symmetry effect in early blind individuals, (n = 19, r = 0.51, p = 0.02, two-tailed), but not in sighted controls participants with a significant interaction between

the IPC activity and groups (n = 38, p = 0.02, two-tailed, left panel). Source data are provided as a Source Data file.

The 4-fold effect in early blind people was also present, although weakened, when we considered each hemisphere separately (One-sample t-test; Left EC: t(18)= 1.88, p = 0.038, Cohen's d = 0.43, 95% CI = [0.016, Inf]; Right EC: t(18)= 1.36, p = 0.095, Cohen's d = 0.31, 95% CI = [- 0.06, Inf], one-tailed, $\alpha = 0.05$, Fig. 5A).

We further investigated the emergence of the 4-fold symmetry in early blind individuals, based on related findings in the literature. Entorhinal 4-fold symmetry in humans has already been observed in two studies, in which sighted participants navigated a virtual reality environment[45,46]. Interestingly, the 4-fold symmetry has been reported to be accompanied by a clustering of the participants' preferred grid orientation along the major axes of the environment[45], suggesting an external anchoring of the entorhinal map. Thus, we tested whether a similar clustering was taking place for the blind individuals in our experiment, considering that in a circular environment, no clustering is expected[36,37]. First, we looked at the phase distribution in the left EC in sighted controls for 6-fold symmetry, and we indeed found that they were uniformly distributed (Bonferroni-corrected across left, right and bilateral hemispheres, Rayleigh test of Uniformity; p = 0.55, two-tailed, $\alpha_{Bonferroni} = 0.01$, Fig. 5D). However, the phases of the 4-fold symmetry in early blind individuals in the same hemisphere were significantly clustered (Bonferroni-corrected across left, right and bilateral hemispheres, Rayleigh test of Uniformity; $p < 0.001$, two-tailed, $\alpha_{Bonferroni} = 0.01$; Fig. 5D). Although this effect was not present in the right hemisphere, the highly significant clustering effect found in the left EC, consistent with the previous report of 4-fold deformation in humans[45], suggests that the emergence of this neural geometry can be related to anchoring behavior on the main axes of the environment.

The disruption of 6-fold symmetry in the EC has been recently related to the adoption of an egocentric perspective during navigation and the increased activity of inferior parietal areas[47]. Since blind individuals tend to adopt mostly egocentric perspectives during navigation, might the emergence of the 4-fold symmetry be related? We explored this possibility by extracting the beta estimates obtained during a univariate whole-brain analysis[48] (Navigation > Rest; see Methods), in the Clock-Navigation experiment, using the inferior parietal cortex cluster obtained during the analysis of the Nav-Math experiment (defined in the contrast ([Navigation > Math] × [early blind

> sighted controls], see above) as an independent ROI. A significant positive correlation emerged between 4-fold symmetry estimates and the activity in the IPC in early blind individuals (Pearson's product-moment correlation; $r = 0.51$, $p = 0.024$, $r^2 = 0.26$, 95% CI = [-0.08, 0.78], Fig. 5E). The same effect did not emerge in sighted controls ($r = -0.089$, $p = 0.71$, $r^2 = 0.007$, 95% CI = [-0.51, 0.38], Fig. 5E). Furthermore, we performed a linear regression analysis to investigate whether this effect was stronger in early blind individuals compared to sighted controls. Indeed, we detected a significant interaction between IPC activity and groups (t-value = -2.33, $p = 0.02$, $r^2 = 0.38$, 95% CI = [-0.31, -0.02], two-tailed, see Table S2) strengthening the hypothesis that the use of an egocentric perspective to navigate the environment influenced the neural geometry of entorhinal cognitive maps in early blind people.

Interestingly, the activity of IPC in early blind people also correlated with their accuracy during the Clock-Navigation experiment ($r = 0.46$, $p = 0.048$, $r^2 = 0.21$, 95% CI = [0.005, 0.75]; Partial Correlation 4-fold: $r = 0.53$, $p = 0.02$), whereas this correlation did not emerge in sighted controls ($r = -0.11$, $p = 0.65$, $r^2 = 0.012$, 95% CI = [-0.53, 0.36]). However, in this case the interaction between IPC activity and Group was only marginal (t-value = -1.8, $p = 0.08$, $r^2 = 0.21$, 95% CI = [0.07, 0.004], two-tailed).

In sum, we documented the emergence of a different neural geometry in early blind individuals' entorhinal cortex during imagined navigation. The grid code detected in early blind people had a periodicity of 90° (4-fold) and was absent in the sighted controls. The 4-fold effect, in blind people, was associated with clustering of the participants' preferred grid orientation along preferred axes of the clock environment and was correlated with univariate activity in the right inferior parietal cortex during navigation.

<u>Compared to the sighted, early blind individuals rely more on egocentric navigation strategies during everyday activities and performed worse during real world navigation.</u>

In order to assess their everyday navigation strategies and abilities, we administered to sighted and blind participants a self-report questionnaire[49]. The questionnaire allowed us to compute a general Navigation Confidence score as well as the relative use of Survey and Route strategies, associated

with Allocentric and Egocentric space representations, respectively[50–55]. The preference to rely more on one of the two strategies was assessed by computing the difference between Route and Survey scores (dRS); a positive value indicates participant preference for Route strategies (see Methods).

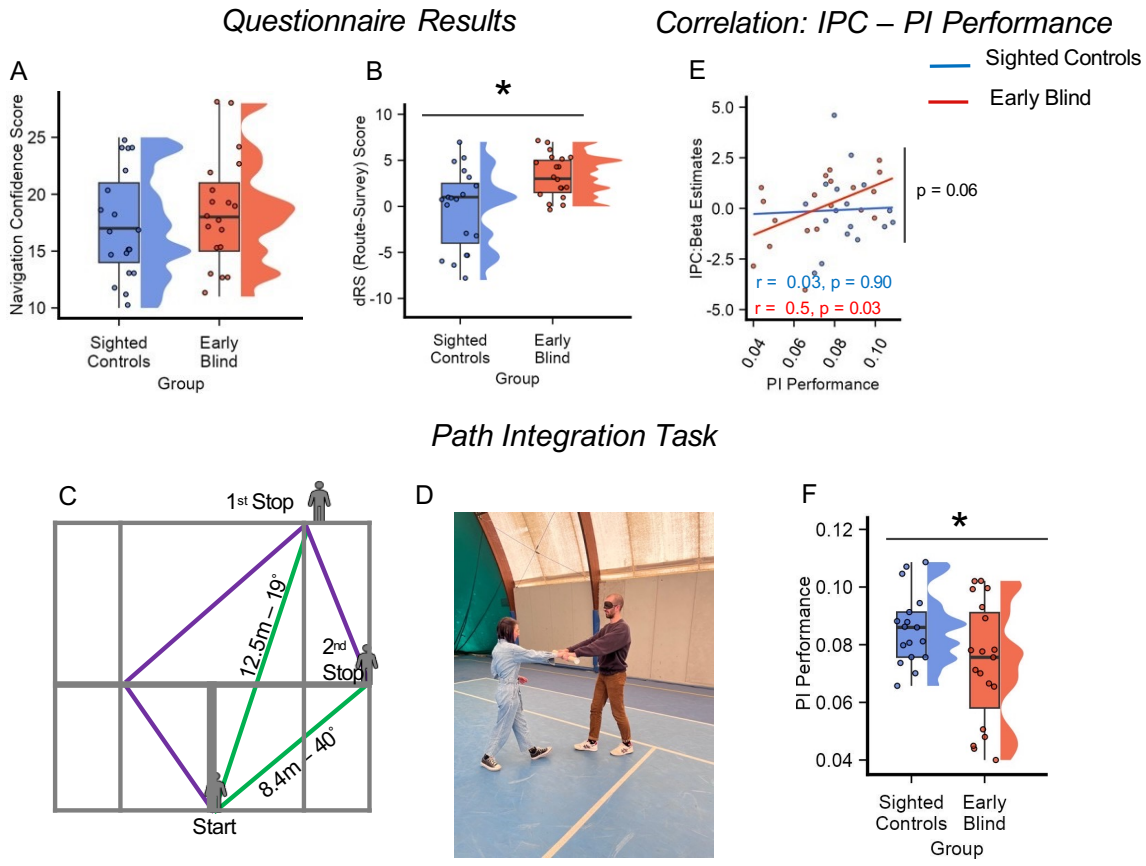


**Fig.6. Compared to sighted controls, early blind individuals relied more on egocentric navigation strategies during everyday life and performed worse in a path integration task.**

(A) – (B) Participants were asked to fill out a self-report questionnaire on their navigation abilities during everyday life. No differences between groups were detected concerning confidence in spatial navigation abilities (A). However, when differentiating between Route and Survey knowledge, we observed a significant difference between the two groups, with early blind participants reporting a greater reliance on Route strategies than sighted controls (B, Wilcoxon ranked-sum test; n = 36, W= 94, p = 0.01, two-tailed). Source data are provided as a Source Data file.

(C) Path integration task: Half of a tennis court (10m × 11m) was used to perform the experiment. The experimenter led the blindfolded participants through several paths (purple lines), created using tennis court lines as a reference. Each path contained two stopping points, at which participants were required to estimate the distance and orientation between their actual position and the starting position (green dashed lines).

(D) During the path integration experiment blindfolded participants were led by the experimenter through the different paths as shown in the picture.
(E) Inferior parietal cortex activity positively correlated with PI Performance in early blind participants (Pearson correlation; n = 19 r = 0.5, p = 0.03) but not sighted controls (Pearson Correlation; n = 17, r = 0.03, p = 0.90). Furthermore, linear regression analysis detected a marginally significant interaction between IPC activity and accuracy during PI experiment (n = 36, t-value = -1.95, p = 0.059, $r^2$ = 0.29 two-tailed). Source data are provided as a Source Data file.
(F) Sighted controls were overall more accurate, during real-world navigation, compared to early blind participants (Two-sample t-test; n = 36, t(34) = 2.10, p = 0.04, two-tailed). Source data are provided as a Source Data file.
In box-plots the boxes indicate the IQR(datapoints included between the first quartile, 25$^{th}$ percentile and the third quartile, 75$^{th}$ percentile), the horizontal black line the median (50$^{th}$ percentile), and the whiskers the distance between the first and third quartile to highest and the lowest value in the sample. The distribution of the data is represented by a density curve beside each box. Significance levels are defined as follow: * p < 0.05; ** p < 0.01; *** p< 0.001.

No difference between the two groups was detected in the expressed confidence in their spatial navigation abilities (Two-sample t-test; Navigation Confidence score: t(36) = -0.77, p = 0.44, Cohens'd = 0.25, 95% CI = [-4.36, 1.94], two-tailed; Fig. 6A).

However, when considering the dRS, a significant difference emerged between the two groups (Wilcoxon ranked-sum test: W = 94, z = -2.27, p = 0.01, r = 0.41, 95% CI = [-6, -1], two-tailed; Fig. 6B), indicating early blind people preference for Egocentric strategies during everyday navigation.

As a final step, we conducted a behavioral path integration (PI, Fig. 6C-D) experiment to investigate whether the stronger reliance on egocentric frame of reference of early blind individuals could influence their accuracy in constructing mental representation of the environments in which they are situated. Path integration, defined as the ability to rely on idiothetic cues to update one's current position in the environment in relation to the previously computed position[56,57], has been reported to be a sensitive hippocampal-entorhinal based test for allocentric spatial memories[58,59]. We thus performed a Path Integration experiment on the same participants who performed the MRI task. Participants (Blindfolded; 17 sighted controls and 19 early blind individuals) walked along 16 different linear paths with the help of an experimenter (see Fig S5 and Table S3). Each path contained two stopping points, at which participants were asked to estimate the distance and the orientation between their actual position and the starting point (Fig. 6C). PI performance was calculated for each participant by combining their accuracy in estimating

distances and orientations (see Methods). Our results showed that, relative to sighted controls, early blind individuals' PI performance was significantly lower (17 sighted controls & 19 early blind; Two-sample t-test; $t(34) = 2.10$, $p = 0.04$, Cohens'd = 0.70, 95% CI = [-0.0004,0.024], two-tailed, Fig. 6F).

Right inferior parietal cortex activity has recently been associated with the accuracy with which people encode spatial information, especially when environmental settings or experimental tasks enhance the use of egocentric spatial representations[46,47]. In line with this evidence, in the Clock-Navigation experiment, we observed a positive correlation in early blind individuals between right IPC activity and the accuracy during imagined navigation (see above). Would IPC activation level also correlate with navigation accuracy in the real world? To answer this, we correlated the beta estimates extracted in the right IPC in the Clock-Navigation experiment with accuracy in the PI experiment. We found a positive correlation between IPC activity and accuracy during the PI task in early blind participants ($r = 0.50$, $p = 0.028$, $r^2 = 0.25$, 95% CI = [0.064, 0.78]; Fig. 6E), which was largely preserved when we controlled for 6-fold symmetry estimates (partial correlation: $r = 0.48$, $p = 0.041$) and 4-fold symmetry estimates (partial correlation: $r = 0.45$, $p = 0.05$). By contrast, no significant correlation was observed in sighted controls between IPC activity and real-world navigation performance (17 sighted controls, $r = 0.031$, $p = 0.91$, $r^2 < 0.001$, 95% CI = [-0.46, 0.50]; Fig. 6E). Comparing the two groups with linear regression analysis we found a marginally significant IPC-activity by Group interaction (17 sighted controls & 19 early blind individuals, t-value = -1.95, $p = 0.059$, $r^2 = 0.29$ two-tailed, 95% CI = [-0.02, 0.0005], Fig. 6E).

Although correlations performed with a limited number of subjects should be taken with caution, these results may be considered as preliminary evidence that an increased activity in inferior parietal cortex, in early blind people, is associated with increased navigation performances both in imagined and real-life navigation. Additional correlation analysis between PI performance and the strength of 4-fold and 6-fold symmetry in both groups did not reveal significant results (all p-values > 0.33), except for a negative correlation between 6-fold symmetry and PI performance in early blind individuals that was, however, clearly driven by outliers and therefore not interpreted (19 early blind individuals; $r = -0.5$, $p = 0.03$, $r^2 = 0.25$, see supplementary materials and Fig. S6).

## Discussion

We investigated the influence of early visual deprivation on the development of the human navigation network (HNN) as well as the development of grid-like coding in the hippocampal-entorhinal system. Here, we discuss the two main findings.

First, the HNN was reliably and selectively activated in both sighted controls and early blind individuals during imagined navigation. Results of the Nav-Math experiment indicate that both groups have greater activation during navigation compared to a mathematics task in the MFG, PPA, SPL/Precu, and OPA. We did not find navigation-specific activity in the hippocampus, in either sighted controls or early blind participants. This, however, can be explained by the familiarity of both groups with the clock environment, which would not have demanded a strong reliance on episodic memory to retrieve its spatial configuration[60]. Indeed, several studies have shown that hippocampal activity decreases during the exploration or recall of a familiar environment, compared to novel ones[61,62].

Two previous studies have tested sighted controls and early blind people performing spatial navigation during fMRI using a sensory substitution device based on tongue stimulation[31] or the haptic navigation of a 3D maze[32]. In both cases, early blind people activated part of the HNN consisting of PPA, MFG, and SPL/Precu. Activity in the parahippocampal regions was stronger in early blind individuals than in sighted controls, and in general, early blind individuals had higher occipital activations (lingual gyrus, cuneus, fusiform gyrus) than matched sighted controls. By contrast, we did not find any difference between groups in the HNN ROIs (including PPA), and occipital regions were not specifically active during navigation in either sighted controls or early blind participants (except for OPA). This discrepancy might be due to the fact that, in previous studies, the navigation task was contrasted either with resting periods[32] or scrambled tongue stimulation[31], which require lower degrees of cognitive control. Here, using a demanding matched-control task with the exact same stimuli (numbers) but requiring a different, non-spatial computation (mathematics), we did not find significantly greater activity in the ventral occipital cortex of early blind individuals. Crucially, when comparing navigation vs. rest, we could see that the occipital cortex was more active in the early blind group than in sighted controls (See Fig. S7), in line with previous reports[31,32]. Nevertheless, such activation cannot be interpreted as strictly navigation relevant. The only brain region that was differentially and specifically activated during

navigation between sighted and blind individuals was the right inferior parietal cortex (IPC), a region of interest known to be important for egocentric spatial representations[44].

This brings us to our second main finding: Early blindness restructured the geometry of entorhinal cognitive maps during the Clock-Navigation task. Our results show that, whereas 6-fold symmetry was detected in sighted controls' entorhinal cortex, replicating previous imagined navigation results[40,41], we did not detect a similar 60° modulation of the BOLD signal in early blind individuals' EC. On the contrary, we found the emergence of 90° sinusoidal modulation (4-fold) in early blind individuals' entorhinal cortex (indicative of a square grid), which was not detected in sighted controls. Although we can provide only a partial explanation for this phenomenon, we hypothesize that 4-fold symmetry derives from the extensive use of an egocentric perspective by blind people during navigation. Egocentric coding of the clock space would increase the reliance on the main axis of the clock, modulating the geometry of grid-cell firing fields and giving rise to a 4-fold symmetry.

The emergence of 4-fold symmetry in the human EC was recently reported in two fMRI studies[45,46] and was generally associated with an anchoring toward the cardinal axes of the environment (north-south; east-west). He and colleagues[45] tested participants in a virtual-reality task, in which they navigated either in an open field or in a hairpin maze. Reflecting the modulation of grid-cell firing fields when rodents navigate a similar maze[60], a 90° rotational symmetry aligned with the main axis of the maze emerged in humans during virtual maze navigation in fMRI[45]. We found a similar anchoring of the 4-fold entorhinal map of early blind participants, despite the absence of barriers in our clock environment (See Fig. 5D), although in our case, grid orientations clustered with a 30° shift from the clock axes that are canonically considered as the main reference (six-twelve and three-nine). In another experiment, Wagner and colleagues[46] found the emergence of 4-fold symmetry when sighted participants had to retrace the path of an avatar that they observed navigating in the previous trial. Similar to our clock experiment, the environment was circular and without barriers. The authors attributed 4-fold symmetry to the possibility that people adopted cardinal axes as a main reference system allowing to compare movement trajectories with these major axes[46]. Although the emergence of the entorhinal 4-fold symmetry could, in principle, be due to different mechanisms in these different experiments, a common factor could be the adoption of an egocentric reference frame during navigation enhanced by the impossibility to collect all the environmental information at a glance (due to the presence of barriers[45]) and by the replication of

previously seen movements from a first person perspective[46]. Interestingly, there is evidence that enhancing participants' self-perception and body awareness during navigation decreases the stability of 6-fold symmetry in the entorhinal cortex and increases activity in the right IPC[47], which, notably, is involved in egocentric spatial coding[42–44]. Moreover, in the experiment by Wagner and colleagues[46], the right IPC activity during the observation of the moving avatar predicted the accuracy during the subsequent path-retracing. Thus, it appears that right IPC activity is associated with both distorted entorhinal geometry and navigation accuracy in tasks that encourage egocentric spatial processing[46,47]. This state of affairs is in keeping with our analysis showing that right IPC activity correlates, in early blind individuals, with the strength of the 4-fold symmetry, and with preliminary evidence associating IPC activity with navigation accuracy in imagined and real-life navigation.

As it emerges from our surveys (Fig. 6B), early blind people relied more on an egocentric coordinate system during everyday navigation[28,30]. The reconstruction of the environment layout in blind people (who cannot perceive several locations at glance) is necessarily more diachronic and sequential than in sighted people[27]. This enhances the reliance on a first-person perspective and on route-based knowledge grounded in the simulation of successive turns[27,63], which can be easily labelled in memory as "left", "right", "front" and "back" turns, thus with a 90° periodicity. Moreover, it has been shown that egocentric coding increases the dependency on the main axes of the environment to establish item positions and moving directions, which are computed as an egocentric bearing from a given axis aligned with the "point of view" from which the environment is typically experienced[64–68]. The navigation strategy reported by most blind participants (see Table S4) – rotating the clock in order to have the starting/ending point in front of them – is indeed suggestive of a calculation of the direction of movement as a function of egocentric rotation (bearing) from the main sagittal axis (six-twelve) from which clocks are usually experienced. If the direction of movement is calculated by egocentric bearing from the main axes, this axis and the perpendicular one become crucial for orientation, which may re-shape grid-cell firing fields[69], giving rise to 90° rotational symmetry.

In this paper, we have shown that the human navigation network is largely resilient to early visual deprivation. Both early blind individuals and sighted people selectively activate the same set of regions during imagined navigation (compared to an arithmetic task), including occipital regions such as the OPA, usually considered to be highly visual[70–72]. However, we also showed different

neural geometries in the entorhinal cortex of sighted and early blind people, with the typical 6-fold symmetry emerging in sighted controls and 4-fold symmetry in early blind individuals. Notwithstanding that the exact mechanisms remain unknown, we report evidence suggesting a relationship between the emergence of 4-fold symmetry and the engagement of the parietal cortex during navigation, together with the anchoring of the entorhinal map to the main axes of the environment. It remains possible that our results could, in part, be related to the specifics of the imagined clock environment, and further studies using different types of environments, as well as auditory or tactile navigation[63] (in which navigation behaviour can be better controlled) are needed to fully understand the differences between sighted and early blind individuals during spatial navigation. However, with this study, we show how early blindness can modulate the neural geometry of entorhinal grid maps, possibly by encouraging an egocentric perspective during navigation, shedding light on the general mechanisms underlying the construction of cognitive maps in the entorhinal cortex and providing an initial insight on the consequences of early blindness on their development. Indeed, one still open and fascinating question is whether differences across sighted and blind people would emerge also during conceptual navigation in non-spatial domains[73–76] of knowledge, across complementary egocentric and allocentric reference frames[76-42] .

## Methods

### Subjects

Thirty-eight participants took part in the MRI experiments. Nineteen participants were early blind individuals (10 females; age: M = 37.37, SD = 6.13; two ambidextrous), and 19 participants constituted the sighted control group (10 females; age: M = 36.21, SD = 6.44; one left-handed). Early blind participants were matched overall by age and sex with sighted control participants, with no significant age difference between the two groups (Paired sample t-test; $t(18) = -1.63$, $p = 0.12$). Thirty-six participants took part in the path integration experiment (two sighted controls participants did not come back to complete the experiment: 19 early blind individuals &17 sighted controls, 8 females; age: M = 35.88, SD = 6.41; one left-handed). Nonetheless, no difference in age between the two groups was detected (Two sample t-test; $t(34) = -0.70$, $p = 0.48$). Early blind

participants were blind since birth or completely lost vision before age 5, reporting, at most, faint light perception and no visual memories. All participants speak Italian fluently, and none reported a history of neurological or psychiatric disorders. The limited sample size was mostly a consequence to the difficulty to find suitable subjects given the rarity of the condition and our strict inclusion criteria. Although this factor should be taken into consideration and future more statistically powerful studies are needed (see also the discussion section), our sample size is comparable to previous studies testing early blind population in spatial navigation and other tasks[31,32,77], as well as to studies testing grid-like coding in virtual/visual[37,78], imagined[40] and conceptual navigation[74]. Moreover, a previous power analysis on studies reporting Hexadirectional coding suggests that a sample size of 20 would have been enough to obtain a .90 power[74]. The ethical committee of the University of Trento approved this study; all participants signed informed consent prior to the experiment and were compensated for their participation. None of the participants was excluded due to excessive head motion (i.e., the maximum head motion of all runs was no more than 3mm in translation or 3˚ in rotation).

Supplementary table 5 shows the demographic information of the early blind.

Clock-Navigation Experiment Stimuli

Experimental paths were designed using AutoCAD (v2019), calculating the angle created by each line that connected each number on the clock, represented by the vertex of a dodecagon, to all the others. Repeated paths (e.g., from 9 to 12 and from 12 to 9), paths connecting two adjacent numbers (e.g., from 1 to 2), and those that traverse the centre of the space were discarded, resulting in a set of 36 unique paths. Twenty-four path combinations were chosen, ensuring that all the degrees ranging from 15˚ to 360˚, in steps of 15˚, were represented, and each number from 1 to 12 was used as starting or ending location an equal number of times (four times per number). We computed the length of each path as the difference between the starting and the target numbers (e.g., from 9 to 12: 9 – 12 = 3), resulting in three different path lengths: (i) Short (distance between numbers: 3); (ii) Medium (distance between numbers: 4) and (iii) Long (distance between numbers: 5) and balanced it within each run so as to have six short paths; six long paths and 12 medium paths.

Instructions were delivered auditorily to participants (48000 Hz, 32-bit, mono), and each number was recorded in both a feminine voice and a masculine voice using an online speech synthesizer (https://ttsfree.com/text-to-speech/italian). The average intensity of all the auditory words was thresholded and equalized at 60 dB using Praat 6.1.01 (http://www.fon.hum.uva.nl/praat/).

Clock-Navigation Experiment Procedure

Participants performed an imagined navigation task in the fMRI scanner. The task was designed similarly to a previous imagined spatial navigation paradigm[40,41]. Participants were asked to imagine themselves within a clock-like environment, with numbers positioned exactly as on a real clock, and to imagine walking from one number to another, according to instructions. Before the experiment began, we instructed participants to perform the shortest and straightest path possible to arrive at the end point, avoiding walking along the perimeter of the clock or stopping or turning in the centre. Participants did not receive any instruction concerning the size of the clock or the speed with which they should have had navigated through it, however, they were aware that the imagination period could last a maximum of four seconds. Each trial concluded with a question about the position of a target number in the space as compared to the participants' imagined position at that moment, as shown in Fig. 1A. Prior to the fMRI session, participants performed behavioral training (4 blocks, 96 trials) to familiarize themselves with the task.

The behavioral training was conducted until participants reached a performance equal to or greater than 80% for two blocks consecutively. The fMRI session consisted of 8 runs of 24 trials each (192 trials). In half of the runs, the chosen path combination (see above) was presented in the standard configuration (namely, “Forward” runs). For the other half, participants were guided in the opposite direction (“Backward” runs; e.g., Forward runs: from 8 to 2 – Reverse runs: from 2 to 8). Forward and backward runs were presented interleaved.

Participants heard two numbers (0.5s each, separated by 0.5s), recited by a female voice, that corresponded to the starting and ending points. After the ending point instruction, they were asked to begin imagining walking across the clock for a variable amount of time between 4 and 6 seconds, at the end of which, a third number (target) was recited (0.5 seconds) by a male voice. Participants were asked to decide whether the target number was situated to the left or the right in relation to the arrival position (4.5 – 6.5s). The press of a button with the right-hand middle finger indicated

the number position was on the left; with the right-hand index finger to indicate the number was situated on the right. Participants were trained to answer before a sound cue played 2 seconds after the end of the target number instruction. This condition was introduced to push participants to navigate the environment during the imagination time window, reducing the possibility that they start imagining only after having heard the target number. The experimental paths were arranged so that for two consecutive trials, the previous ending point corresponded to the next trial's starting point; when this condition was violated, participants heard a "jump" (In Italian, "salto", 0.5s) instruction, which indicated that the starting point of the new trial would be different from the ending point of the previous one. They were given 4 seconds after the jump instruction to reorient themselves according to the new starting position. The target numbers associated with each trial were pseudo-randomized across runs, while making sure that they were different from the numbers used as starting and ending positions and were not adjacent to the ending point. Moreover, the positions of the target numbers in space were counterbalanced within each run so that they appeared an equal number of times (12) on the left and on the right side of the space. Target numbers were also counterbalanced across runs in such a way that, for the same trajectory, in half of the runs, the target number was situated on the left and the other half of the runs on the right.

During the entire duration of the experiment, participants were blindfolded and received instruction through MRI-compatible earphones using Psychtoolbox 3.0.14 (http://psychtoolbox.org/). Answers were given using an MRI-compatible response box connected to the testing PC. Stimuli presentation in the behavioral training, as well as the fMRI experiment, were displayed using Matlab releases 2014b (Behavioral Training) and 2017b (fMRI).

Nav-Math Experiment Stimuli

Pairs of numbers (i.e., paths for the navigation blocks) were chosen to be identical between math and navigation tasks.

Only the order of presentation of each combination was shuffled across tasks and blocks. Twenty combinations were pseudo-randomly selected out of the 36 available (see above) to make sure that each path was presented only once and not repeated backward. Each number between 1 and 12 was presented at least once and a maximum of six times to avoid number oversampling. Space resolution was not taken into account in the construction of the navigation blocks, as it was not a

crucial feature for univariate analysis contrasting navigation and mathematics. Stimuli recording criteria were the same as those used for the main experiment (see above).

Nav-Math Experiment Procedure

During the Nav-Math experiment, participants were asked to complete a navigation task and a mathematic task. The navigation task was similar to the one in the Clock-Navigation experiment (see above). Participants heard three different numbers consecutively, referring to a starting point, an ending point, and a target number, respectively. Each number was played for 0.5 seconds, interleaved by 0.25 seconds of silence. Right after the third number was recited, participants had 3 seconds to decide whether the target number was on the left or on the right of the implied trajectory. Participants were required to answer as quickly and accurately as possible by pressing two keys using the index and middle fingers of the right hand.

At the beginning of the mathematic task, participants heard a target number (0.5s) for the entire block. Then, each trial in the block had the same structure as in the navigation task. In each trial, three numbers were played (0.5s each, separated by silence of 0.25s). Participants had to sum the first two numbers, subtract the third number from the sum, and then decide within 3 seconds whether the resulting absolute value was greater or smaller than the target number they had heard at the beginning of the block. Participants pressed buttons with their right-hand index finger if the result of the arithmetic operation was less than the target number and with their right-hand middle finger if it was greater. Left/Right and Greater/Smaller responses were counterbalanced within each block (10 times each condition). In both tasks, the first two numbers were recited in a feminine voice, whereas the third number was recited in a masighted controlsuline voice. The Nav-Math experiment consisted of 4 blocks (2 navigation blocks and 2 mathematic blocks) of 20 trials each, interleaved, and counterbalanced across participants. Prior to each block, instructions were played as to which task would be performed. There were 15 seconds of silence between blocks, allowing the BOLD signal to decay.

Blindfolded participants underwent two runs of the Nav-Math experiment (80 trials for each task). Before participating in the MRI session, all participants performed a brief behavioral training (2 blocks for each condition, 40 trials per condition) to be familiarized with the experimental design.

Audio stimuli were delivered with MRI-compatible headphones using Psychtoolbox 3.0.14 (http://psychtoolbox.org/), and button presses were recorded using an MRI-compatible response box. Behavioral training and the fMRI sessions were performed using Matlab releases 2014b (Behavioral) and 2017b (fMRI).

MRI data collection

Echo-planar images (EPI) were acquired with a 3T Siemens Prisma scanner using a 64-channel coil. Functional images were acquired with the following parameters: Field of View (FoV) = 200mm; Voxel Size = 3x3x3mm; Number of slices: 66; Time Repetition (TR) = 1000ms; Time Echo (TE) = 28ms; Multi-band acceleration (MB) factor = 6 and a flip angle of 59°. Signal loss in the medial temporal lobe region was addressed by tilting the slice of 15° compared to the anterior-posterior commissure line (ACPC, direction: anterior edge of the slice towards the check). Moreover, to avoid slice group interference, we made sure that the ratio between the number of slices and the MB factor was equal to an odd number[79] (66/6 = 11). Gradient-echo Field maps were acquired for distortion correction of the functional images using the following parameter: FoV = 200mm; Voxel Size = 3x3x3mm$^3$; TR: 768ms; TE = 4.92 and flip angle of 60°. These images were acquired by adding a fat band to avoid the presence of wrap-around artifacts in the images. In addition, a Multi-Echo MPRAGE (MEMPRAGE) sequence was used to acquire a T1-weighted structural image for each participant with the following parameters: FoV = 256mm; Voxel Size = 1x1x1 mm; TR = 2530 ms; TE1 = 1.69ms; TE2 = 3.55ms; TE3 = 5.41ms; TE4 = 7.27ms and a flip angle of 7°.

fMRI data pre-processing

Images underwent standard preprocessing procedures using Statistical Parametric Mapping (SPM12 https://www.fil.ion.ucl.ac.uk/spm/software/spm12/) in Matlab 2020a. Field maps were used to calculate the voxel displacement matrix to reduce distortion artifacts. Functional images were spatially realigned and corrected with the voxel displacement matrix using the 'Realign and Unwarp' tool in SPM. Structural images (T1) were realigned to the mean of functional images, and the functional images were normalized to the Montreal Neurological Institute (MNI) space using unified segmentation methods. Images were smoothed with a 6 mm full-width-at-half-

maximum (FWHM) spatial kernel. Whole-brain analyses were implemented on the smoothed images in the MNI space; ROI analyses in the EC were implemented on the unsmoothed images in the native space.

Nav-Math Experiment: Whole brain analysis

First, five conditions were modeled in the General Linear Models (GLMs) at the first level: navigation instructions, mathematic instructions, mathematic target number, navigation task, and mathematic task. The duration of the navigation and mathematic tasks was calculated from the onset of the first number until the participants' responses (Purple boxes, Fig. 1B-C). The produced boxcar functions were convolved with the hemodynamic response function (HRF). The six-rigid head motion parameters, computed during the spatial realignment in SPM, were included in the GLMs to control for head motions. Furthermore, slow drifts in the signal were removed using a high-pass filter at 1/256 Hz. Second, we performed a non-parametric permutation analysis using the SnPM toolbox for SPM (http://nisox.org/Software/SnPM13/). One-sample t-test (early blind individuals and sighted controls independently) or two-sample t-test (Sighted controls > early blind and early blind > sighted controls) were computed on each participant's beta maps obtained by contrasting the two tasks (Navigation > Math and Math > Navigation) and by contrasting each task with the resting state periods (Navigation > Rest and Math > Rest). An Explicit mask of the main brain areas involved in navigation processing was set in the model. The HNN ROI was obtained by searching for the term 'navigation' in Neurosynth (https://www.neurosynth.org/) which integrated brain activation from 77 studies (cluster of activation thresholded at $p_{FDR} < 0.01$). We ran 10000 permutations, and no variance smoothing was performed. A voxel-level FDR corrected $p = 0.05$ was set as the threshold for multiple comparisons. In addition, group-level analysis using the same data reported above was performed on unmasked images, allowing exploratory whole-brain analysis. Lastly, small volume correction (SVC) analysis was performed on beta maps resulting from the group and task contrast ([Navigation > Math] × [early blind > sighted controls]) to assess possible group difference in the parietal cortex with the voxel-level significant threshold at $p < 0.001$ and the cluster-level significant threshold at $p_{FWE} < 0.05$.

ROI Definition

Subject-specific entorhinal cortex in the left and right hemispheres were cytoarchitectural defined and converted from surface space to volume space using the 'mri_convert' function in Freesurfer (v7.1.1, https://surfer.nmr.mgh.harvard.edu/). The obtained masks were co-registered to the mean functional image to obtain the same spatial resolution (3x3x3 $m^3$). On average, sighted controls' left EC included 116 voxels and right EC 96 voxels, and early blind individuals' left EC included 106 voxels and right EC 93 voxels. Analyses were conducted both using individual hemisphere EC masks and bilateral EC masks combining both hemispheres[37].

Clock Navigation Experiment: Grid-like signal analyses

Four-way cross-validation has been applied to quadrature filter analysis previously used to detect grid-like coding in humans' EC during spatial navigation tasks[36,40,78]. The eight experimental runs were divided into 4 partitions of 2 runs each, combining a 'forward' and a 'backward' run (see above). For each iteration, three partitions (6 runs) were used in GLM-1 to estimate the preferred grid orientation, and the remaining partition (2 runs) was used in GLM-2 to test the strength of the grid-like representation in the EC. The process was iterated until each partition was used for GLM-1 (Estimate) three times and for GLM-2 (Test) once (4 iterations). Within each partition, trajectories' degrees were equally represented. In both GLMs, the signal was high-pass filtered at a threshold of 1/128 Hz to remove the slow drift, and the six-rigid head motion parameters computed during the spatial realignment in SPM were modeled as nuisance regressors. Both GLMs also included two regressors of no interest: the 'jump instruction' period and the period computed from the onset of the 'target number instruction' event until participants' responses.

More specifically, GLM-1 was first used to estimate the preferred grid orientation for each participant in their native space. Imagined navigation periods (purple box, Fig. 1A) were modulated by two parametric regressors: $cos(6\theta_t)$ and $sin(6\theta_t)$, where $\theta_t$ indicates the trajectory's angle at trial 't.' The factor '6' indicates that six-fold symmetry rotational periodicity was tested. Resulting beta maps, $\beta_1$ and $\beta_2$, were used to calculate each voxel's grid orientation as:

$$(1)\ \varphi = \left(\arctan\left[\frac{\beta_2}{\beta_1}\right]\right) / 6$$

Participants' preferred grid orientation was calculated as a weighted mean across all the voxels within the EC ROI. The weight of the mean reflected the amplitude of the voxel response calculated as follows:

$$(2)\ \sqrt{\beta_2^2 + \beta_1^2}$$

Second, the remaining partition was used in the GLM-2 to test the emergence of a 60°sinusoidal modulation of the BOLD by calculating the cosine of the trajectories' angle performed by participants realigned with their preferred grid orientation as in:

$$(3)\ \cos(6\ (\theta_t\text{-}\varphi))$$

The magnitude of grid-like representation in each participant was quantified by averaging the parametric regressors estimated in the GLM-2 across all the iterations. Finally, to better visualize the effect, we divided the trajectories' angles into 12 bins aligned with each participant's mean grid orientation (60° modulo 0) or misaligned (60° modulo 30) and averaged the corresponding regressors across participants (Fig. 4B middle). All the analyses were conducted on the periodicity of interest (6-fold) as well as on control models (4-, 5-, 7-, 8- Fold symmetries)

Finally, we modeled a group-level GLM to conduct an exploratory whole-brain analysis. One-sample t-test (independently for sighted controls and early blind individuals) was conducted on beta maps obtained in the GLM-2 to investigate which brain areas were sensible to 6-fold symmetry.

Path Integration Experiment procedure

The path Integration behavioral experiment was constructed following[78] experimental design. Differently from the classical path integration tasks, where participants were asked either to estimate the distance or orientation of a target point from a single location, this experimental design required participants to both estimate distance and orientation of a target point from two different locations in the space. The use of multiple locations enabled the collection of a greater amount of data points, which would provide a more accurate calculation of the PI errors. Moreover, distance and orientation measurements acquired from different points in space might reduce the biases in the estimations that could arise when participants need to provide a single answer at the end of the

walked path[78]. Here, we used half of a tennis field (10.97 × 11.88 m) to construct eight unique paths following the field's predefined lines (Fig. S3). In Each path, two stopping points were introduced with distances from the starting location ranging from 4m to 14m and angles from 37° to 122°.

Participants were blindfolded before the entrance into the experimental environment. They were provided with a compass attached to a string around their necks and a cardboard stick in their hands during navigation. Before the experiment started, they received verbal instructions about the task, and once they confirmed to have understood all the instructions, the experiment started. During the experiment, participants placed both hands on the stick. The experimenter stood in front of them, with a hand on the cardboard stick, and led them to walk along the path. Once reached the first stopping point, the experimenter asked participants to first estimate in meters and centimeters the Euclidean distance between their actual position and the starting point and then to point toward the direction of the starting position using the compass. The answers were transcribed by the experimenter. Participants completed eight paths, repeated twice (16 paths), and none of them reported to have recognized the repeated paths. At the start and the end of the experiment, participants completed two standardization paths used in the analyses to correct their distance estimations (see the 'Path Integration analyses' paragraph). They were asked to walk two straight paths of 5m and 10m and to guess the walking distance in meters. Moreover, at the end of the experiment, they were asked whether they had heard any external cues that helped them to orient in the space during the task, but this was not the case for any of the participants.

Supplementary table 2 reports the list of the performed paths with their associated measurements.

Path Integration analyses

As for the experimental design, analyses were conducted following[78]. Participants' distance estimations were corrected using the standardization paths data to reduce the biases in the computation of the error not directly ascribable to the participants' path integration ability but rather to their tendency to underestimate or overestimate distances in real life. First, the participants' answers obtained at the beginning and the end of the experiment in the

'standardization paths' were averaged for each specific distance, 5m and 10m. Subsequently, we calculated the correction factor ($C_f$) for both distances as follows:

$$(4)\ C_f = d_{standardize}/d_{response}$$

Where $d_{standardize}$ was the actual length of the path, and $d_{response}$ was the participants' answer. Second, the computed correction factors were multiplied by the participants' estimated distances during the task. Reported distances from 4m to 7.5m were corrected using the 5m $C_f$ , and those greater than 7.5m using the 10m $C_f$. Corrected distances ($d_{corrected}$) and orientations (Ori) estimations of each stopping point were combined to calculate the x and y coordinates of the presumed starting position:

$$(5)\ x_{presumedStart} = x_{stop} + d_{corrected} * \cos\cos(Ori)$$
$$y_{presumedStart} = y_{stop} + d_{corrected} * \sin(Ori)$$

Where $x_{real}$ and $y_{real}$ corresponded to the real coordinates of the starting position of each trial. In order to compute the path integration error of each stopping point, the Euclidean distance between the stopping point and the presumed starting point estimated at the previous stopping point was calculated (PI Error). For the first stopping point, the previous presumed starting position corresponded to the real starting position of the path. This procedure allowed us to calculate PI independently for each path segment, reducing the possible biases produced by a cumulative computation of it. Lastly, the calculated errors were averaged across stopping points and trials, and the performance was computed as follows:

$$(6)\ PI_{performance} = \frac{1}{PI_{error}}$$

Questionnaires

Participants were asked to fill out two questionnaires after the fMRI experiment: one self-made questionnaire investigating which strategies they were using to navigate within the clock environment (See supplementary table 4) and a self-report questionnaire aimed to investigate

participants' navigation strategies in their everyday life[49]. The scores from the QOS were obtained by summing the points of specific questions following the guidelines provided by the authors[49] (Navigation Confidence: question 3 + question 4+ question 5s+ question 10 + question 11 + question 13; Route knowledge: q5r + q6r; Survey knowledge: q5s + q6s + $q9_{sp}$ - $9_{verb}$). The dRS scores were computed by subtracting the Survey knowledge score from the Route knowledge score so that a positive value would indicate participants' tendency to rely on more egocentric strategies during their everyday life navigation, and negative values would have indicated the opposite.

Statistical analyses

Statistical analyses were conducted using SPM and SnPM in Matlab 2020a for whole brain analyses and R (v4.2.2) for ROI analyses. The distributions of the grid orientations (Fig. 3I) were assessed using the function in the CircStat toolbox in Matlab 2020a. Results of both the whole-brain and the ROI analysis were computed using one sample t-test to investigate single-group effects and a two-sample t-test to investigate the effect between groups. The Wilcoxon-Signed-Rank test was used if the data obtained from the ROI analyses were not normally distributed. The normal distribution of the estimated parameters was checked using the Shapiro-Wilk test.

We computed Pearson's product-moment correlations to assess the relationship between parietal cortex activity and fold symmetries or path integration performance. The correlations with brain activity in the EC were conducted using the 4-fold beta estimates in the bilateral EC of both sighted controls and early blind individuals, whereas the correlations with 6-fold symmetry were conducted on the left EC beta estimates for sighted controls and the bilateral EC beta estimates for the early blind individuals. The significance threshold was set at $\alpha < 0.05$ and the p-value computed two-tailed, unless specified. For each statistical test, effect sizes were computed using R (v4.2.2). The behavioural and the ROI results were represented using box-plot and raincloud plots, where the boxes indicate the interquartile Range (IQR), meaning the datapoints included between quartile 1 (Q1, lower quartile, 25$^{th}$ percentile) to quartile 3 (Q3, upper quartile, 75$^{th}$ percentile), the horizontal black line indicates the median of the values of the sample, and the whiskers indicate the distance between the upper and lower quartile to highest and the lowest value in the sample. Moreover, in raincloud plots, the distribution of the data is represented by a density curve beside each box. The sample size for all the analyses was of 19 participants in the sighted control group

and 19 participants in the early blind group unless differently specified. Asterisks upon the graphs represent significance level as follow: * $p < 0.05$; ** $p < 0.01$; *** $p < 0.001$.

Data availability: The neuroimaging and behavioral data generated in this study have been deposited in the Zenodo database under accession code https://doi.org/10.5281/zenodo.10794697[80]. Source data are provided with this paper and are available under accession code https://doi.org/10.5281/zenodo.10794697[80]. The raw and pre-processed neuroimaging data are protected and are not available due to data privacy laws, access can be obtained by forwarding a formal inquiry to the corresponding author (federica.sigismondi@unitn.it).

Code availability: The codes to generating the main figures and for the behavioural task have been deposited in the Zenodo database under accession code https://doi.org/10.5281/zenodo.10694439[80]

**References**


1. Tatler BW, Land MF. Vision and the representatio§n of the surroundings in spatial memory. *Philosophical Transactions of the Royal Society B: Biological Sciences*. Published online February 27, 2011. doi:10.1098/rstb.2010.0188

2. Piccardi L, De Luca M, Nori R, Palermo L, Iachini F, Guariglia C. Navigational Style Influences Eye Movement Pattern during Exploration and Learning of an Environmental Map. *Frontiers in Behavioral Neuroscience*. 2016;10. Accessed May 9, 2023. https://www.frontiersin.org/articles/10.3389/fnbeh.2016.00140

3. Matthis JS, Yates JL, Hayhoe MM. Gaze and the Control of Foot Placement When Walking in Natural Terrain. *Current Biology*. 2018;28(8):1224-1233.e5. doi:10.1016/j.cub.2018.03.008

4. Nau M, Julian JB, Doeller CF. How the Brain's Navigation System Shapes Our Visual Experience. *Trends in Cognitive Sciences*. 2018;22(9):810-825. doi:10.1016/J.TICS.2018.06.008

5. Bird CM, Burgess N. The hippocampus and memory: insights from spatial processing. *Nat Rev Neurosci*. 2008;9(3):182-194. doi:10.1038/nrn2335

6. Chersi F, Burgess N. The Cognitive Architecture of Spatial Navigation: Hippocampal and Striatal Contributions. *Neuron*. 2015;88(1):64-77. doi:10.1016/j.neuron.2015.09.021

7. Epstein RA, Patai EZ, Julian JB, Spiers HJ. The cognitive map in humans: spatial navigation and beyond. *Nat Neurosci*. 2017;20(11):1504-1513. doi:10.1038/nn.4656

8. Epstein RA. Parahippocampal and retrosplenial contributions to human spatial navigation. *Trends in Cognitive Sciences*. 2008;12(10):388-396. doi:10.1016/j.tics.2008.07.004

9. Julian JB, Keinath AT, Marchette SA, Epstein RA. The Neurocognitive Basis of Spatial Reorientation. *Current Biology*. 2018;28(17):R1059-R1073. doi:10.1016/j.cub.2018.04.057

10. Clark BJ, Simmons CM, Berkowitz LE, Wilber AA. The retrosplenial-parietal network and reference frame coordination for spatial navigation. *Behavioral Neuroscience*. 2018;132(5):416-429. doi:10.1037/bne0000260

11. Patai EZ, Spiers HJ. The Versatile Wayfinder: Prefrontal Contributions to Spatial Navigation. *Trends in Cognitive Sciences*. 2021;25(6):520-533. doi:10.1016/j.tics.2021.02.010

12. Tolman, E. C. (1948). Cognitive maps in rats and men. *Psychological review*, *55*(4), 189.

13. O'Keefe J, Dostrovsky J. The hippocampus as a spatial map. Preliminary evidence from unit activity in the freely-moving rat. *Brain Research*. 1971;34(1):171-175. doi:10.1016/0006-8993(71)90358-1

14. Taube JS, Muller RU, Ranck JB. Head-direction cells recorded from the postsubiculum in freely moving rats. I. Description and quantitative analysis. *J Neurosci*. 1990;10(2):420-435. doi:10.1523/JNEUROSCI.10-02-00420.1990

15. Hafting T, Fyhn M, Molden S, Moser MB, Moser EI. Microstructure of a spatial map in the entorhinal cortex. *Nature*. 2005;436(7052):801-806. doi:10.1038/nature03721

16. Thinus-Blanc, C., & Gaunet, F. (1997). Representation of space in blind persons: vision as a spatial sense?. *Psychological bulletin*, *121*(1), 20.

17. Pasqualotto A, Proulx MJ. The role of visual experience for the neural basis of spatial cognition. *Neuroscience and Biobehavioral Reviews*. 2012;36:1179-1187. doi:10.1016/j.neubiorev.2012.01.008

18. Schinazi VR, Thrash T, Chebat DR. Spatial navigation by congenitally blind individuals. *Wiley Interdisciplinary Reviews: Cognitive Science*. 2016;7(1):37-58. doi:10.1002/wcs.1375

19. Taube JS, Muller RU, Ranck JB. Head-direction cells recorded from the postsubiculum in freely moving rats. II. Effects of environmental manipulations. *J Neurosci*. 1990;10(2):436-447. doi:10.1523/JNEUROSCI.10-02-00436.1990

20. Fenton AA, Csizmadia G, Muller RU. Conjoint Control of Hippocampal Place Cell Firing by Two Visual Stimuli: I. the Effects of Moving the Stimuli on Firing Field Positions. *Journal of General Physiology*. 2000;116(2):191-210. doi:10.1085/jgp.116.2.191

21. Scaplen KM, Gulati AA, Heimer-McGinn VL, Burwell RD. Objects and landmarks: Hippocampal place cells respond differently to manipulations of visual cues depending on size, perspective, and experience. *Hippocampus*. 2014;24(11):1287-1299. doi:10.1002/hipo.22331

22. Pérez-Escobar, J. A., Kornienko, O., Latuske, P., Kohler, L., & Allen, K. (2016). Visual landmarks sharpen grid cell metric and confer context specificity to neurons of the medial entorhinal cortex. *Elife*, *5*, e16937.

23. Chen G, Manson D, Cacucci F, Wills TJ. Absence of Visual Input Results in the Disruption of Grid Cell Firing in the Mouse. *Current Biology*. 2016;26(17):2335-2342. doi:10.1016/j.cub.2016.06.043

24. Asumbisa K, Peyrache A, Trenholm S. Flexible cue anchoring strategies enable stable head direction coding in both sighted and blind animals. *Nat Commun*. 2022;13(1):1-15. doi:10.1038/s41467-022-33204-0

25. Save E, Cressant A, Thinus-Blanc C, Poucet B. Spatial Firing of Hippocampal Place Cells in Blind Rats. *J Neurosci*. 1998;18(5):1818-1826. doi:10.1523/JNEUROSCI.18-05-01818.1998

26. Ungar S. Cognitive mapping without visual experience. In: *Cognitive Mapping*. Routledge; 2000.

27. Ottink L, van Raalte B, Doeller CF, Van der Geest TM, Van Wezel RJA. Cognitive map formation through tactile map navigation in visually impaired and sighted persons. *Sci Rep*. 2022;12(1):11567. doi:10.1038/s41598-022-15858-4

28. Iachini T, Ruggiero G, Ruotolo F. Does blindness affect egocentric and allocentric frames of reference in small and large scale spaces? *Behavioural Brain Research*. 2014;273:73-81. doi:10.1016/j.bbr.2014.07.032

29. Gori M, Cappagli G, Baud-Bovy G, Finocchietti S. Shape Perception and Navigation in Blind Adults. *Frontiers in Psychology*. 2017;8. Accessed May 4, 2023. https://www.frontiersin.org/articles/10.3389/fpsyg.2017.00010

30. Noordzij ML, Zuidhoek S, Postma A. The influence of visual experience on the ability to form spatial mental models based on route and survey descriptions. *Cognition*. 2006;100(2):321-342. doi:10.1016/j.cognition.2005.05.006

31. Kupers R, Chebat DR, Madsen KH, Paulson OB, Ptito M. Neural correlates of virtual route recognition in congenital blindness. *Proceedings of the National Academy of Sciences of the United States of America*. 2010;107(28):12716-12721. doi:10.1073/pnas.1006199107

32. Gagnon L, Schneider FC, Siebner HR, Paulson OB, Kupers R, Ptito M. Activation of the hippocampal complex during tactile maze solving in congenitally blind subjects. *Neuropsychologia*. 2012;50(7):1663-1671. doi:10.1016/j.neuropsychologia.2012.03.022

33. Halko MA, Connors EC, Sánchez J, Merabet LB. Real world navigation independence in the early blind correlates with differential brain activity associated with virtual navigation. *Human Brain Mapping*. 2014;35(6):2768-2778. doi:10.1002/hbm.22365

34. Chebat DR, Chen JK, Schneider F, Ptito A, Kupers R, Ptito M. Alterations in right posterior hippocampus in early blind individuals. *NeuroReport*. 2007;18(4):329. doi:10.1097/WNR.0b013e32802b70f8

35. Fortin M, Voss P, Lord C, et al. Wayfinding in the blind: Larger hippocampal volume and supranormal spatial navigation. *Brain*. 2008;131(11):2995-3005. doi:10.1093/brain/awn250

36. Doeller CF, Barry C, Burgess N. Evidence for grid cells in a human memory network. *Nature*. 2010;463(7281):657-661. doi:10.1038/nature08704

37. Nau M, Navarro Schröder T, Bellmund JLS, Doeller CF. Hexadirectional coding of visual space in human entorhinal cortex. *Nat Neurosci*. 2018;21(2):188-190. doi:10.1038/s41593-017-0050-8

38. Julian JB, Keinath AT, Frazzetta G, Epstein RA. Human entorhinal cortex represents visual space using a boundary-anchored grid. *Nat Neurosci*. 2018;21(2):191-194. doi:10.1038/s41593-017-0049-1

39. Giari G, Vignali L, Xu Y, Bottini R. MEG frequency tagging reveals a grid-like code during attentional movements. *Cell Reports*. 2023;42(10):113209. doi:10.1016/j.celrep.2023.113209

40. Horner AJ, Bisby JA, Zotow E, Bush D, Burgess N. Grid-like Processing of Imagined Navigation. *Current Biology*. 2016;26(6):842-847. doi:10.1016/j.cub.2016.01.042

41. Bellmund JL, Deuker L, Navarro Schröder T, Doeller CF. Grid-cell representations in mental simulation. *eLife*. 2016;5:e17089. doi:10.7554/eLife.17089

42. Bottini R, Doeller CF. Knowledge Across Reference Frames: Cognitive Maps and Image Spaces. *Trends in Cognitive Sciences*. 2020;24(8):606-619. doi:10.1016/j.tics.2020.05.008

43. Parkinson C, Liu S, Wheatley T. A Common Cortical Metric for Spatial, Temporal, and Social Distance. *Journal of Neuroscience*. 2014;34(5):1979-1987. doi:10.1523/JNEUROSCI.2159-13.2014

44. Schindler A, Bartels A. Parietal Cortex Codes for Egocentric Space beyond the Field of View. *Current Biology*. 2013;23(2):177-182. doi:10.1016/j.cub.2012.11.060

45. He 2019. Environmental Barriers Disrupt Grid-like Representations in Humans during Navigation | Elsevier Enhanced Reader. doi:10.1016/j.cub.2019.06.072

46. Wagner IC, Graichen LP, Todorova B, et al. Entorhinal grid-like codes and time-locked network dynamics track others navigating through space. *Nat Commun*. 2023;14(1):231. doi:10.1038/s41467-023-35819-3

47. Moon HJ, Gauthier B, Park HD, Faivre N, Blanke O. Sense of self impacts spatial navigation and hexadirectional coding in human entorhinal cortex. *Commun Biol*. 2022;5(1):1-12. doi:10.1038/s42003-022-03361-5

48. Kunz L, Schroder TN, Lee H, et al. Reduced grid-cell-like representations in adults at genetic risk for Alzheimer's disease. *Science*. 2015;350(6259):430-433. doi:10.1126/science.aac8128

49. Francesca Pazzaglia, Cesare Cornoldi, Rossana De Beni. Differenze individuali nella rappresentazione dello spazio e nell'abilità di orientamento: presentazione di un questionario autovalutativo. *Giornale italiano di psicologia*. 2000;(3):627. doi:10.1421/310

50. Siegel AW, White SH. The Development of Spatial Representations of Large-Scale Environments. In: Reese HW, ed. *Advances in Child Development and Behavior*. Vol 10. JAI; 1975:9-55. doi:10.1016/S0065-2407(08)60007-5

51. Shelton AL, Gabrieli JDE. Neural Correlates of Individual Differences in Spatial Learning Strategies. *Neuropsychology*. 2004;18(3):442-449. doi:10.1037/0894-4105.18.3.442

52. Wolbers T, Weiller C, Büchel C. Neural foundations of emerging route knowledge in complex spatial environments. *Cognitive Brain Research*. 2004;21(3):401-411. doi:10.1016/j.cogbrainres.2004.06.013

53. Latini-Corazzini L, Nesa MP, Ceccaldi M, et al. Route and survey processing of topographical memory during navigation. *Psychological Research*. 2010;74(6):545-559. doi:10.1007/s00426-010-0276-5

54. Chrastil ER. Neural evidence supports a novel framework for spatial navigation. *Psychon Bull Rev*. 2013;20(2):208-227. doi:10.3758/s13423-012-0351-6

55. Zhang H, Zherdeva K, Ekstrom AD. Different "routes" to a cognitive map: dissociable forms of spatial knowledge derived from route and cartographic map learning. *Mem Cogn*. 2014;42(7):1106-1117. doi:10.3758/s13421-014-0418-x

56. Gallistel CR. *The Organization of Learning*. The MIT Press; 1990:viii, 648.

57. Whishaw IQ, Wallace DG. On the origins of autobiographical memory. *Behavioural Brain Research*. 2003;138(2):113-119. doi:10.1016/S0166-4328(02)00236-X

58. Hartley T, Bird CM, Chan D, et al. The hippocampus is required for short-term topographical memory in humans. *Hippocampus*. 2007;17(1):34-48. doi:10.1002/hipo.20240

59. Howett D, Castegnaro A, Krzywicka K, et al. Differentiation of mild cognitive impairment using an entorhinal cortex-based test of virtual reality navigation. *Brain*. 2019;142(6):1751-1766. doi:10.1093/brain/awz116

60. Eichenbaum H. The role of the hippocampus in navigation is memory. *Journal of Neurophysiology*. 2017;117(4):1785-1796. doi:10.1152/jn.00005.2017

61. Kaplan R, Horner AJ, Bandettini PA, Doeller CF, Burgess N. Human hippocampal processing of environmental novelty during spatial navigation. *Hippocampus*. 2014;24(7):740-750. doi:10.1002/hipo.22264

62. Cheng S, Frank LM. New Experiences Enhance Coordinated Neural Activity in the Hippocampus. *Neuron*. 2008;57(2):303-313. doi:10.1016/j.neuron.2007.11.035

63. Ottink L, Hoogendonk M, Doeller CF, Van der Geest TM, Van Wezel RJA. Cognitive map formation through haptic and visual exploration of tactile city-like maps. *Sci Rep*. 2021;11(1):15254. doi:10.1038/s41598-021-94778-1

64. Burgess N. Spatial memory: how egocentric and allocentric combine. *Trends in Cognitive Sciences*. 2006;10(12):551-557. doi:10.1016/j.tics.2006.10.005

65. Diwadkar VA, McNamara TP. Viewpoint Dependence in Scene Recognition. *Psychol Sci*. 1997;8(4):302-307. doi:10.1111/j.1467-9280.1997.tb00442.x

66. McNamara TP, Rump B, Werner S. Egocentric and geocentric frames of reference in memory of large-scale space. *Psychonomic Bulletin & Review*. 2003;10(3):589-595. doi:10.3758/BF03196519

67. Mou W, McNamara TP. Intrinsic frames of reference in spatial memory. *Journal of Experimental Psychology: Learning, Memory, and Cognition*. 2002;28(1):162-170. doi:10.1037/0278-7393.28.1.162

68. Shelton AL, Mcnamara TP. Multiple views of spatial memory. *Psychonomic Bulletin & Review*. 1997;4(1):102-106. doi:10.3758/BF03210780

69. Ginosar G, Aljadeff J, Las L, Derdikman D, Ulanovsky N. Are grid cells used for navigation? On local metrics, subjective spaces, and black holes. *Neuron*. Published online April 11, 2023. doi:10.1016/j.neuron.2023.03.027

70. Dilks DD, Julian JB, Paunov AM, Kanwisher N. The Occipital Place Area Is Causally and Selectively Involved in Scene Perception. *J Neurosci*. 2013;33(4):1331-1336. doi:10.1523/JNEUROSCI.4081-12.2013

71. Julian JB, Ryan J, Hamilton RH, Epstein RA. The Occipital Place Area Is Causally Involved in Representing Environmental Boundaries during Navigation. *Current Biology*. 2016;26(8):1104-1109. doi:10.1016/j.cub.2016.02.066

72. Kamps FS, Julian JB, Kubilius J, Kanwisher N, Dilks DD. The occipital place area represents the local elements of scenes. *NeuroImage*. 2016;132:417-424. doi:10.1016/j.neuroimage.2016.02.062

73. Bao X, Gjorgieva E, Shanahan LK, Howard JD, Kahnt T, Gottfried JA. Grid-like Neural Representations Support Olfactory Navigation of a Two-Dimensional Odor Space. *Neuron*. 2019;102(5):1066-1075.e5. doi:10.1016/j.neuron.2019.03.034

74. Park SA. Inferences on a multidimensional social hierarchy use a grid-like code. *Nature Neuroscience*. 2021;24:27.

75. Viganò S, Rubino V, Soccio AD, Buiatti M, Piazza M. Grid-like and distance codes for representing word meaning in the human brain. *NeuroImage*. 2021;232:117876. doi:10.1016/j.neuroimage.2021.117876

76. Viganò S, Bayramova R, Doeller CF, Bottini R. Mental search of concepts is supported by egocentric vector representations and restructured grid maps. *Nat Commun*. 2023;14(1):8132. doi:10.1038/s41467-023-43831-w

77. Kanjlia S, Lane C, Feigenson L, Bedny M. Visual cortex of congenitally blind individuals responds to symbolic number. *Journal of Vision*. 2015;15(12):194. doi:10.1167/15.12.194

78. Stangl M, Achtzehn J, Huber K, Dietrich C, Tempelmann C, Wolbers T. Compromised Grid-Cell-like Representations in Old Age as a Key Mechanism to Explain Age-Related Navigational Deficits. *Current Biology*. 2018;28(7):1108-1115.e6. doi:10.1016/j.cub.2018.02.038

79. Nau M. Functional imaging of the human medial temporal lobe. Published online 2020. doi:10.17605/OSF.IO/CQN4Z

80 Sigismondi, F. (2024). Altered Grid-like coding in Early Blind people - Datasets and Scripts [Data set]. Zenodo. https://doi.org/10.5281/zenodo.10694439

**Acknowledgments:**

This work was supported the by the European Research Council grant (ERC-StG NOAM - 804422 awarded to R.B.)
We are thankful to our blind and sighted participants for their collaboration. We are furthermore grateful to Jorge Jovicich, Nicola Pace, Stefano Tambalo, Manuela Orsini and Ilaria Mirandola for technical assistance in developing fMRI acquisition sequences. Finally, we thank all the members of the BottiniLab for the insightful discussion about this project.

**Author contribution:**

Conceptualization: F.S., Y.X., R.B., M.S
Methodology: F.S., Y.X, R.B,
Investigation: F.S., M.S, R.B.
Formal Analysis: F.S., Y.X, R.B.
Supervision: R.B
Writing – Original Draft: F.S., Y.X., R.B
Data Curation: F.S

**Competing interests:** Authors declare that they have no competing interests

**Supplementary materials:**

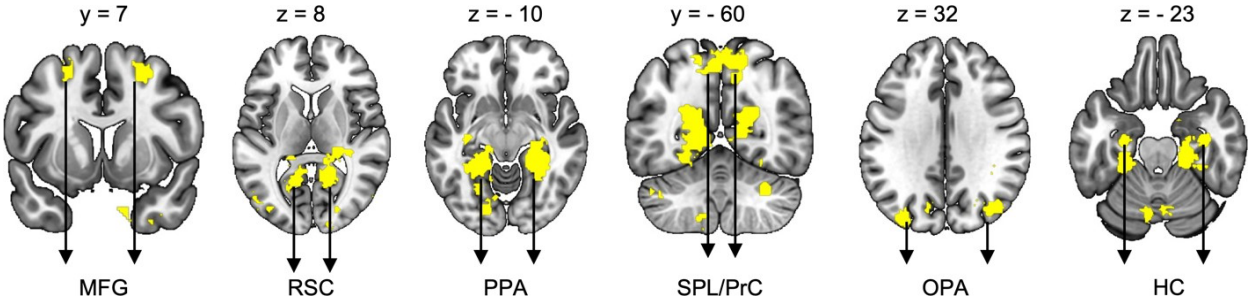


**Figure S1. The brain mask of the human navigation network**

The mask of the human navigation network consisted of (bilateral) medial frontal gyrus (MFG), retrosplenial cortex (RSC), parahippocampal place area (PPA), superior parietal lobe/precuneus (SPL/PrC), occipital place area (OPA), and hippocampus (HC). The mask was obtained from the term- based meta-analysis on *Neurosynth*[1] across 77 studies (pfdr < 0.01, the term was "navigation"). The mask is overlapped with the MNI-152 T1 template.

**Supplementary Table 1. Brain regions more active in the navigation task than in the math task (pFDR< 0.05)**

| Brain Regions | MNI Coordinates of the Peak Voxel | | | Peak T Value |
|---|---|---|---|---|
| | X | Y | Z | |
| **Sighted Controls** | | | | |
| Left Middle Frontal Gyrus | -21 | 8 | 53 | 4.5 |
| Right Middle Frontal Gyrus | 24 | 2 | 53 | 5.89 |
| Left Retrosplenial Cortex | -9 | -46 | 8 | 5.29 |
| Right Retrosplenial Cortex | 15 | -55 | 11 | 5.85 |
| Left Parahippocampal Place Area | -27 | -43 | -10 | 4.14 |
| Right Parahippocampal Place Area | 27 | -37 | -13 | 4.73 |
| Left Superior Parietal Lobe/Precuneus | -12 | -70 | 53 | 7.04 |
| Left Occipital Place Area | -33 | -82 | 32 | 5.47 |
| Right Occipital Place Area | 36 | -76 | 17 | 5.54 |
| **Early Blind Individuals** | | | | |
| Left Middle Frontal Gyrus | -21 | 4 | 56 | 3.03 |
| Right Middle Frontal Gyrus | 24 | 5 | 50 | 3.70 |
| Left Retrosplenial Cortex | -12 | -55 | 11 | 3.73 |
| Right Retrosplenial Cortex | 21 | -52 | 5 | 4.62 |
| Left Parahippocampal Place Area | -33 | -37 | -16 | 3.29 |
| Right Parahippocampal Place Area | 30 | -43 | -10 | 3.09 |
| Left Superior Parietal Lobe/Precuneus | -15 | -70 | 56 | 4.89 |
| Left Occipital Place Area | -33 | -85 | 20 | 4.04 |
| Right Occipital Place Area | 42 | -79 | 11 | 4.10 |

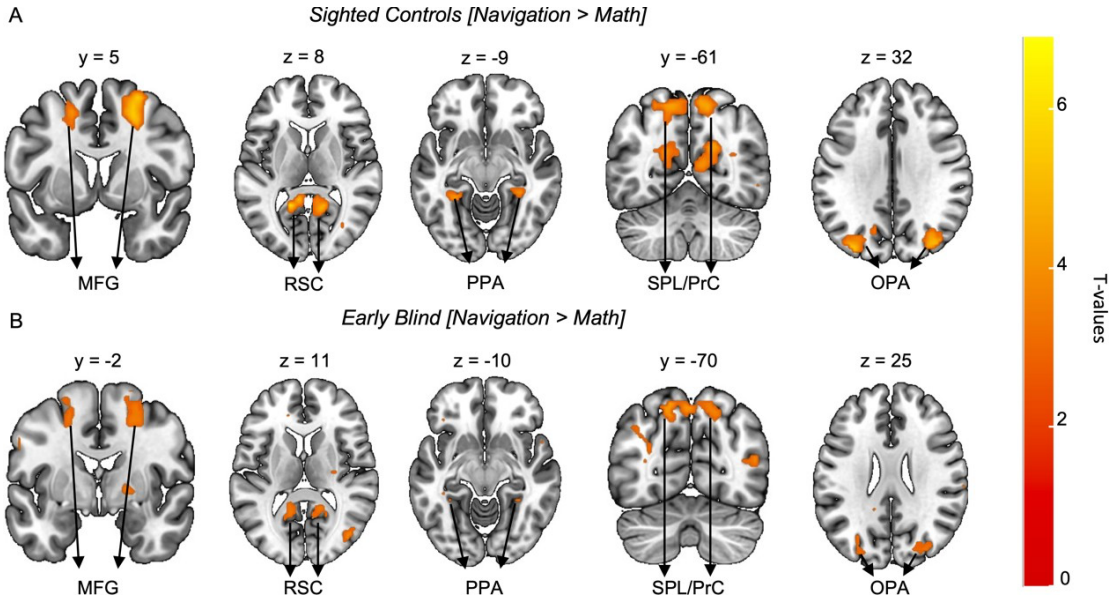


**Figure S2. Results of Navigation vs. Math contrast without the predefined mask**

Whole-brain results of the Nav-Math experiment demonstrated that both sighted controls (A, n = 19) and early blind individuals (B, n = 19) activated the same network of regions (i.e., the human navigation network) during the imagined navigation of the clock space (Navigation > Math). The activations were thresholded at $p < 0.01$ uncorrected and overlapped on the MNI-152 T1 template.

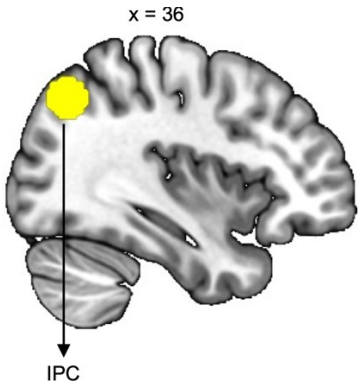


**Figure S3. Early blind individuals relied more on the inferior parietal cortex (IPC) during navigation than SC.**

Small Volume correction analyses were performed with a 10mm sphere around the peak coordinates from an independent study (MNI coordinates: 36/-68/44, Schindler et al., 2013), which investigated egocentric representation during an imagined navigation task. Results demonstrate a significant activation within the region of interest, suggesting that the early blind individuals (n = 19), compared to the sighted controls (n = 19), had greater activation in the IPC during the imagined navigation task than the math task ($p_{fwe} < 0.05$; i.e., [Navigation > Math] □ [early blind > sighted controls]).

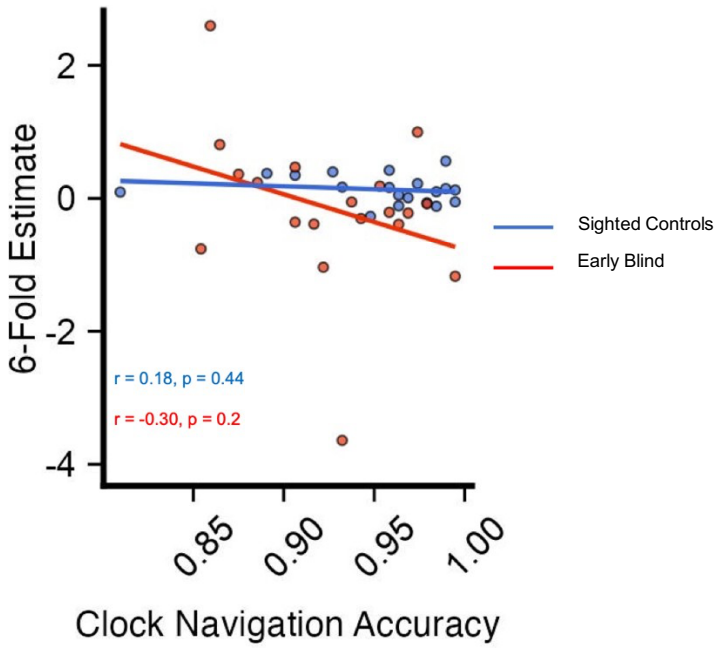


**Figure S4. Correlation between the accuracy in the Clock Navigation Experiment and 6-fold grid-like coding**

We did not find significant evidence that the accuracy in the Clock Navigation experiment correlated with the 6-fold symmetry estimate (Left EC for sighted controls and bilateral EC for early blind individuals), neither in sighted controls ($n = 19$, $r = -0.18$, $p = 0.44$, $r^2 = 0.03$) nor in early blind individuals ($n = 19$, $r = -0.30$, $p = 0.2$, $r^2 = 0.09$). However, it is worth noting that, although not significant, there was a negative trend in the early blind group, where participants with the higher accuracy scores also expressed a lower grid-like coding in the EC. This result support the hypothesis that the reduced 6-fold signal in the early blind was not attributable to the difference in task performance between the two groups. Source data are provided as a Source Data file.

**Supplementary Table 2. 4-fold Symmetry Score Predicted by IPC Activity**

*Linear regression*

| **Coefficients** | **Estimate** | **Std. Error** | **T-value** | **Pr (>\|t\|)** |
|---|---|---|---|---|
| Intercept | 0.311 | 0.085 | 3.656 | 0.0008*** |
| IPC Activity | 0.153 | 0.052 | 2.95 | 0.005** |
| Group | - 0.41 | 0.12 | - 3.4 | 0.0017** |
| IPC Activity : Group | - 0.18 | 0.07 | - 2.33 | 0.02* |

*$R^2$ = 0.38; Adjusted $R^2$ = 0.32; F(3,34) = 6.95; p = 0.0009. All p-values are two-tailed*

Source data are provided as a Source Data file.

**Supplementary Table 3. Path information in the path integration task**

| START | FIRST STOP | SECOND STOP | DISTANCE: START-FIRST | DISTANCE: START-SECOND | ANGLE (□1) START-FIRST | ANGLE (□2) START-SECOND |
|---|---|---|---|---|---|---|
| N | D | O | 14.5 | 4.1 | 34.7˚ | 107.8˚ |
| I | C | A | 7.2 | 10.15 | 53.7˚ | 31.7˚ |
| G | O | Q | 7.6 | 11.5 | 50.5˚ | 33.7 |
| G | P | C | 10.4 | 7.2 | 37.9˚ | 115.5˚ |
| I | Q | O | 6.5 | 7.6 | 77.9˚ | 57.3˚ |
| B | P | H | 14.4 | 7.2 | 55.3˚ | 55.3˚ |
| O | D | L | 12.5 | 8.4 | 19.1˚ | 40.6˚ |
| N | I | O | 10.4 | 4.1 | 73.7˚ | 122.7˚ |

*θ is the inner angle of the performed segment (starting point – stopping point).*

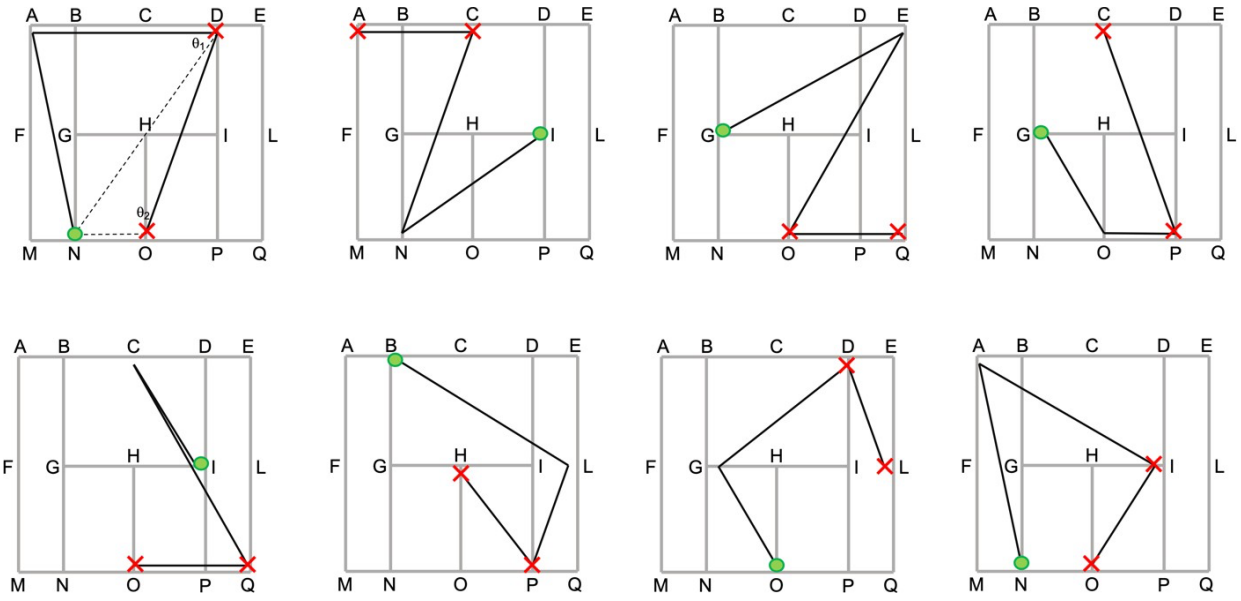


**Figure S5. Illustrations of the paths in the path integration task.**

Participants performed eight unique paths, repeated twice throughout the experiment. Each path was constituted by a starting point (green dots) and two different stopping points (red crosses). At each stopping point, blindfolded participants were required to estimate the distance and orientation of the starting point compared to their own position. The details of the paths are described in Supplementary Table 3.

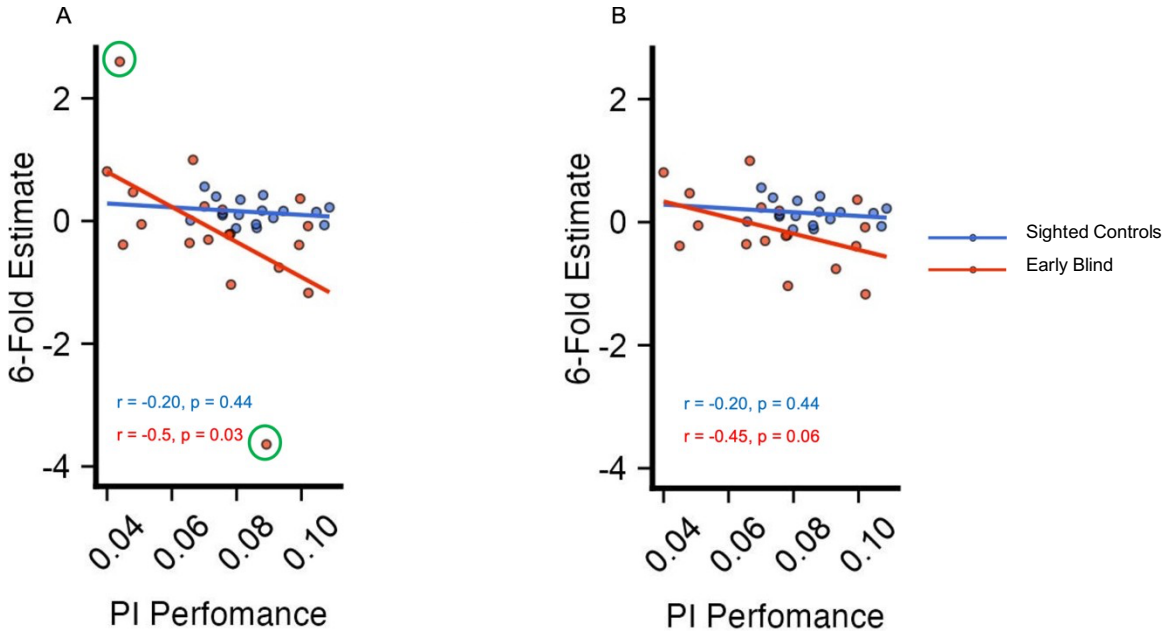


**Figure S6. Path Integration (PI) ability negatively correlated with 6-fold symmetry in Early Blind participants.**

(A) 6-Fold symmetry estimates (Left EC for sighted controls and bilateral EC for early blind individuals) negatively correlated with PI Performance in early blind participants, suggesting that sighted-like representation of space might be dysfunctional for navigating without vision (Pearson's product-moment correlations; n = 19, r = -0.5, p = 0.03). However, this correlation might be biased by the presence of two outliers (green circles) in the early blind population. No significant correlation was found in the sighted control group (n = 17, r = -0.19, p = 0.44). (B) Removing the outliers in the early blind group weakened the negative correlation between 6-fold symmetry estimates and PI performance (n = 17, r = -0.45, p = 0.06). Source data are provided as a Source Data file.

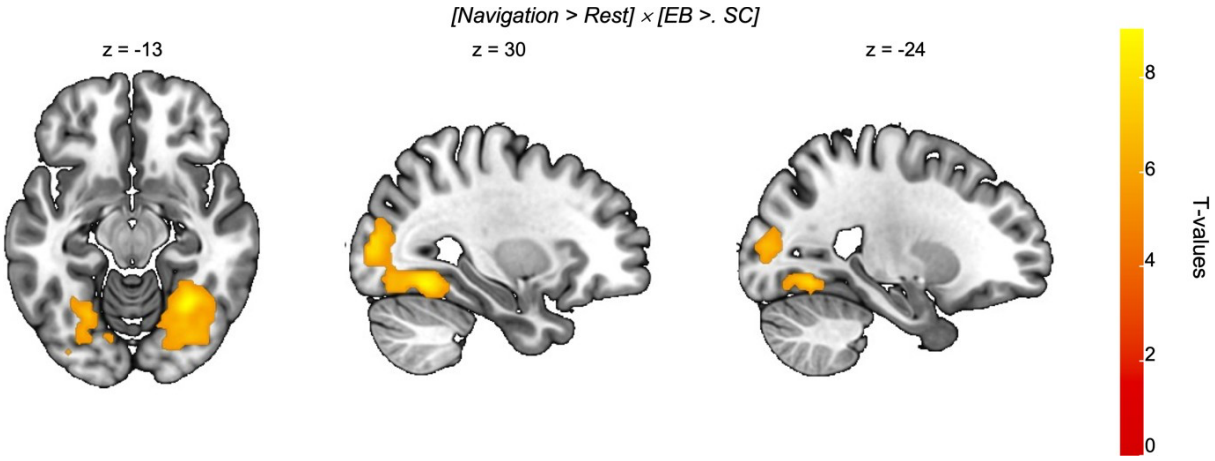


**Figure S7. The occipital cortex was more activated in early blind than in sighted controls.**
Although no differences between sighted controls (n = 19) and early blind individuals (n = 19) were detected when the navigation task was compared to the math task, when comparing the navigation task against rest ([Navigation > Rest] □ [early blind > sighted controls]), we could find the emergence of clusters of activity in several occipital areas among which bilateral inferior occipital gyrus; occipital fusiform gyrus; fusiform gyrus and lingual gyrus in early blind individuals more than sighted controls, which is in line with previous results2,3 (The activations were thresholded at pFWE < 0.05 and overlapped on the MNI-152 T1 template).

**Supplementary Table 4. Strategies for imagined navigation during the Clock Navigation experiment.**

| Code | Strategies |
|---|---|
| **Sighted Controls (SC)** | |
| SC01 | Thinking about the path I need to perform |
| SC02 | Divide the clock in two halves by tracing a line from the first to the second point |
| SC03 | Walk through the clock from the first to the second number |
| SC04 | Bird-view of the clock to locate the starting and ending position |
| SC05 | Walk through the clock from the starting to the ending point |
| SC06 | Divide the clock space with a line |
| SC07 | Visualize the clock from the starting point |
| SC08 | Walk through the clock |
| SC09 | Rotate the clock space according to my position |
| SC10 | Rotate the clock space according to the starting point position |
| SC11 | Bird-view of the clock |
| SC12 | Divide the clock in two halves from the starting to the ending point |
| SC13 | Walk through the clock |
| SC14 | Bird-view of the clock space tracing a line from the starting to the ending point |
| SC15 | Imagine the path to perform within the clock |
| SC16 | Walk through the clock |
| SC17 | Imagine walking from one number to the other |
| SC18 | Walk through the clock |
| SC19 | Imagine walking from one point to the other of the space |
| **Early Blind (EB)** | |
| EB01 | Trace a line from one point to the other |
| EB02 | Rotate the clock according to the starting point location and walk until the target point |
| EB03 | Imagine always looking at the ending point being at the starting position |
| EB04 | Imagine having the ending point in front of me |
| EB05 | Imagine two points on the clock |
| EB06 | Rotate the clock to have the starting point in front of me |
| EB07 | Imagine myself within the clock space |
| EB08 | Imagine the clock space divided in two halves according to the starting and ending point |
| EB09 | Rotate the clock to have the starting point in front of me |
| EB10 | Rotate the clock to always face the ending point |
| EB11 | Walk from one number to the other |
| EB12 | Imagine the path to perform |
| EB13 | Rotate the clock to have the starting point in front of me |
| EB14 | Rotate the clock to have the starting point in front of me |
| EB15 | Rotate the clock to have the starting point in front of me |
| EB16 | Imagine the ending point in front of me |
| EB17 | Divide the clock with a line |
| EB18 | Imagine the ending point in front of me |
| EB19 | Imagine the ending point in front of me |

**Supplementary Table 5. Demographic information of the early blind individuals (EB) and their matched sighted controls (SC)**

| EB CODE | AGE RANGE | GENDER | TOTAL BLINDNESS | ETIOLOGY | SC CODE | AGE RANGE | GENDER |
|---|---|---|---|---|---|---|---|
| EB01 | 46-56 | M | Birth | Optic nerve hypoplasia | SC01 | 39-49 | M |
| EB02 | 31-41 | M | Birth | Retinitis pigmentosa | SC02 | 27-37 | M |
| EB03 | 39-49 | M | Birth | Retinal burnt in the incubator | SC03 | 38-48 | M |
| EB04 | 28-38 | F | Birth | Microphthalmia | SC04 | 24-34 | F |
| EB05 | 31-41 | F | Birth | Premature retinopathy | SC05 | 28-38 | F |
| EB06 | 29-39 | F | Birth | Bilateral aplasia | SC06 | 26-36 | F |
| EB07 | 37-47 | F | Birth | Retrolenticular fibroplasia | SC07 | 40-50 | F |
| EB08 | 29-39 | M | Birth | Leber congenital amaurosis | SC08 | 26-36 | M |
| EB09 | 29-39 | F | 8 months | Congenital retinitis pigmentosa | SC09 | 31-41 | F |
| EB10 | 32-42 | M | Birth | Bilateral congenital anophthalmos | SC10 | 36-46 | M |
| EB11 | 30-40 | F | 2 years | Bilateral retinoblastoma | SC11 | 26-36 | F |
| EB12 | 27-37 | F | Birth | Premature retinopathy | SC12 | 25-35 | F |
| EB13 | 29-39 | M | Birth | Premature retinopathy | SC13 | 30-40 | M |
| EB14 | 33-43 | M | Birth | Optic nerve hypoplasia | SC14 | 29-39 | M |
| EB15 | 30-40 | F | Birth | Congenital retinitis pigmentosa | SC15 | 32-42 | F |
| EB16 | 32-42 | F | Birth | Premature retinopathy | SC16 | 29-39 | F |
| EB17 | 24-34 | M | 5 years | Dominant optic atrophy | SC17 | 25-30 | M |
| EB18 | 31-41 | F | Birth | Premature retinopathy | SC18 | 34-44 | F |
| EB19 | 48-58 | M | Birth | Bilateral congenital glaucoma | SC19 | 48-58 | M |

**Supplementary References**


1. Yarkoni, T., Poldrack, R. A., Nichols, T. E., Van Essen, D. C. & Wager, T. D. Large-scale automated synthesis of human functional neuroimaging data. *Nat. Methods* **8**, 665–670 (2011).

2. Gagnon, L. *et al*. Activation of the hippocampal complex during tactile maze solving in congenitally blind subjects. *Neuropsychologia* **50**, 1663–1671 (2012).

Kupers, R., Chebat, D. R., Madsen, K. H., Paulson, O. B. & Ptito, M. Neural correlates of virtual route recognition in congenital blindness. *Proc. Natl. Acad. Sci. U. S. A.* **107**, 12716–12721 (2010).

# III

## Introduction to the Sound Navigation Experiment

The second part of my PhD had been dedicated to the development of an fMRI experimental paradigm to investigate the emergence of entorhinal cortex cognitive maps in blind individuals during a conceptual navigation task. Given the characteristics of the special population we aimed to test (i.e., early blind) it was not possible to rely on pre-existing conceptual navigation paradigms that were shown to be sensitive enough to elicit a grid-like signal in humans' entorhinal cortex, as they all rely to some extent on visual stimuli. Therefore, we needed to implement a paradigm that completely rely on other senses such as hearing. We developed an auditory analogy task in which participants were prompted with two sound pairs and were asked to report whether the same relationship existed between them, or not (see below). Given the importance of adopting a task that is sensitive enough to elicit grid-like activity with a limited number of early blind participants, considering as well the novelty of the paradigm and the relatively low signal-to-noise ratio in the EC, before the experimental testing of blind people and related sighted controls, we conducted a pilot experiment on an independent group of sighted individuals (N= 19). Before going into the details of the main experiment, therefore, I'll sum up the methods and results of this pilot study.

# VISUAL EXPERIENCE INFLUENCES GRID-LIKE CODING IN CONCEPTUAL NAVIGATION

## Introduction

Imagine the situation in which, during university, you have to choose which exam to prepare first. To make the best choice you'll need to carefully select the topic in which you can prepare better. However, the solution will come to your mind in a rather effortless way. Indeed, intelligent systems' distinctive characteristic concerns the ability to acquire knowledge from the context in which they are immersed and usefully store it so that can be re-used to adaptively interact with it [1–3]. How this knowledge is acquired and flexibly reused is a question that inspired different fields in animal and human cognition as well as computational modeling [4–7]. One possibility is that animals and humans store each specific information acquired at each specific moment in separate chunks and retrieve them when needed. However, this solution, behind requiring the use of an incredible number of cognitive resources, would lack the flexibility needed to rapidly adapt to external conditions. Alternatively, the acquired knowledge could be summarized and aggregated in separate clusters divided by 'core features'. This solution will guarantee flexibility and generalization other than being costless [1,8–11]. This latter representation is what Tolman in 1984 defines as cognitive maps [12,13]. Groundbreaking research on rodents' electrophysiology attributes the hippocampal-entorhinal system to a crucial role in the creation of allocentric cognitive maps. Here different types of spatially tuned neurons such as place [14], head direction [15] and grid cells [16] provide information on whether the agent is located within the environment. While place and head direction cells encode the agent's actual location and heading direction respectively [14,15], grid cells [16], with their multiple firing fields, tile the navigable surface in a hexagonal latex providing information concerning the movements of the agent. In humans, a grid-like coding, usually associated with grid cell activity, can be detected through the use of non-invasive neuroimaging techniques, such as fMRI, as a 60° modulation of the BOLD signal, during different types of spatial navigation tasks [1,17–21], suggesting that, cognitive maps subtend humans spatial navigation similarly to what happens in animals. Interestingly, the same neural correlate has been found in humans' EC

also during more abstract tasks such as navigation of a bird [22], odor [23], social [24,25] and word space [26] and it seems to subtend also more complex cognitive processes such as decision making [27–29]. This evidence suggests a similarity in the processing and encoding of the spatial and abstract relations, as if, concepts are stored in cognitive maps and explored in the same way we explore spatial locations.

The influence of how we navigate in space on how we organize conceptual information in our minds is not new in the field of cognitive neuroscience. Think about, for example, the way humans organize numbers on a line with smaller values on the left and bigger numbers on the right [30–32] or how we talk about time usually using spatial metaphors such as 'leave the past behind'[33,34]. Several studies have indeed demonstrated that humans tend to attribute spatial values to non-spatial stimuli to successfully encode and remember them. The influence of space on concepts can be observed both at the behavioral level and neuroimaging level where the role of the medial parietal lobe and hippocampus seems to be prevalent [30–32,35–37]. However, the relation between spatial and conceptual knowledge in the field of cognitive maps remains unclear. Indeed, it could be that the detection of a grid-like coding in both spatial and conceptual navigation is the result of the influence exerted by spatial navigation neural mechanism, ontogenetically evolved, on conceptual navigation, or on the contrary that navigation in the two domains, albeit relying on a common (and possibly innate) memory code, develop independently.

There's a general agreement in the scientific community in attributing to vision a crucial role in extracting spatial relations in humans[38,39]. Vision, contrarily to other senses, allows the simultaneous encoding of multiple information concerning distances and location of salient landmarks allowing the rapid creation of allocentric cognitive maps[40–42]. However, little is known about the response of the neural correlates of cognitive maps, when the visual experience is lacking. Animal studies suggest that whereas place cells firing field stability is not affected by the absence of visual experience [43], head direction cells signal [44], albeit present, became more unstable. On the contrary, there is no evidence concerning grid cells firing stability in the absence of visual experience in animals. In humans, a recent study compared sighted and early blind individuals in an imagined spatial navigation task [45]. In this study participants were asked to imagine to navigate a clock-like environment going from one number to the other. Authors observed the emergence of a grid-like coding in the entorhinal cortex of sighted participants but a reduced 6-fold symmetry in early blind individuals, while doing the task. Crucially, the authors observed the emergence of

an alternative neural geometry of entorhinal cortex cognitive maps in early blind individuals performing the imagined spatial navigation task, a 4-fold symmetry [45]. This alteration in the grid-like coding in blind people's EC has been associated with a higher parietal cortex activity, usually associated with the egocentric encoding of spatial information [46].

Does early lack of visual deprivation influence, also, the development of abstract cognitive maps similar to what is observed in spatial cognitive maps? To address this question, we designed an fMRI study where we asked blindfolded sighted and early blind individuals to perform a conceptual navigation task based on sound analogies while undergoing two fMRI sessions. In this study, participants heard two pairs of sounds that changed in pitch and duration and were asked to judge whether the changes between the two pairs of sounds were comparable or not (i.e., whether the following analogy was true or false: sound 1: sound 2 = sound 3 : sound 4, see methods). Unbeknown to participants the changes between each pair of sounds created a precise trajectory in a 2-dimensional pitch-duration space. The conceptual space participants navigated was sampled at a granularity of 30˚ to provide enough spatial resolution to detect grid-like signals in the human entorhinal cortex [22,24]. Before the experiment participants underwent extensive training to get familiar with the experiment and the sound space they needed to navigate. We first piloted this experiment on an independent group of sighted participants.

**Pilot Experiment**

**Methods:**

Participants

Nineteen sighted participants took part in the experiment (12 females and 7 males; age: M = 23.05, SD = 3.44; 1 left-handed and 18 right-handed). All participants were Italian native speakers and none of them reported a history of neurological disorders. Before the experiment participants signed an informed consent and were reimbursed for their participation after the fMRI sessions. None of the participants were excluded from neuroimaging analyses due to excessive head motion (i.e., the maximum head motion for each run in each participant was smaller than 3mm in

translation and 3° in rotation). The ethical committee of the University of Trento approved the study.

Stimuli construction and presentation

The experimental stimuli were constituted by 16 pure tones which vary between each other by duration and pitch. The tones do not contain any melodic information. In total, there were 4 different duration levels and 4 different pitch levels making it so that the stimuli could be arranged in a 4X4 grid. The levels of duration and pitches were defined a priori and no psychophysiological measurement was collected to compute the Just Noticeable Difference (JND) for sound discrimination for each participant due to time constraints. However, a behavioral pilot conducted using these stimuli confirmed that chosen durations and pitch intervals were sufficient to allow the discrimination of the sounds. Specifically, pitch levels (435-, 587-,788-,1040-Hz, see Fig.1) followed a non-linear increase (differences between levels: 152, 201, and 252 respectively, see Fig. 1A) where each term increased approximately 50 units. Similarly, duration levels (160-, 320-, 640-, 1280-ms, see Fig.1A) followed an exponential growth where each duration was double the previous one. The tones were created using Matlab 2022a. First, we've calculated the audio sampling rate:

$$x_{time} = 0 : \frac{1}{sample\ frequency} : duration\ range$$

where 'sample frequency' was the predefined frequency of the tones (48000Hz) and 'duration range' was the different levels of durations of the tones reported above. Then, we computed the audio signal as follows:

$$y_{audio} = \sin(2\pi * (x_{time} * frequency\ range))$$

where 'frequency range' was the predefined pitch level (see above). Finally, to avoid clip artifacts in the sounds we've added 0.1 secs fade at the beginning at the end of each sound. The adjunction of a fade did not affect durations. To create the experimental trials (from now on trajectories) each sound was paired with each other except itself to have 256 sound pairs. For each sound pair, we've calculated the raw degree angle of each trajectory as:

$$\theta_{raw} = atan\frac{(x_2 - x_1)}{(y_2 - y_1)}$$

Where '$x_1$' and '$x_2$' indicated the duration of the first and second sound respectively (from 1 to 4) and '$y_1$' and '$y_2$' indicated the pitch of the first and second sound respectively (from 1 to 4). The raw degrees were then grouped in 30° bins. We then computed the Euclidean Distance (ED) of each sound pair and excluded too-long and too-short trajectories (ED <=1.14 and ED >=4) to avoid imbalances in difficulty between trials. Finally, each of the remaining sound pairs (152 in total) was paired with each other except itself, resulting in 11476 combinations. The experiment was constituted of 192 trials (i.e., quadruplets of sounds) divided into 8 runs of 24 trials each. The first 4 runs were constituted by unique 96 trials selected from the available combinations mentioned above, whereas the remaining 4 runs were constructed by swapping the order of appearance of the sounds' pairs (e.g., in Run 5 the first sound pair played was the second sound pair played in Run 1, to that the first and second sounds in Run 5 were the third and the fourth sounds played in Run 1). Trials for each run were selected so that, within the entire dataset each quadruplet of sound appears just once (also accounting for the swapped order), and the relationship between the two sound pairs (increasing/decreasing in pitch/duration) produces feasible change also in the other sound pairs, again accounting for swapped trials. For instance, if the fourth sound had a duration of 4 (i.e., level 4) and between the first and second sounds there was an increase in duration of 2 levels, this would have led the fourth sound to have a duration of 6 which was out of the 4X4 grid boundaries, the same reasoning could be applied to pitch. These cases were removed from the possible candidates to constitute the final dataset. Moreover, each run had to have the following characteristics: (I) 12 trials should be constituted by quadruplets that had the same characteristics (i.e., the $\theta_{raw}$ and ED of the two sound pairs were the same, from now on match trials, Fig. 1A) and the remaining 12 trials by quadruplets that have different characteristic (i.e., the $\theta_{raw}$ and ED of the two sound pairs were different, from now on mismatch trials, Fig. 1A); (II) among the 24 trials each degree bin (from 0 to 330 in step of 30) should appear four times (twice among the first pairs of sounds, and twice among the second pair of sounds).

Sound Space experiment procedure: Participants performed a conceptual navigation experiment by solving a novel analogy task with sounds (Fig. 1A). The task was inspired by previous

conceptual navigation studies [24,29]. Participants heard four different sounds, that constituted two independent sound pairs, and were asked to decide whether there was the same relationship between the two sound pairs. Specifically, the same relation exists only if the amount of change in duration and pitch between the first two sounds (sound 1 and sound 2) was identical in the last two sounds (sound 3 and sound 4). To give an example, the same relationship exists if, between sound 1 and sound 2, there was an increase in duration of 2 levels and a decrease in pitch of one level and the same was true for sound 3 and sound 4. Therefore, the task participants had to perform could be compared to the resolution of an analogy where:

$$A : B = C : D$$

In other terms:

Sound 1 : Sound 2 = Sound 3 : Sound 4

The arrangement of the sound in a 4X4 grid was never made explicit to participants. Moreover, to avoid any spatial bias during the description of the task the experimenter never used spatial-related terms (e.g., direction of change). Given the complexity of the analogy task participants underwent extensive training prior to the fMRI sessions. The training was structured so that there were 4 different steps of increasing difficulty. The 4 different steps could be divided into two phases: a stimuli familiarization phase and a task familiarization phase. The stimuli familiarization phase consisted of 3 different steps, in which participants first were asked to simply listen to the audio stimuli (passive hearing task), and then, they had the opportunity to directly compare all the different sound and duration levels to each other through two pairwise comparison tasks (one accounting for 1-dimension at the time, and the other accounting for both dimensions, see below).During the passive hearing, participants heard all the different durations of the stimuli while not changing the pitch, the same procedure was applied to all the different pitches while, in this case, not changing the duration. Participants, at this stage, had the opportunity to listen to the different durations and pitches as many times as they wanted in a self-paced way. Subsequently, they performed the first pairwise comparison task: here, participants were asked to focus only on one sound's characteristic, either pitch or duration, and decide which among the two sounds lasted more or had the highest pitch. Participants heard two sounds separated by an Inter Stimulus Interval (ISI) of 2.5 seconds. After the second sound was played, they had 1.5 seconds to think which sound lasted more, or had the highest pitch before a cue word, either 'duration' ('durata') or 'pitch'

('tono'), was played. After the cue word, they had 2 seconds to answer by pressing one of the two buttons, on which their fingers were placed prior to the beginning of the task, and received feedback after their response. Participants knew before each run to which of the two sound features (pitch or duration) they had to pay attention. This task was performed until participants reached 100% accuracy. The same rationale was applied to the second pairwise comparison task, where the only difference was that this time the sound's pair changed in both the pitch and the duration. Specifically, after having heard the second sound, participants had 1.5 seconds to think about the changes in pitch and duration, then, in a random order, they were first asked to say which of the two sounds lasted more (cue word: duration) and which of the two sounds had the highest pitch (cue word: pitch). Participants had 1.5 seconds after each cue word to respond by pressing one of the two buttons on which their fingers were placed and receive feedback after their response. This task was performed until they reached at least 80% of accuracy. Finally, participants were trained in the analogy task they will perform in the fMRI (task familiarization phase). Participants heard the first two sounds separated by an ISI of 1.2 secs, after the second sound they had a jittered interval between 3.5 and 4.5 seconds to extract the relationship between the first sound pair (i.e., whether there was an increase or a decrease in duration and or pitch or whether either pitch or duration did not change. First relation extraction period, from now on). After that, participants hear the second sound pair (sound 3 and sound 4, ISI 1.2 secs). After the fourth sound, they had to say whether there was the same relationship between the two sounds' pairs or not. Participants have a jittered time window (6.5-7.5 seconds) to understand the relation between the second sound pair (second relation extraction period from now on) and decide whether the same relation exists between the two sound pairs (match trials, Fig. 1A) or not (mismatch trials, Fig. 1A). Only in the case of a correctly detected mismatch trial, participants were prompt with a second question in which they were asked to say whether the trial was a mismatch because the relationship was different both at the duration and pitch level, or whether the relationship was preserved in one of the two dimensions but different in the other. This second question was introduced using the cue word 'both' (entrambi, in Italian). For example, if in the first sound pair, there was an increase in duration of 1 level and the pitch remained unchanged, and in the second sound pair there was a decrease in duration of 1 level, but the pitch remains unchanged, the relationship between the two sounds' pairs was not the same due to the change in duration. In this case, participants should have answered 'no' to the second question. Crucially, the second question was added to prevent

participants from focusing just on one dimension (either pitch or duration) in mismatch trials. After each answer they receive feedback, and if they responded out of the time window they heard the word 'time' ('tempo', in Italian). Within the scanner, participants underwent one fMRI session constituted by 8 runs, the only difference between the analogy task performed during the training and the fMRI one was that no feedback was given after the participants' responses in the fMRI task.

fMRI data collection: Echo-Planar Images (EPI) were acquired with a 3T Siemens Prisma using a 64-channel coil for all the participants except two (one early blind and respective sighted control participant) where due to their head size, we had to use a 20-channel coil. Functional images were acquired as follows: Field of View (FoV)= 220mm; voxel size= 2.5mm$^3$ isotropic; number of slices= 65; Time Repetition (TR)= 1000ms; Time Echo= 22ms; Multi-Band acceleration factor (MB)= 5 and a flip angle of 62°. The number of slices and MB were chosen so that the ratio between the two corresponds to an odd number (65/5=13) to reduce slice group interference. Moreover, to minimize signal loss in the medial temporal lobe the acquisition box was tilted at 15° from the Anterior-Posterior Commisure (ACPC; direction: anterior edge of the slice toward the check). Furthermore, we collected a gradient-echo field map for distortion correction with the following parameters: FoV= 220ms; voxel size= 2.5mm$^3$ isotropic; TR= 760ms; TE1= 492ms; TE2= 7.38ms, flip angle= 62°. Finally, T1 structural images were acquired with a Multi-Echo MPRAGE (MEMPRAGE) sequence: FoV= 250; voxel size= 1mm$^3$ isotropic; TR=2530ms; TE1= 1.69ms; TE2= 3.55ms; TE3= 5.41ms; TE4= 7.2ms and flip angle of 7°.

fMRI data preprocessing

Images underwent standard preprocessing procedures using Statistical Parametric Mapping (SPM12 https://www.fil.ion.ucl.ac.uk/spm/software/spm12/) and MATLAB 2020a. Functional images were spatially realigned and corrected for distortions using the 'realign an unwarp' tool in SPM12. The correction took place using a Voxel Displacement Matrix (VDM) computed using the acquired field maps of each participant. The structural (T1) and functional images were coregistered to the mean functional images and normalized to the Montreal Neurological Institute (MNI) space, using unified segmentation methods. Finally, functional images were smoothed with

a 5mm Full-Width-Half-Maximum (FWHM) spatial Kernell. The images were preprocessed separately for each fMRI session. ROI analyses in the EC were implemented on unsmoothed images in the native space.

ROI Definition

Entorhinal cognitive masks were cytoarchitecturally defined for each participant using Freesurfer (v7.1.1, https://surfer.nmr.mgh.hardvard.edu/). The obtained masks were then coregistered to each participant's mean functional images obtained from the preprocessing to match the functional images' spatial resolutions (2.5 isotropic). Analyses were conducted both on a single hemisphere and considering both hemispheres together. For this latter case, we computed a mask of bilateral entorhinal cortex by merging the masks of the two hemispheres using the built-in 'ImCalc' function in the Statistical Parametric Mapping software (SPM12 https://www.fil.ion.ucl.ac.uk/spm/software/spm12/)

Grid-Like Coding Analyses

To detect grid-like coding we've applied two-way-crossvalidation to quadrature filter analyses. The eight experimental runs were divided into two partitions of 4 runs each in which trajectories' degrees were equally represented. For each iteration, one partition was used to estimate the mean grid orientation of each participant (GLM1) and the remaining partition to test the mean grid orientation (GLM2). This process was iterated until all the partitions were used both for GLM1 and GLM2.The analyses were conducted by defining the regressor of interest as either the first relation extraction period (after sound 2, see Fig. 1A) or the second relation extraction period (after sound 4, see Fig. 1A). The duration of the time window of interest (i.e., either the first or the second relation extraction period) was determined on a trial-by-trial basis using each participant's Reaction Times (RTs, second relation extraction period) or the double of participants' RTs (first relation extraction period; see the Results section for more details). Additionally, the regressor of interest in both GLMs (GLM1 and GLM2) was modulated by parametric regressors that account for the trajectory's angle ($\theta$) of each trial (see below for details). In each GLM we've modelled as regressor of no interest the two sound pairs and the response period. Moreover, we modeled the

six-rigid head motion parameters, computed during the realignment stage of the preprocessing using SPM, as nuisance regressor and we filtered the signal with a 1/128Hz high-pass filter to remove slow drift in the signal.

The quadrature filter analyses consisted of two GLMs. In the first GLM, the mean grid orientation for each participant was estimated in its native space. To do so, the two relation extraction periods were modulated by two parametric regressors: *cos(6$\theta_t$) and sin(6$\theta_t$)* where *6$\theta_t$* indicates the angle ($\theta$) of the trajectory for each trial (t) and the factor '6' indicate that 60° sinusoidal modulation of the BOLD signal was tested. The resulting beta maps ($\beta_1$ and $\beta_2$ respectively) were then used to calculate the phase of all the voxel within a pre-defined, subject-specific, entorhinal cortex ROI (see above) as in:

$$\varphi = \frac{\left(arctan\left[\frac{\beta_2}{\beta_1}\right]\right)}{6}$$

We then computed a weighted mean across the phases of the voxels within the EC mask, where the weights of the mean were defined as the amplitude of each voxel response calculated as follows:

$$\sqrt{\beta_2^2 + \beta_1^2}$$

The mean grid orientation was then tested on an independent set of data (second partition) in GLM2 by modulating each relation extraction period with the cosine of trajectories' angles realigned to each participant's preferred orientation as in:

$$\cos\big(6(\theta_t - \varphi)\big)$$

The magnitude of grid-like response in the entorhinal cortex in each participant was computed by averaging the mean activation across iterations for each relation extraction period separately. The same analyses were applied also to alternative periodicities (4-,5-,7- and 8-fold symmetry) used as control models.

**Results:**

Behavioral Results: Nineteen blindfolded sighted individuals took part in the sound navigation experiment. This experiment was inspired by similar studies in the field of cognitive maps for abstract knowledge, yet, it is worth highlighting the novelty of the task used here. Indeed, within the scanner, participants were engaged in a sound analogy task in which they had to decide whether or not the same relation was present between two sound pairs (Sound1: Sound2 = Sound3: Sound4) and if not, whether there was not the same relation because across the two sound pairs both the relations in pitch and duration were different or, on the contrary, whether the relation was different in just one of the two dimensions (see methods paragraph. Fig.1A). We first performed a behavioral analysis to investigate participants performance during the task, separately for each question. Considering the difficulty of the task, participants' performance was in line with the one reported in other studies that rely on a similar paradigm [24], both in the first question (Same or different relation: Mean = 74.1%; SD = 0.12, see Fig. 1B) and the second question (completely different relation or partially preserved relations: Mean = 61 %; SD = 0.12, see Fig. 1B). We furthermore analyze participants' Reaction Times (RTs) both for the first (mean RTs = 1.38 seconds; SD = 0.53, see Fig. 1C) and the second question (mean RTs = 1.10 seconds; SD = 0.37 seconds, see Fig.1C). Collectively these results suggest that participants were able to solve the task, successfully navigating the conceptual sound-space.

Neuroimaging Results: We've then analyzed the neuroimaging data from the sound navigation experiment to investigate whether during the two relation extraction periods (i.e., after participants heard the second sound and after participants heard the fourth sound respectively, see Fig.1A) we could observe a grid-like coding in participants' EC. In literature, there is a general consensus that a proxy of grid cell activity can be observed with fMRI as a 60° modulation of the BOLD signal, namely a grid-like coding (see methods. Fig. 2A). To detect grid-like coding in the EC of sighted participants we had applied a 2-way crossvalidation procedure to quadrature filter analysis (see methods). Thus, we split our dataset into two halves and used one half (4 runs) to estimate participants' mean grid orientation ($\varphi$) and the other half (4 runs) to test the orientation. We repeated this procedure twice so all the runs contributed an equal amount of time to the estimation and the testing of the signal (see methods paragraph). Accounting for the velocity with which

participants performed the task (see above), for each participant, we decided to use the RTs of each trial, to define the duration of the two events of interest (i.e., first relation and second relation extraction period). While for the second relation extraction period the RTs reflected exactly the moment in which participants took a decision, the duration of the first relation extraction period could only be estimated since no response was required. We've decided to set the duration of this period at double the RTs of each specific trial in the second relation extraction period. Indeed, we have reasoned that, compared to the second relation extraction period a longer latency would have been possibly needed given the need to accurately extract the relation between the first and second sound to correctly solve the task and due to the impossibility to predict the relation at all. Based on prior literature[17,19], the underlying neural mechanisms involved in the formation of cognitive maps should manifest as a positive periodic (sinusoidal) modulation of the BOLD signal. To test this, we conducted one-tailed t-tests or Wilcoxon tests (depending on whether the sample distribution was normal or non-normal), where the one-tailed t-tests assessed whether the observed modulation was significantly greater than zero. Conversely, to compare the two groups (sighted and early blind), we conducted two-sample t-tests.

Similarly to the previously described experiment (see Chapter 2), given the lack of a priori hypothesis about grid-like coding lateralization in the brain, we first estimated each participant's mean grid orientation within a combined left and right EC Region of Interest (ROI)[21,45]. Quadrature filter analyses detected a significant 60° modulation of the BOLD signal in sighted participants bilateral EC (one-sample t-test; $t(18) = 2.11$, $p = 0.024$, $\alpha = 0.05$, one-tailed. Fig. 2B) in the first relation extraction period (after sound 2, see Fig. 2A). The same analyses performed on alternative periodicities (4-, 5-, 7-, 8- Fold symmetries) in the first relation extraction period did not reveal any significant modulation of the BOLD signal by any of the remaining alternative periodicities tested (Bonferroni corrected across tested periodicities, one sample t-test, 4-Fold: $t(18) = 0.35$, $p = 0.36$; 7-Fold: $t(18) = 0.1$, $p = 0.46$, and 8-Fold: $t(18) = 0.72$, $p = 0.23$. Wilcoxon signed rank exact test; 5-Fold: $V = 135$, $p = 0.06$, $\alpha_{Bonferroni} = 0.01$, all results one-tailed. Fig. 2B) supporting the specificity of our 6-Fold result. We then investigated the strength of the 6-Fold BOLD modulation in the two hemisphere separately and we observed a significant grid-like coding in participants' left EC (one sample t-test; $t(18) = 2.38$, $p = 0.014$, $\alpha = 0.05$, one-tailed. Fig. 2C) but not in the right EC (one sample t-test; $t(18) = 0.38$, $p = 0.35$, $\alpha = 0.05$, one-tailed. Fig. 2C). These latter results might suggest a slight lateralization of the signal in the left EC.

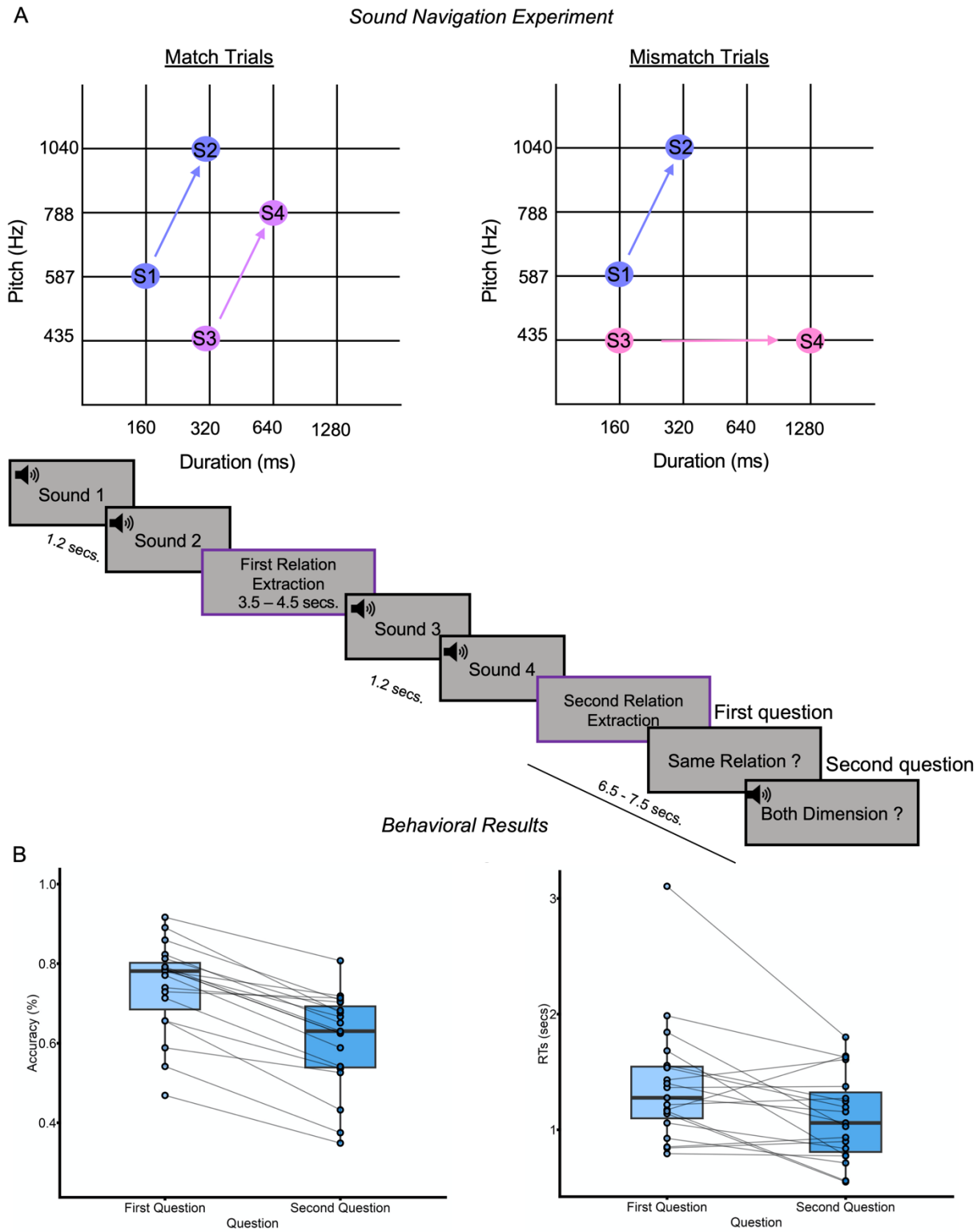


**Fig.1: A** Timeline of the sound navigation experiment and two examples of a match and a mismatch trial (on the top). Blindfolded participants in fMRI heard two different sound pairs. For each sound pair, they

were required to extract the relation between the two sounds (increasing/decreasing/stability of duration/pitch. First relation extraction and second relation extraction periods). At the end of the fourth sound participants, after having extracted the relation, were also asked to indicate whether the same relation existed (first question) between the two sound pairs (match trials, upper left) or not (mismatch trials, upper right). In the case of mismatch trials, they were furthermore required to indicate whether the difference relation was attributable to a change in both pitch and duration or just one of the two dimensions (second question). Purple boxes indicate the time window of interest for the quadrature filter analyses. **B** Behavioral analyses revealed no difference in accuracy (left) nor in reaction times (RTs, right) across the first (same or different relation) and the second (one or two dimensions) questions of the experiment. The boxes indicate the interquartile range (IQR, i.e., data points included between the first and the third quartile). The horizontal black lines indicates the median of the values of the sample and the whiskers indicate the distance between the highest and the lowest values in the sample from the estimated first and third quartiles. The dots represent single participant to the experiment.

We then performed the same analyses on the second relation extraction period (after sound 4, see Fig. 2A) where we did not observe a significant 60° sinusoidal modulation when we considered the left and right hemisphere combined (one sample t-test: $t(18) = 1.49$, $p = 0.07$, $\alpha = 0.05$, one-tailed. Fig. 2B) nor any other BOLD modulation by the remaining alternative periodicities (Bonferroni corrected across tested periodicities, one sample t-test, 4-Fold: $t(18) = -0.009$, $p = 0.5$; 5-Fold: $t(18) = 0.16$, $p = 0.43$, 7-Fold: $t(18) = 0.49$, $p = 0.31$, and 8-Fold: $t(18) = -2.47$, $p = 0.23$, $\alpha_{bonferroni} = 0.98$, all results one-tailed. Fig. 2B). Similarly, analyses on single hemisphere did not detect any grid-like coding (one sample t-test; left EC: $t(18) = 1.17$, $p = 0.12$; Right EC: $t(18) = 0.27$, $p = 0.41$, $\alpha = 0.05$, all results one-tailed. Fig. 2C). However not significant, it is worth to notice that, the 6-Fold symmetry in the combined hemisphere was the rotational symmetry that elicited the higher modulation of the BOLD signal approaching significance (one sample t-test: $t(18) = 1.49$, $p = 0.07$, $\alpha = 0.05$, one-tailed. Fig. 2B). The reduced 6-fold symmetry we observed during the second relation extraction period might be related to a noisier signal detected in this time window compared to the one we've detected in the first relation extraction's time window. Indeed, whether in the first relation period, participants had only to focus to navigate from the first to the second sound, in the second relation extraction period participants not only had to navigate from the third to the fourth sound understanding the relation between them, but also, comparing the just extracted relation to the one they have extracted previously.

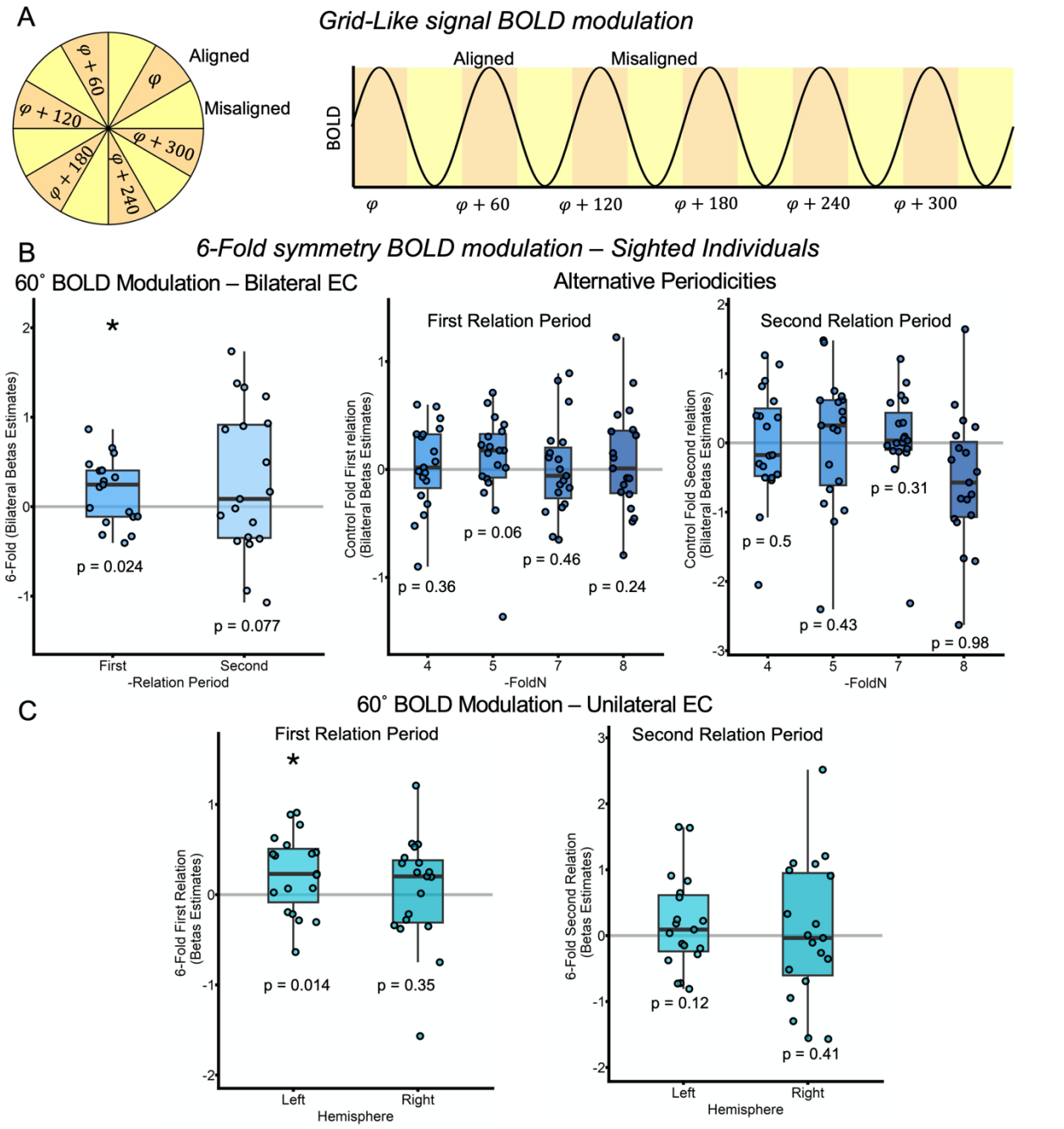


**Fig.2: A** Grid-like coding can be detected with fMRI as a 60˚(hexagonal) sinusoidal modulation of the BOLD signal, where movements aligned with the grid axes (φ, orange) elicit a greater modulation of the BOLD signal compared to misaligned movements (yellow).**B** Quadrature filter analyses were performed on the first and second relation extraction periods separately. Results showed a significant 6-fold symmetry in the bilateral EC of sighted individuals during the first relation extraction period (one sample t-test; $t(18) = 2.11$, $p = 0.024$, Left) and a trend toward significance in the second relation extraction period (one sample t-test; $t(18) = 1.49$, $p = 0.077$, Left). No other modulation of the BOLD signal was detected by any of the remaining alternative periodicities tested nor in the first (middle), nor in the second (right) relation extraction period (all results one-tailed. The significance threshold was set at $p < 0.05$ for 6-fold symmetry

and $p_{Bonferroni} < 0.01$ for alternative periodicities). **C** Similar results were obtained when we investigated the presence of a grid-like coding in the two hemispheres separately for the two relation extraction periods. Although a significant 6-fold symmetry was detected only in the left EC in the first relation extraction period (Left, one sample t-test; $t(18) = 2.38$, $p = 0.014$) there was no significant difference across the two hemispheres (all results one-tailed. No significant grid-like coding was detected in the two hemispheres during the second relation extraction period. The significance threshold was set at $p < 0.05$). In figure 2B-C the boxes indicate the IQR. The horizontal black lines indicate the median and the whiskers indicate the distance between the highest and the lowest values in the sample from the estimated first and third quartiles. The dots represent single participant to the experiment. Asterisk above the boxes indicates significant levels of $p < 0.05$ uncorrected.

Therefore, it could be hypothesized that, during the second relation extraction period, working memory and attention-related processes, that would have helped participants to keep in mind the relation between the first two sounds and compare it with the one of the last two sounds took place. The engagement of the above-cited additional cognitive processes, useful to solve the task, in which neural correlates reside also in the medial temporal lobe [47,48], might have influenced the strength of the detected signal in the EC explaining the observation of a reduced grid-like coding in the second relation period.

**Conclusion:**

We've conducted a pilot experiment to investigate whether, with an innovative auditory analogy paradigm, which did not rely on visual stimuli, we were able to detect a grid-like signal in the EC of sighted individuals. This pilot was necessary as there are no studies on conceptual navigation that investigate the emergence of a 6-fold symmetry in sighted individuals using purely auditory stimuli. We observed a significant 6-fold symmetry during the first relation extraction period using a bilateral mask. Hemispheric investigation showed that the effect was stronger, at least numerically, in the left hemisphere. A grid-like effect, instead, was only marginal in the second relation extraction period. Such a weaker effect was expected since, in this period, participants may have held in mind both the first and the second mental trajectory (for comparison), making the signal noisier. This pilot study provides us with important indications to refine our predictions in the main experiment with early blind individuals and sighted control participants.

**Main Experiment**

The experimental design and stimuli remained largely unchanged across the pilot experiment and the main experiment. However, marginal changes were introduced concerning duration intervals and the presentation of the second question (see methods below) to make the experiment slightly easier and faster considering that participants would have had to perform two fMRI sessions instead of one. Finally, I would like to remark that, at the moment of the writing of this thesis, this second project is still a work in progress as already mentioned in the introduction.

**Methods:**

Subjects

Forty-seven individuals took part in the experiment. Twenty-four participants were sighted controls (14 Male; M: 35.7, SD = 9.22) and twenty-three participants were early blind (13 Male; M = 39.13, SD = 8.04). Early blind participants were matched by age and sex with sighted controls (maximum year difference ± 5 years) with no significant differences between the age of the two groups (Paired sample t-test; $t(22) = 1.11$, $p = 0.27$). The introduction of the additional sighted control did not influence the age difference statistics (Two-sample t-test; $t(45) = 1.35$, $p = 0.18$) and therefore was added to the analyses. Participants were all Italian native speakers. Blind individuals who lose completely their sight at birth or by the age of 3 (except for one who loses their sight completely at the age of 5), report at least dark/light perception and no visual memory. None of the participants reported having a history of neurological disorders. None of the participants had been excluded due to excessive head motion (i.e., the maximum head motion for each run in each participant was smaller than 3mm in translation and 3° in rotation). Prior to the experiment all the participants signed an informed consent form and were reimbursed for their participation. The ethical committee of the University of Trento approved this study.

Although conscious about the difficulties, originally, we aimed for a sample size of seventy participants (35 sighted and 35 early blind individuals) to perform the experiment, as this is the sample size typically reported in conceptual navigation experiments [29]. Due to time constraints related to the writing of this thesis, and fMRI availability, this goal was not reached. However, we

reserve the possibility to test more participants, if this will allow a significant increasing of the sample.

Table 3 shows the demographics of sighted and early blind individuals.

Sound-Navigation Experimental Stimuli

The experimental stimuli were the same compared to those used in the pilot experiment (see above). Briefly, the experiment consisted of 16 pure tones that vary between each other in their durations and pitches. The levels of the different pitches were (435-, 587-,788-,1040-Hz, see Fig.1). Compared to the pilot study, intending to increase the accuracy and make the different levels of durations of the sounds more distinguishable, we've optimized the intervals between one duration level and the other by following an exponential increment. Thus, the different duration levels in this experiment were (160-, 368-, 810-, and 1620-ms, see Fig.3A). As for the pilot study reported above, the sounds were created using Matlab 2022a by first calculating the time points at which the audio signal should be sample and then computed the sine wave of the sound. Additionally, a fade of 0.1 seconds has been added at the beginning and the ending of the sounds to avoid clip artifacts.

The experimental trials and trajectories were the same as those used in the pilot (see methods section above for details on their construction)

Instructions were delivered auditorily to participants by the experimenter. All the stimuli were sampled at a frequency range of 48000Hz, 32-bit, mono, equalized at a threshold of 60db, and delivered to the participants through MRI-compatible headphones.

Sound-Navigation Experimental Procedure

Participants performed a conceptual navigation experiment equal to the one of the pilot experiments described above. Prior to the fMRI session, participants underwent extensive training that aimed to let them familiarize themselves with the task and construct the sound space they had to navigate. The training was divided into 4 parts of increasing difficulty: a passive hearing task, two pairwise comparisons task, and, finally, a simulation of the task they would have had to perform in the MRI scanner (the analogy task, see above). The only difference between the training

that participants underwent in this experiment compared to the pilot one, was the introduction of a guided tutorial of the fMRI task that participants performed prior doing the task on their own. Throughout the tutorial, participants had the opportunity to focus only on the task they had to perform as the experiment was pressing the button for them and no time window for the answer was set. Moreover, in this tutorial participants had the opportunity to listen again to the trial if they gave the wrong answer. Briefly, the analogy task (Fig. 3A) consisted of listening to two sound pairs and deciding whether there was the same change in pitch and duration between them. Participants listen to the first two sounds, separated by an Inter Stimulus Interval of 1.2 secs. After the ending of sound 2, they had a jitter period of time between 3.5 and 4.5 seconds, in which they were asked to think about what changed between the two sounds (increase/decrease in duration/pitch) and the magnitude of the change. Subsequently, they were asked to use the same logic to extract the relation between the third and the fourth sounds they heard. Finally, they had to decide whether or not the changes in pitch and duration were the same (match trials, Fig. 3A) across the two sound pairs considering both the direction of the change (increasing/decreasing or no change) and the magnitude or not (mismatch trials, Fig. 3A). Participants had a jitter time window between 3.5 and 4.5 seconds to extract the relation between the last two sounds and give and answer. Differently from the pilot study, where a second question anticipated by the cue word 'both' ('entrambi') was played after every correctly detected mismatch trial, in both the fMRI sessions, it was played just in 3 trials out of 12 possible mismatch trials. Participants were naïve about how many times they would have been asked to answer the second question, however, they were instructed that, when the second question was played, they would have had additional time to answer (response time window 9.5 seconds after the end of sound 4).

The arrangement of the sounds in a 4X4 grid was never made explicit to participants. Moreover, to avoid any spatial bias during the description of the task the experimenter never used spatial-related terms (e.g., the direction of change, magnitude of the change).

Participants underwent 2 fMRI sessions constituted by 8 runs each. During the entire duration of the experiment (fMRI sessions and behavioral training), participants belonging to both groups (sighted and blind individuals) were blindfolded. The stimuli in the fMRI were delivered through MRI-compatible headphones and answers were recorded through fMRI fMRI-compatible response box connected to the experimental computer. The experiment was performed using

Matlab 2014b (behavioral training) and 2022b (fMRI experiment) and psychtoolbox 3.0.14 (http://psychtoolbox.org/)

Sound-Navigation Experiment: Whole Brain Analyses

We've investigated the emergence of brain activity correlated with pitch perception and Euclidean distance by performing two separate general linear models (GLMs). Specifically, grounding on the idea that subsequential similar stimuli would elicit higher BOLD adaptation [49] we've conducted two adaptation-like analyses using as parametric modulators the absolute differences between two sound pitches and the Euclidean distance of the two sound pairs. In the first GLM, we modeled as a regressor of interest the onset of the second and the onset of the fourth sound and modulated this regressor with the absolute difference in the pitches between the two different sound pairs (i.e., the difference in pitches between sound 1 and sound 2, and difference in pitches between sound 3 and sound 4). The durations for the regressor of interest were defined using a stick function. Similarly, in the second GLM, we defined one regressor of interest as the onset of the second and the onset of the fourth sounds and modeled it parametrically with the distance participants should have navigated between two sounds in the sound space (i.e., the Euclidean distance between sound 1 and sound 2, and the Euclidean distance between sound 3 and sound 4). The duration of the regressor of interest was defined with a box-car function using as duration intervals the RTs, specific to each run, of each participant in answering the first question. In both GLMs, we also modeled three regressors of no interest: the first sound played, the third sound played, and the participants' responses. Furthermore, to control for head motion we included, in both GLMs, the six-rigid head motion parameters computing during the spatial realignment step in the preprocessing by SPM12. Finally, we used a high-pass filter at 1/128Hz to account for slow drift in the signal.

The obtained beta maps were used to perform both a one-sample t-test in each group separately, and a two-sample t-test to contrast the two groups (Sighted controls > early blind; early blind > sighted controls and sighted controls + early blind). The significant threshold was set at $p < 0.001$ voxel-level and $p_{fwe} < 0.05$ cluster-level unless differently specified.

fMRI data preprocessing

Functional images underwent a standard preprocessing procedure, separate for each session, as described in detail in the method section of the pilot experiment (see above). We used SPM12 to spatially realign the images and normalize them to the MNI space. Moreover, we accounted for distortion artifacts by correcting functional images with VDM computed on the acquired field maps specifically for each session. Furthermore, the normalized images were smoothed with a 5mm Full-Width-Half-Maximum (FWHM) spatial Kernell.

Whole brain analyses were performed on normalized and smoothed images whereas ROI analyses in the EC were implemented on unsmoothed images in the native space.

ROI Definition

The ROI definition was performed equally to what was described in the method section of the pilot experiment (see above). Briefly, we have cytoarchitecturally defined the entorhinal cortex masks for each participant using Freesurfer (v7.1.1). The obtained masks were then coregistered using SPM12 to match the spatial resolution of the functional images (2.5x2.5x2.5mm). The bilateral entorhinal cortex mask was obtained by combining the left and right entorhinal cortex masks for each participant.

Grid-like Coding analyses

Two-way crossvalidation has been applied to standard quadrature filter analyses[19,21,45] as described in detail in the method section of the pilot experiment (see above). We used all the runs (8) of one fMRI session to estimate participants' mean grid orientation (GLM1) and the other fMRI session to test it (GLM2). The process was repeated so that the fMRI session used in the first iteration to estimate the mean grid orientation would have been used in the second interaction to test the grid orientation, and, the fMRI session used to test the mean grid orientation in the first iteration will be used to estimate it in the second iteration of the crossvalidation. The analyses were conducted separately for the two relation extractions. Briefly, in GLM1, either the first (after sound 2) or the second (after sound 4) relation extraction period was modulated by two parametric modulators defined as $cos(6\theta_t)$ *and* $sin(6\theta_t)$, where $\theta_t$ indicate the angle created by the trajectory at trial 't' and

the number '6' indicates the fold symmetry of interest. The resulting beta maps were then used to compute the mean grid orientation within each participant's subject-specific EC ROI as in: $\varphi = (arctan[\beta_2/\beta_1])/6$ where $\beta_1$ and $\beta_2$ correspond to the sine and the cosine beta maps previously calculated. Finally, the emergence of a 60° sinusoidal modulation of the BOLD signal was tested in an independent set of data (8 runs) by modulating the regressor of interest (either first or second relation extraction period) with a parametric modulator reflecting the cosine of the trajectories' angles performed by participants realigned with each participant mean grid orientation: $cos(6(\theta_t - \varphi))$. The magnitude of grid-like coding was assessed by averaging the results of the two iterations of the crossvalidation. The same analyses conducted on the periodicity of interest (6-Fold) were also conducted on alternative models (4-,5-,7- and 8-Fold symmetry).

An additional GLM was computed to better visualize the 60° sinusoidal modulation of the BOLD signal in the EC. In this GLM we've divided each trajectories' angle into 12 bins with a spatial resolution of 30° that could be aligned (0 mod 60) or misaligned (0 mod 30) to the participants' mean grid orientation and we averaged the regressors across participants. Finally, we performed group-level analyses on the contrast obtained in GLM2 to investigate exploratorily the presence of other brain areas, besides EC, sensible to a 60° modulation.

Statistical Analyses

Statistical analyses were conducted both using SPM12 for whole brain analyses and RStudio (v4.2.2) for ROI and behavioral analyses. The mean grid orientations in the Hexadirectional coding analyses were computed for each participant using the functions implemented in the CircStat toolbox in Matlab 2020a. Whole brain and ROI results were computed using a one-sample t-test for within-group analyses and a two-sample t-test for between-group analyses. The $\alpha$ threshold was set at 0.05 and statistical results were reported two-tailed unless differently specified. The normal distribution of the data was estimated using the Shapiro-Wilk test and Wilcoxon Singed-Ranked exact test was performed in case of a non-normal distribution of the data.

Whole brain results were displayed by overlapping the estimated brain activity on the MNI152 template provided by SPM12. Behavioral and ROI results were displayed using boxplots and raincloud plots. In these graphs, the boxes indicate the interquartile range (IQR, i.e., data points included between the first and the third quartile). The horizontal black line indicates the median of

the values of the sample and the whiskers indicate the distance between the highest and the lowest values in the sample from the estimated first and third quartiles.

## Results

Sighted and Early blind individuals successfully navigated the sound space

Twenty-four blindfolded sighted and twenty-three blindfolded early blind individuals were engaged in a conceptual navigation task, in which they were asked to decide whether or not the changes in pitches and durations between two sound pairs were equal or not while undergoing two separate fMRI sessions. After receiving extensive training before the first fMRI session, the participant, within the scan, performed an analogy task (see methods). Briefly, in each trial, participants heard four different sounds that constituted two separate sound pairs (the first and second sounds constituted the first sound pair, and the third and fourth one constituted the second sound pair). Participants were asked to decide whether the same relation occurs between the two sound pairs, in other terms, they were asked to decide whether the analogia was true or false. To do so, after each sound pair, they had a jittered time widow between 3.5 to 4.5 seconds to navigate in the sound space and understand whether between the two just heard sounds there was and increasing or decreasing in the pitch or in the duration (or in both) or whether either pitch and duration did not change between the two sounds (first and second relation extraction respectively, see Fig. 3A). Moreover, during the second relation period (i.e., after the fourth sound was played), they were asked to say whether the changes between the first and second sound and the third and fourth sound were identical both in the direction (increasing/decreasing/stability) and in the magnitude of the change (match trials, see Fig. 3A) or not (Fig. 3A). Occasionally, participants were prompted with a second question in which they were asked to say whether in a mismatch trial, the relation between the two sounds pairs was not the same because the relation in both dimensions (i.e., pitch and duration) changed or because only one sound's feature among pitch and duration changed. In this latter case, a longer time window was available for participants (see methods, see Fig. 3A). The task was first piloted (see above) to control for its feasibility and sensitivity in detecting activation in the EC of participants, furthermore, it was inspired by similar

conceptual navigation tasks from previous studies [24,29]. Behavioral analyses were conducted on 24 sighted control and 22 early blind individuals as due to technical problems one early blind individual performed just one fMRI session. For the same reason, this participant was excluded from Hexadirectional coding analyses (see below). First, we investigated whether the accuracy of the task differs between the two fMRI sessions. Considering that the second questions were presented to participants only 3 times in each run (out of 24 total number of trials in each run) the accuracy was computed only considering the first question, that was whether or not there was the same relation across the two sound pairs. In both sighted and early blind groups we did not observe any significant difference in participants' performance across the two fMRI sessions (Repeated measure ANOVA; SC: $F(1,23) = 0.004$, $p = 0.9$; EB: $F(1,21) = 0.51$, $p = 0.47$, two-tailed, Fig. 3B). Furthermore we did not detect any difference in accuracy between the two groups (Repeated measure ANOVA; main effect of group: $F(1,44) = 0.34$, $p = 0.56$; accuracy × group interaction: $F(1,44) = 0.30$, $p = 0.52$, two-tailed, Fig. 3A). We then performed similar analyses to investigate the pattern of Reaction Times (RTs) across the two fMRI sessions both within and across groups. Analyses did not detect any significant difference in the RTs in the sighted control group across the two fMRI sessions (Linear Mixed Model; main effect of session: $\chi^2(1) = 0.45$ $p = 0.5$, two-tail, Fig. 3C) but a significant effect on RTs in the early blind group (main effect of session: $\chi^2(1) = 8.32$ $p = 0.004$, two-tailed, Fig. 3B) with early blind responding generally faster during the second fMRI session compared to the first one. Moreover, a difference in RTs approaching significance has been detected between sighted and blind individuals across sessions, which is likely driven by the previously observed results that early blind individuals were significantly faster in responding in the second session (Linear mixed model; main effect of group: $\chi^2(1) = 0.75$ $p = 0.38$; main effect of session: $\chi^2(1) = 6.45$, $p = 0.01$; session × group interaction: $\chi^2(1) = 2.92$, $p = 0.09$, two-tail, Fig. 3B). Finally, we've analyzed the data obtained from the questionnaire participants were asked to fill at the end of each fMRI sequence, to investigate the presence of possible differences in the perceived task difficulty across groups and sessions. We did not observe any significant difference in the perceived general task difficulty across fMRI sessions nor in the sighted individual group (Repeated measure ANOVA: main effect of difficulty: $F(1,23) = 0.85$, $p = 0.4$, two-tailed, Fig. 2D) nor in the early blind individuals' group (Repeated measure ANOVA: main effect of difficulty: $F(1,21) = 2.3$, $p = 0.14$, two-tailed, Fig. 2D). Moreover no difference in the perceived task difficulty was detected across groups (Repeated measure ANOVA: main effect of difficulty:

$F(1,43) = 0.79$, $p = 0.78$; main effect of group: $F(1,43) = 3.94$, $p = 0.05$; difficulty × group interaction: $F(1,43) = 2.8$, $p = 0.1$; two-tailed, Fig. 2D). Finally, we've performed a binomial test to calculate the accuracy threshold which indicates a non-random performance by the participants, that was set at 58%. Three early blind participants who performed below this threshold (thus, could not reliably perform the task) were excluded from the Hexadirectional coding analyses (see below).

Similar brain regions encode sound pitch and conceptual distance in sighted and early blind participants

Before investigating the presence of a grid-like coding in sighted and early blind participants' EC we performed two whole-brain analyses with a dual aim: first, we wanted to ensure the quality of the neuroimaging data we've collected, and second, we wanted to investigate whether sighted and early blind participants were relying on similar neural correlates to navigate in the sound space. In our experiment, we used sounds that vary in pitch and duration as experimental stimuli. In literature, there is evidence that sound processing and recognition rely on different sets of brain areas among which are frontal, parietal, and superior temporal cortices [50–53].Within the superior temporal cortex is situated the primary sensory region deputed to process sounds' low-level characteristics: the auditory cortex and more specifically the Heschel's gyrus. Sound pitches are, arguably, the feature that makes two sounds distinguishable one from the other in an easy and immediate way. The engagement of the auditory cortex during pitch discrimination tasks has been widely demonstrated in humans and was often associated with a higher BOLD-adaptation response as a function of the presentation of two sounds with similar pitch [54,55]. Therefore, to assess our first aim, we performed an adaptation analysis modulating the BOLD signal with the absolute pitch distance of the two sound pairs separately (see methods).

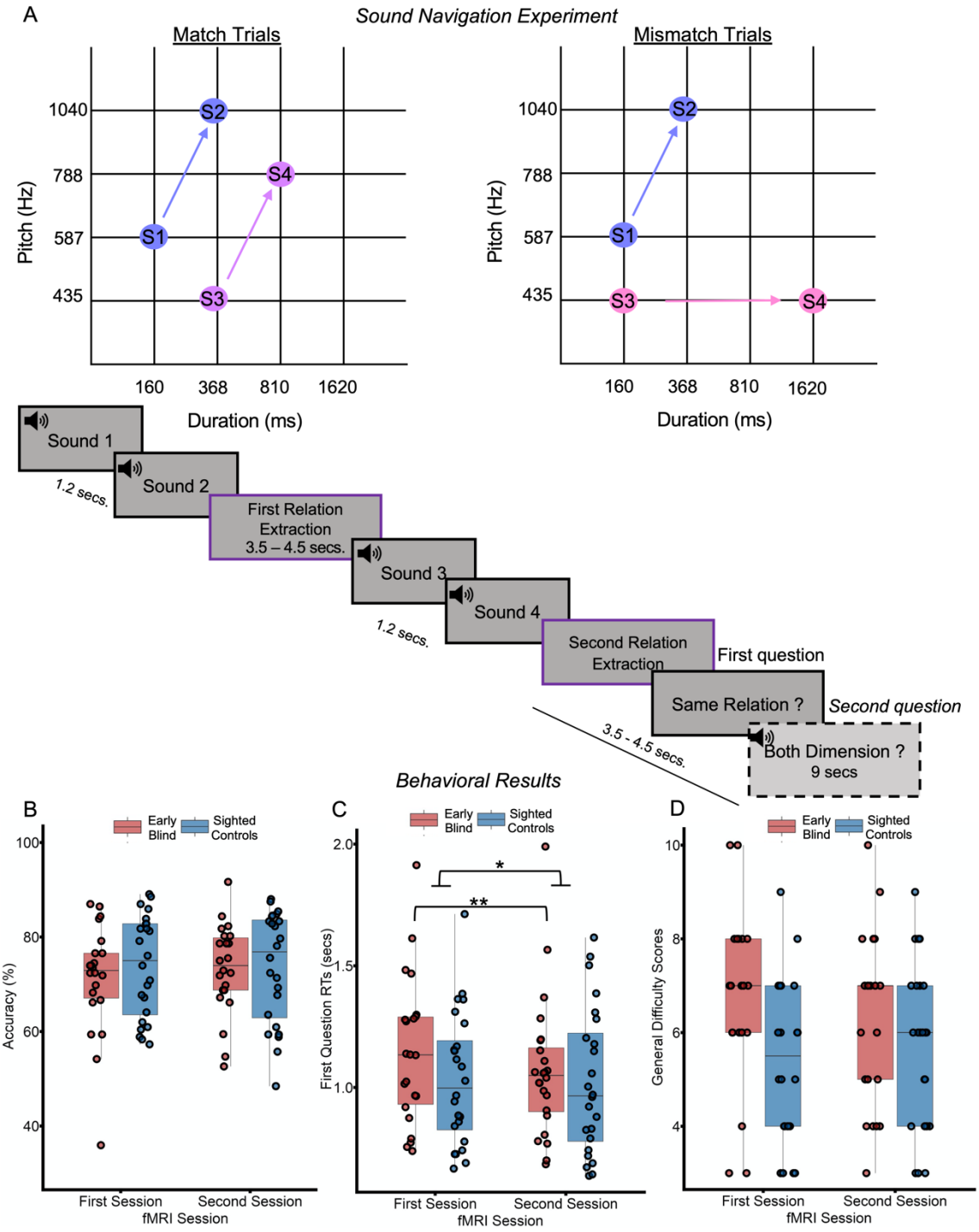


**Fig.3: A** Timeline of the conceptual sound analogy experiment (bottom) and examples of a match and a mismatch trials (top). Equally, to the pilot experiment, participants within the fMRI heard two different sound pairs and were asked to report whether or not there was the same relation between the two sound pairs. Differently from the pilot experiment, the second question (dashed box) was presented to participants only 3 times out of 24 trials. Purple boxes indicate the period of interest for quadrature filter analyses. **B**

Behavioral analyses were conducted within and between groups across testing sessions (2) and across groups. No differences were detected in the accuracy scores of sighted and early blind individuals nor within groups and across sessions or groups (left). **C**. On the contrary, we detected a significant difference across fMRI sessions in early blind participants (middle, Linear mixed model; $\chi^2(1) = 8.12$, $p < 0.004$) with them being faster during the second session compared to the first one possibly related to learning mechanism. The same difference across sessions was not detected in sighted individuals (middle). Finally, we detected a main effect of session when we compared the two groups (middle, Linear mixed model; $\chi^2(1) = 6.45$, $p = 0.01$) that might be driven by early blind patters of response (significantly faster in the second session compared to the first one) which can be attributed to the significant difference in RTs between sessions in early blind participants. **D.** Lastly, scores obtained from a questionnaire participants had to fill up at the end of every fMRI session reveal no difference across sessions nor across groups in the task perceived difficulty (right). All the presented results were two-tailed and the threshold for significance was set at $p < 0.05$. In figure 3B-C and D, the boxes indicate the IQR. The horizontal black lines indicate the median and the whiskers indicate the distance between the highest and the lowest values in the sample from the estimated first and third quartiles. The dots represent single participant to the experiment. Asterisk above the boxes indicates significant levels of $*p < 0.05$ and $**p<0.01$ uncorrected.

Results from these analyses revealed in both sighted and early blind participants a greater BOLD signal modulation for the biggest pitch differences (repetition enhancement effect) in bilateral auditory cortex (Fig. 4A and Table S1. All results thresholded at $p = 0.001$ voxel-level and $p_{fwe} = 0.05$ cluster level), with no differences between the two groups. Accounting for the absence of significant differences between sighted and blind individuals, we merge the two datasets to have a clearer view of the modulation of the BOLD signal exerted by pitch difference. This analysis confirms the presence of a strong bilateral repetition enhancement in the Heschel's gyrus shared across the two groups (Fig. 4A and Table S1. All results were thresholded at $p = 0.001$ voxel-level and $p_{fwe} = 0.05$ cluster level), and no other significant cluster emerged from these analyses. Although, our predictions revolved around a suppression of the BOLD signal correlated with the similarity between two pitches (i.e., small absolute differences), repetition enhancement in this domain has been already observed in animals and humans, and has been associated with a low-level processing of sound frequencies that could be detected when two auditory stimuli are separated by a considerable amount of time (from ~500ms to 1000ms)[56,57]. Our sound stimuli were separated by an Inter Stimulus Interval (ISI) of 1.2 seconds, and, accounting also for the duration of the sounds themselves (ranging from 160ms to 1620ms), we could hypothesize that the repetition enhancement we've observed in sighted and early blind individuals was a signature of the processing of low-level sound information in both sighted and early blind individuals' auditory cortex.

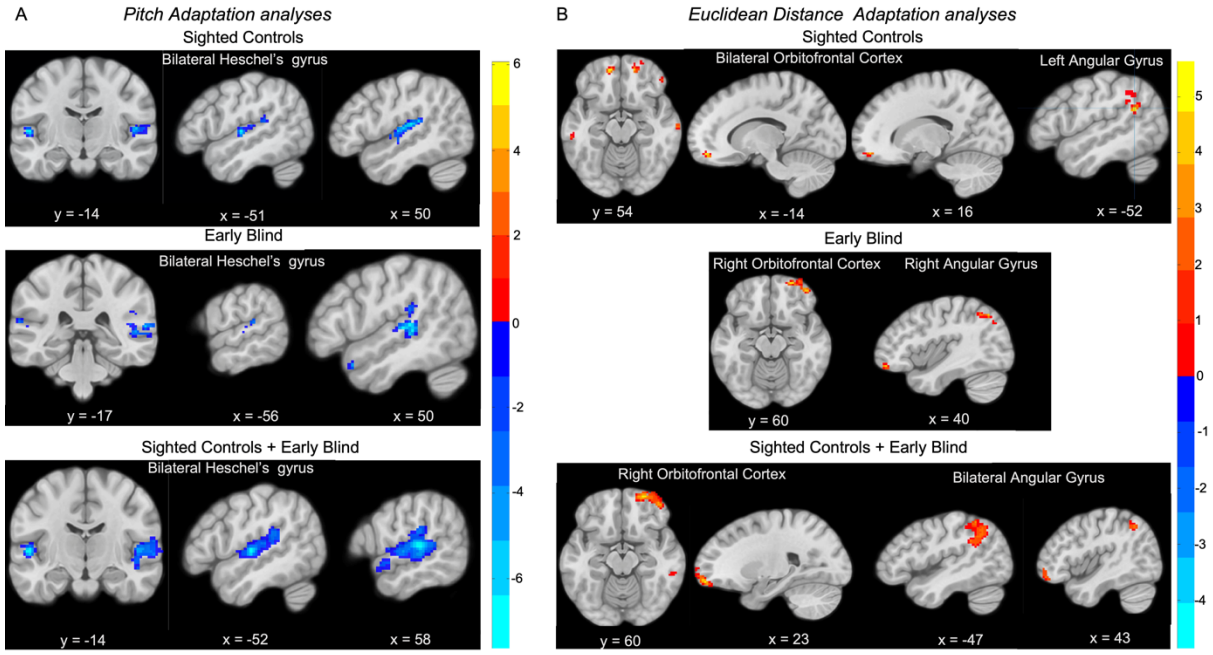


**Fig.4:** Adaptation analyses conducted on the absolute distance between the pitches of the two sounds (separately for the first and second sound and for the third and fourth sound) revealed a BOLD-enhancement (i.e., enhance BOLD modulation for small absolute differences between two pitches) in the auditory cortex, specifically in the Heschel's gyrus of both sighted (top) and blind individuals (middle) with no difference between the two groups. Accounting for the absence of difference between groups, we merged the dataset of sighted and blind and performed the same analysis (bottom). This analysis revealed even stronger recruitment of bilateral Heschel's gyrus, confirming the results obtained in single groups (all results thresholded at a $p = 0.001$ voxel-level and $p_{fwe} < 0.05$ cluster-level. The activation overlaps with the MNI-152 T1 template, color bars indicate the t-value interval). **B** Euclidean distance computation in both sighted (top) and early blind (middle) individuals revealed a BOLD-adaptation (i.e., reduced BOLD modulation for closer distances) in the orbitofrontal cortex and angular gyrus, more left-lateralized in the sighted and right-lateralized in the early blind, with no difference across groups. When the results of the two groups were merged (bottom) BOLD-adaptation was observed in the bilateral angular gyrus and in the right orbitofrontal cortex (all results thresholded at a $p = 0.001$ voxel-level and $p_{fwe} < 0.05$ cluster-level. The activation overlaps with the MNI-152 T1 template, color bars indicate the t-value interval)

Following a similar rationale, we've performed a second set of whole brain analyses to investigate BOLD-adaptation response as a function of the Euclidean distance in the 2D duration-pitch space, between the first and the second sound of each pair. Spatial distance processing and perception, across egocentric and allocentric frames of reference, have been correlated with frontal, parietal, and medial-temporal brain areas [58–60]. Recently, similar neural correlates in parietal and frontal regions have been observed also during the navigation of conceptual spaces [24,26,29,61]. We, therefore, investigate whether a similar pattern of brain activity could be observed in our task in sighted and

blind individuals. Specifically, we investigate whether the BOLD signal was significantly suppressed as a function of the distance traveled by the participants in the sound space. Adaptation analyses revealed higher repetition suppression (i.e., the closer two sounds were the more the BOLD signal was suppressed) in the angular gyrus and orbitofrontal cortex of both groups, which was more left-lateralized in sighted and more right-lateralized in early blind (Fig. 4B and Table S2a, all results thresholded at $p = 0.001$ voxel-level), but with no difference across groups. Similarly to what had been done for the analyses on sound pitches, we pull together the sighted and early blind individual dataset to get a clearer picture of the BOLD adaptation in response to Euclidean distances. This further step corroborate evidence of a shared distance processing between sighted and blind individuals in the right orbitofrontal cortex and bilateral angular gyrus (Fig. 4B and Table S2b. All results thresholded at $p = 0.001$ voxel-level and $p_{fwe} = 0.05$ cluster level).

In sum, the pitch-based adaptation results in the bilateral STG served as a first quality check of our data and revealed a similar engagement of auditory cortices during the task in both sighted and blind, excluding any group difference in terms of perceptual processing. More importantly, adaptation analysis based on Euclidean distance showed the emergence of distance coding in several expected brain regions, again with no difference across groups. Distance coding can be taken as a clear index of conceptual navigation [29,61] and, together with the behavioral results, support the hypothesis that both sighted and blind engaged mental trajectories in a cognitive map in order to solve the task.

Reduced Grid like coding in early blind individuals during conceptual navigation

Next, we investigated the emergence of a grid-like code in sighted and early blind individuals' EC during the sound navigation task. Grid-like coding had already been detected with fMRI in conceptual navigation studies [22,24,25,29], characterized by a hexadirectional modulation of the BOLD signal (60° sinusoidal modulation) in which movements aligned with the grid axes elicit a higher BOLD modulation compared to those misaligned (see Fig. 2A), equally to what observed in spatial navigation tasks (see Fig. 2A)[17]. The precise cellular mechanism underlying the detection of such

modulation remains unclear; it may correlate with increased spiking activity of conjunctive grid-by-head direction cells during movements aligned, as opposed to misaligned, with the main grid axes[62]. Another possibility is that the 60° BOLD signal modulation reflects a repetition suppression phenomenon, where movements aligned with the grid recruit fewer different grid cells compared to misaligned movements. Consequently, the modulation of the BOLD signal may reflect an adaptation in neuronal response[62].

We thus apply two-way crossvalidation to quadrature filter analysis in which we used one fMRI session to estimate each participant's mean grid orientation (φ) and the remaining fMRI session to test the magnitude of the 6-Fold symmetry (see method section). The presence of grid-like coding in the EC of sighted and early blind was tested separately for each relation extraction period. Relying on the same rationale as the pilot study (see above), we conducted one-tailed tests (either t-tests or Wilcoxon tests) to investigate signatures of grid-like coding within each group and two-sample t-tests to compare sighted and early blind individuals. The first relation extraction period begins at the end of the second sound, when participants, in principle, should have navigated in the sound space going from the first to the second sound (Fig. 3A).

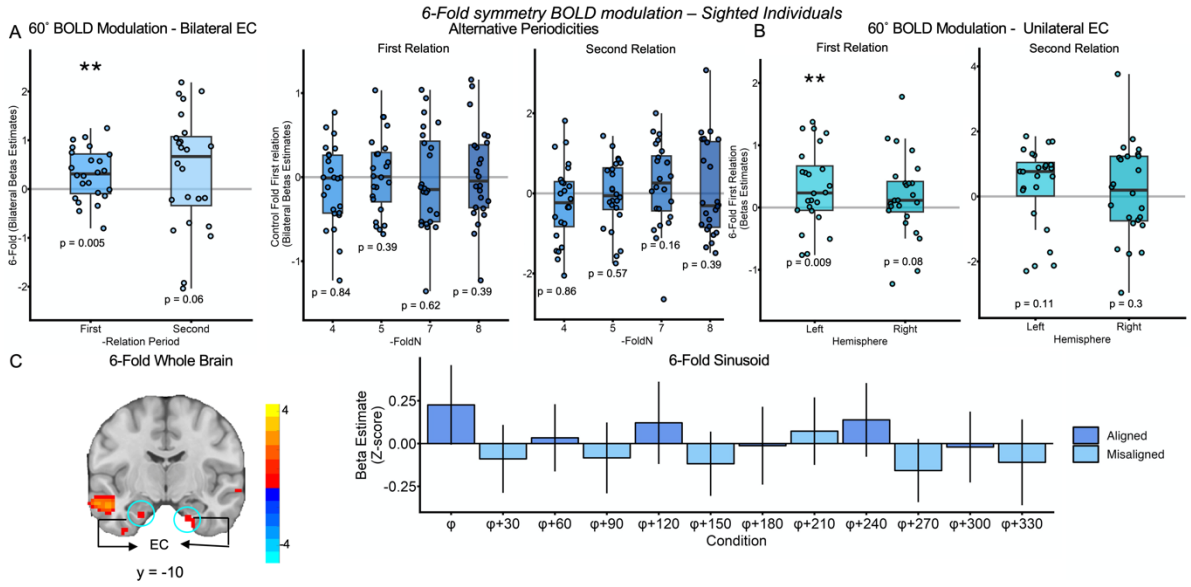


**Fig.5: A** Quadrature filter analysis revealed a significant 6-fold symmetry in sighted individuals' bilateral entorhinal cortex (left, one sample t-test; $t(23) = 2.81$, $p = 0.005$) in the first relation extraction period and a trend toward significance in the second relation extraction period (left, one sample t-test; $t(23) = 1.56$, $p = 0.06$) similarly to what observed in the pilot study, and no other modulation of the BOLD signal by any of the remaining alternative periodicities nor in the first not in the second relation extraction period (middle, all results one-tailed. The significance threshold was set at $p < 0.05$ for 6-fold symmetry and $p_{bonferroni} < 0.01$

for alternative periodicities). **B** Analyses on the two hemispheres separately revealed a significant 60° modulation of the BOLD signal in the left EC (right, one sample t-test; $t(23) = 2.5$, $p = 0.009$) and a trend toward significance in the right EC (right, one sample t-test; $t(23) = 1.41$, $p = 0.08$) in the first relation extraction period but no significant 6-fold symmetry detected in the second relation extraction period (right, Wilcoxon signed rank exact test; Left EC: $V = 194$, $p = 0.11$. One sample t-test; Right EC: $t(23) = 0.51$, $p = 0.3$, all results one-tailed. The significance threshold was set at $p < 0.05$ for 6-fold symmetry). **C** Left: whole brain analyses performed meaning the beta maps of the two relation extraction periods revealed a cluster of activation in bilateral EC (whole brain threshold $p < 0.05$, for display purposes only. The activation overlaps with the MNI-152 T1 template). Right: the grid-like coding can also be visualized as 60° sinusoids. In this case, experimental trajectories aligned with each participant's grid orientation ($\varphi$) and its 60° multiples would elicit a higher BOLD modulation compared to those misaligned with the grid (mean of the 6-fold symmetry detected in the two relation extraction periods, for display purposes only). In figure 5A-B D, the boxes indicate the IQR. The horizontal black lines indicate the median and the whiskers indicate the distance between the highest and the lowest values in the sample from the estimated first and third quartiles. The dots represent single participant to the experiment. Asterisk above the boxes indicates significant levels of **p<0.01 uncorrected.

Following pilot results, we expected to find a significant grid-like coding in sighted individuals in bilateral entorhinal cortex with a possible slight lateralization of the signal in the left hemisphere. Thus, we first analyzed the data from sighted control participants combining the left and right EC, estimating a common grid orientation for both hemispheres [21,45]. We observed a significant 6-fold modulation in the bilateral entorhinal cortex of sighted individuals (one sample t-test; $t(23) = 2.81$, $p = 0.0048$, $\alpha = 0.05$, one-tailed, Fig. 5A-5C). Supporting the specificity of our results, no other significant modulation of the BOLD signal was observed for any of the remaining tested periodicities (One sample t-test; 4-Fold: $t(23) = -1.01$, $p = 0.84$; 5-Fold: $t(23) = 0.27$, $p = 0.39$; 7-Fold: $t(23) = -0.3$, $p = 0.62$; 8-Fold: $t(23) = 0.26$, $p = 0.39$, $\alpha_{Bonferroni} = 0.016$ corrected across tested periodicities, one-tailed, Fig. 5A). Interestingly, the signal was present, albeit weakened, when we considered the two hemispheres separately: it was significant in the left EC (one-sample t-test; $t(23) = 2.5$, $p = 0.009$, one-tailed, Fig. 5B) and approached significance in the right EC (one-sample t-test; $t(23) = 1.41$, $p = 0.08$, $\alpha = 0.05$, one-tailed, Fig. 5B). No other significant modulation of the BOLD signal were detected in neither of the two hemisphere (One-sample t-test; Left EC: 4-Fold: $t(23) = -0.77$, $p = 0.77$; 5-Fold: $t(23) = -0.49$, $p = 0.68$; 7-Fold: $t(23) = 0.2$, $p = 0.41$; 8-Fold: $t(23) = 0.03$, $p = 0.48$. Right EC: 4-Fold: $t(23) = -0.22$, $p = 0.58$; 5-Fold: $t(23) = -0.15$, $p = 0.44$; 7-Fold: $t(23) = -1.05$, $p = 0.84$; 8-Fold: $t(23) = -0.86$, $p = 0.8$; $\alpha_{Bonferroni} = 0.005$ corrected across tested periodicities and hemispheres (5X2), one-tailed). The evidence of, albeit only numerical, stronger

grid-like coding in the left EC compared to the right EC was also present in the pilot experiment (see above) and might suggest a slight lateralization of the signal. Equal analyses were performed on the second relation extraction period which began at the end of the fourth sound (Fig. 3A). In this extraction period, to correctly solve the task a double computation was needed: first participants had to navigate from the third to the fourth sound to extract the relation between this second sounds' pair, then, they had to perform a comparison between the two sounds pairs and decide whether the sound analogy was true or not (sound 1 : sound 2 = sound 3 : sound 4). The results from the second relation extraction period revealed a 6-fold symmetry in the bilateral EC, approaching significance (one-sample t-test; $t(23) = 1.56$, $p = 0.06$, $\alpha = 0.05$, one-tailed, Fig. 5A–5B), and no other significant BOLD modulation by any of the remaining alternative models (One sample t-test; 4-Fold: $t(23) = -1.14$, $p = 0.86$; 5-Fold: $t(23) = -0.19$, $p = 0.57$; 7-Fold: $t(23) = 1$, $p = 0.16$. Wilcoxon signed rank exact test; 8-Fold: $V = 160$, $p = 0.39$, $\alpha_{Bonferroni} = 0.016$ corrected across tested periodicities, one-tailed, Fig. 5A). When we considered the two hemispheres separately, no significant 60° BOLD modulation was detected nor in the left EC not in the Right EC (Wilcoxon signed rank exact test; Left EC: 6-Fold: $V = 194$, $p = 0.11$. One sample t-test; Right: 6-Fold: $t(23) = 0.51$, $p = 0.3$, $\alpha = 0.05$ one-tailed). Similarly, we did not find any modulation of the BOLD signal by the remaining tested periodicity in the Left EC (One sample t-test; 4-Fold: $t(23) = -0.24$, $p = 0.59$; 5-Fold: $t(23) = -1.04$, $p = 0.84$; 7-Fold: $t(23) = -0.21$, $p = 0.58$; 8-Fold: $t(23) = 1.39$, $p = 0.08$; $\alpha_{Bonferroni} = 0.005$, corrected across tested periodicities and hemispheres (5X2), one-tailed) nor in the right EC (One sample t-test; 4-Fold: $t(23) = -1.79$, $p = 0.95$; 7-Fold: $t(23) = 1.39$, $p = 0.09$; 8-Fold: $t(23) = -1.48$, $p = 0.92$. Wilcoxon signed rank exact test; 5-Fold: $V = 152$, $p = 0.48$, $\alpha_{Bonferroni} = 0.005$ corrected across tested periodicities and hemispheres, one-tailed). Mirroring once again the results obtained in our pilot study, the 6-fold symmetry obtained in the second relation extraction period was weaker and only approaching significance in the bilateral EC. As mentioned before, in the second relation extraction period participants not only had to understand the relation between the third and the fourth sound, but they were also asked to compare that relation to the one they had extracted before, between the first and the second sound they heard. Therefore, it is plausible that the reduced grid-like coding observed in this relation period is due to the fact that participants were holding in mind two different trajectories (often with a different angle) in a short temporal window. However, we detect no difference in the magnitude of the grid-like coding in the two different relation extraction periods in sighted individuals

bilateral EC (Paired sample t-test; t(23) = -0.27, p = 0.78, $\alpha = 0.05$, two-tailed, Fig. 5A-5B). The same analyses were performed on early blind individuals to investigate the emergence of a 60° modulation of the BOLD signal in the EC. We first considered the first relation extraction period and did not detect any significant grid-like coding in early blind participant bilateral EC (One sample t-test; t(18) = -0.82, p = 0.79, $\alpha = 0.05$, one-tailed, Fig. 6A) not by any of the alternative tested periodicity (One sample t-test; 4-Fold: t(18) = -0.67, p = 0.74; 5-Fold: t(18) = -0.81, p = 0.78; 7-Fold: t(18) = 0.32, p = 0.37, $\alpha_{Bonferroni} = 0.016$, corrected across periodicities, one-tailed, Fig. 6A), except for a 8-Fold symmetry (~ 22° modulation of the BOLD) which however did not survive multiple comparison across tested periodicities (One sample t-test; 8-Fold: t(18) = 1.89, p = 0.037, $\alpha_{Bonferroni} = 0.016$ corrected across tested periodicities, one-tailed, Fig. 6A).

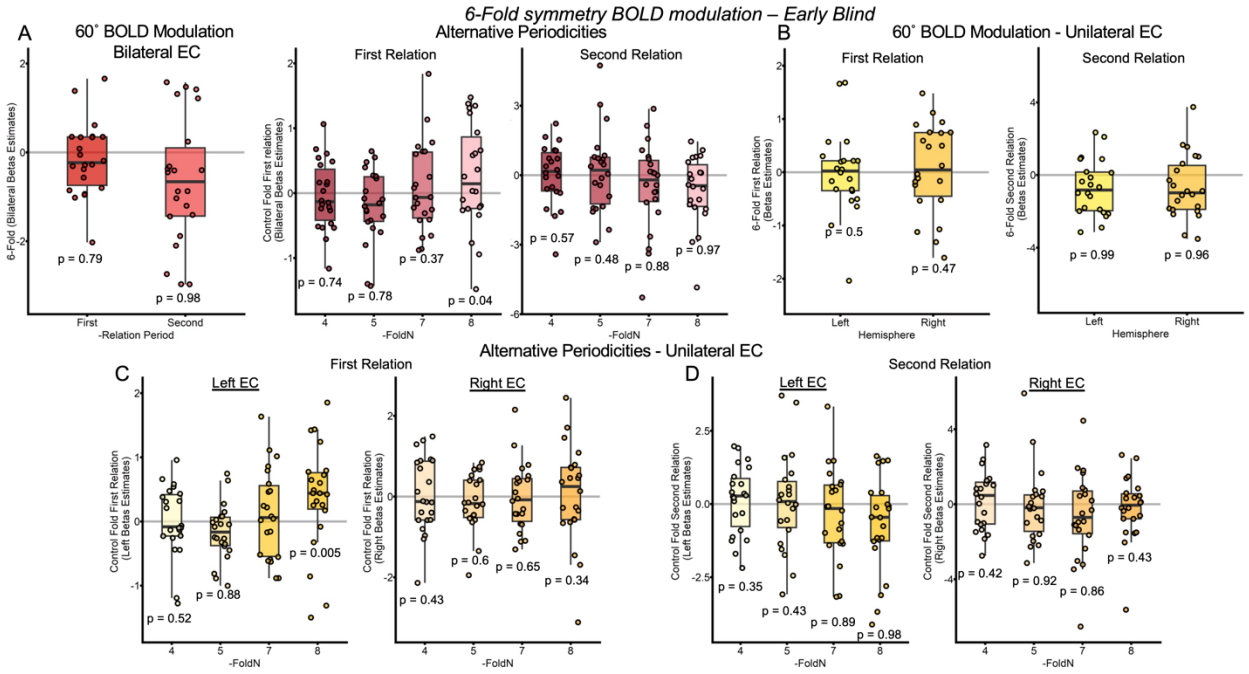


**Fig.6: A – B** Quadrature filter analysis conducted on early blind individuals did not detect any 60° modulation of the BOLD signal in any of the two relations extractions period nor when we considered bilateral EC (A left, one sample t-test; First relation: t(18) = -0.82, p = 0.79; Second relation: t(18) = -2.46, p = 0.98) nor single hemispheres (B, one sample-test; First relation, Left EC: t(18) = 0.005, p = 0.5; Right EC: t(18) = 0.49, p = 0.47. Second relation, Left EC: (18) = -2.46, p = 0.99, Right: (18) = 1.96, p = 0.96). Alternative periodicities did significantly modulate the BOLD signal in any of the two relation extraction periods (middle), except for an 8-fold symmetry (one sample t-test; t(18) = 1.89,p = 0.04) in the first relation extraction period which however did not survive multiple comparisons across the tested periodicities (5, all results one-tailed. The significance threshold was set at $p < 0.05$ for 6-fold symmetry and $p_{bonferroni} < 0.01$ for alternative periodicities). **C – D** Alternative periodicities in single hemispheres did not elicit a significant

BOLD modulation not in the first relation extraction period (C) nor in the second relation extraction period (D). During the first relation extraction period in the left EC, a significant 8-fold symmetry emerged (one sample t-test; $t(18) = 2.82$, $p = 0.0056$), however, similarly to what was observed in bilateral EC, this alternative neural geometry emerging did not survive multiple comparisons across periodicities and hemispheres (5x2, all results one-tailed. The significance threshold was set at $p < 0.05$ for 6-fold symmetry and $p_{bonferroni} < 0.005$ for alternative periodicities). The boxes indicate the IQR. The horizontal black lines indicate the median and the whiskers indicate the distance between the highest and the lowest values in the sample from the estimated first and third quartiles. The dots represent single participant to the experiment.

We then analyze the two hemispheres separately and found no significant BOLD modulation by any of the tested periodicities in the right EC (One sample t-test; 4-Fold: $t(18) = 0.17$, $p = 0.43$; 5-Fold: $t(18) = -0.27$, $p = 0.6$; 6-Fold: $t(18) = 0.47$, $p = 0.31$; 7-Fold: $t(18) = -0.40$, $p = 0.65$, $\alpha_{Bonferroni} = 0.005$ corrected across periodicities and hemispheres (5X2), one-tailed, Fig. 6B-6C). In the left EC, we again detected a significant 8-Fold symmetry which, however, did not survive multiple comparisons correction across hemispheres and tested periodicities (One sample t-test; 8-Fold: $t(18) = 2.82$, $p = 0.0056$, $\alpha_{Bonferroni} = 0.005$ corrected across periodicities and hemispheres, one-tailed, Fig.6C) and no other modulation of the BOLD signal (One sample t-test; 4-Fold: $t(18) = -0.05$, $p = 0.52$; 5-Fold: $t(18) = -1.24$, $p = 0.88$; 6-Fold: $t(18) = 0.005$, $p = 0.49$; 7-Fold: $t(18) = 0.45$, $p = 0.32$, $\alpha_{Bonferroni} = 0.005$ corrected across periodicities and hemispheres, one-tailed, Fig. 6C). Analyses on the second relation extraction period reveal a similar pattern of results, with no 60° modulation of the BOLD signal in early blind individuals bilateral EC (one sample t-test; 6-Fold: $t(18) = -2.46$, $p = 0.98$,; $\alpha = 0.05$, one-tailed, Fig. 6A) not in the left EC (one sample t-test; 6-Fold: $t(18) = -2.46$, $p = 0.98$, $\alpha = 0.05$, one-tailed, Fig. 6B) nor right EC (one sample t-test; 6-Fold: $t(18) = -1.96$, $p = 0.96$, $\alpha = 0.05$, one-tailed, Fig. 6B). Furthermore we did not detect any other modulation of the BOLD signal by the remaining tested alternative periodicities in bilateral EC (One sample t-test; 4-Fold: $t(18) = =0.17$, $p = 0.53$; 5-Fold: $t(18) = 0.06$, $p = 0.47$; 7-Fold: $t(18) = -1.2$, $p = 0.87$; 8-Fold: $t(18) = -1.97$, $p = 0.98$; $\alpha_{Bonferroni} = 0.005$ corrected across periodicities and hemispheres, one-tailed, Fig. 6A) nor left EC (One sample t-test; 4-Fold: $t(18) = 0.4$, $p = 0.34$; 5-Fold: $t(18) = 0.18$, $p = 0.42$; 7-Fold: $t(18) = -1.2$, $p = 0.89$; 8-Fold: $t(18) = -2.16$, $p = 0.97$; $\alpha_{Bonferroni} = 0.005$ corrected across periodicities and hemispheres, one-tailed, Fig. 6D) or the right EC (One sample t-test; 4-Fold: $t(18) = 0.19$, $p = 0.42$; 7-Fold: $t(18) = -1.13$, $p = 0.86$. Wilcoxon signed rank exact test; 5-Fold: $V = 61$, $p = 0.91$; 8-Fold: $V = 100$, $p = 0.42$; $\alpha_{Bonferroni} = 0.005$ corrected across periodicities and hemispheres, one-tailed, Fig. 6D). Critically, when comparing the six-fold

symmetry magnitude across the two groups, considering both the relation extraction periods, we observed a significant main effect of group (Repeated measure ANOVA ; $F(1,41)$, $p < 0.001$, $\alpha = 0.05$, two-tailed, Fig. 7A) indicating a stronger 6-fold symmetry in sighted compared to blind. The ANOVA also revealed the absence of a main effect of relation periods ($F(1,41) = 1.66$, $p = 0.2$, $\eta^2 = 0.019$), and no relation × group interaction ($F(1,41) = 3.17$, $p = 0.17$).

Finally, when we consider all the periodicities (folds) tested in the analyses, in the two relation extraction periods, we observed a significant interaction between tested periodicity and groups, largely driven, it seems, by the difference in 6-fold symmetry (Linear mixed model; main effect of tested periodicities: $\chi^2(4)= 0.125$, $p = 0.97$; main effect of relation period : $\chi^2(1)= 2.73$, $p = 0.1$; main effect of group: $\chi^2(1)= 5.04$, $p = 0.03$; tested periodicities × relation interaction: $\chi^2(4) = 1.01$, $p = 0.39$; tested periodicities × group interaction: $\chi^2(4) = 3.01$, $p = 0.02$; relation × group interaction: $\chi^2(1) = 3.87$, $p = 0.057$; tested periodicities × relation × group interaction: $\chi^2(4) = 2.12$, $p = 0.08$; $\alpha = 0.05$, two-tailed, Fig. 7B)

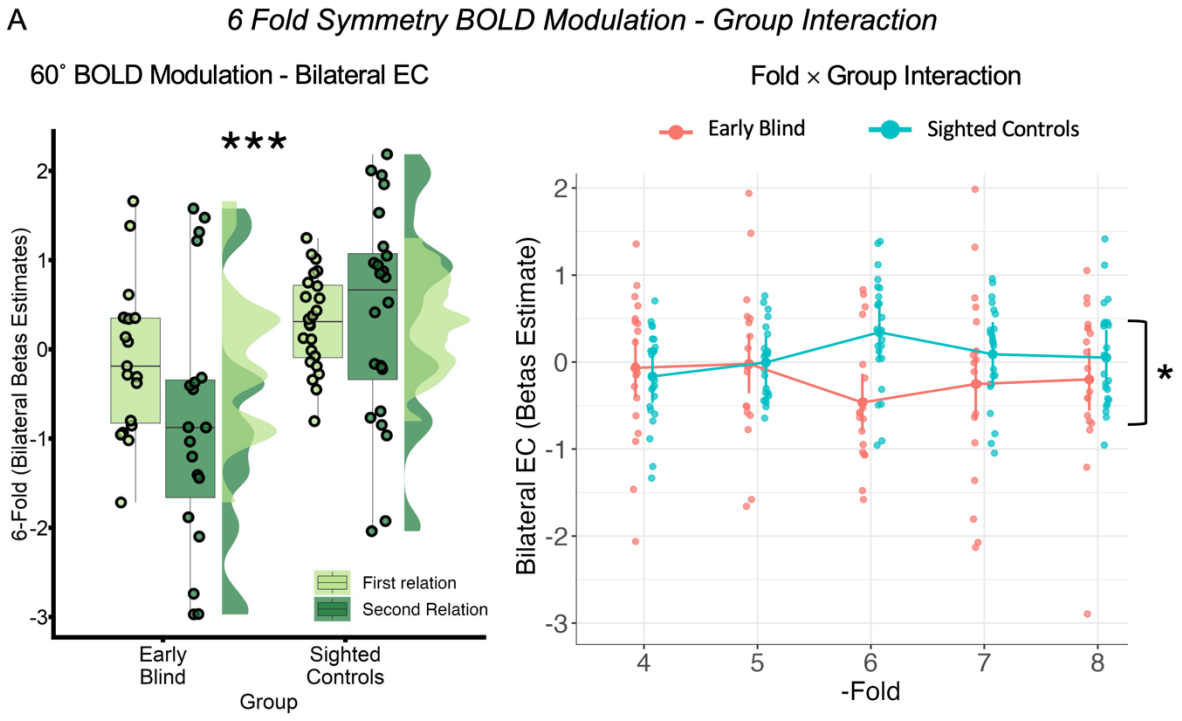

**Fig.7: A** The magnitude of the 6-fold symmetry was significantly greater in sighted compared to early blind individuals, considering both relation extraction periods (left, repeated measure ANOVA; $F(1,41) = 3.17$, $p < 0.001$, two-tailed). Moreover, linear mixed models on all the tested periodicities revealed a significant fold × group interaction (right, $\chi^2(4) = 3.01$, $p = 0.02$, two-tailed), and a significant effect of group (right, $\chi^2(1) = 5.04$, $p = 0.03$). These results, albeit driven by the observed higher 6-fold symmetry in sighted individuals, possibly suggest a general influence of visual experience on the overall pattern of BOLD modulation exerted by the different periodicities. The boxes (left) indicate the IQR. The horizontal black lines indicate the median and the whiskers indicate the distance between the highest and the lowest values in the sample from the estimated first and third quartiles. The dots, in both graphs represent single participant to the experiment. Asterisk above the boxes indicates significant levels of ***p<0.001 and *p<0.05.

In sum, a significant 6-fold symmetry was observed in the bilateral EC, and to some extent also in the left and right EC, of sighted control individuals during a conceptual navigation task in a sound space. Conversely, a reduced 6-fold symmetry has been observed in the EC of early blind individuals. Crucially, the magnitude of the grid-like coding detected in the sighted group was significantly higher compared to early blind individuals. Interestingly, a significant general difference between the two groups has been detected across all the tested periodicities, however, these results might be driven by the higher 6-fold symmetry detected in the sighted group. Finally, the emergence of an 8-fold symmetry during the first relation extraction and a negative 6-fold symmetry during the second relation extraction (one sample t-test; 6-Fold = $t(18)$, $p = 0.02$, two-tailed) is interesting, although neither of the two results survive correction for multiple comparisons.

**Discussion**

We've investigated the influence of early visual experience on the development of entorhinal cortex cognitive maps during conceptual navigation. Specifically, we investigated whether early blind individuals showed a 60° sinusoidal modulation (i.e., grid-like coding) in the EC during a conceptual navigation task in a sound space environment, similar to those observed in previous studies[22–26,29] and in a previously conducted pilot experiment (see above) in sighted individuals. Here we report two main findings.

First, we showed that early blind and sighted control participants performed the task and navigated the sound space in a highly-similar way. Indeed, behavioral results showed no difference in accuracy between the two groups while solving the task. Additionally, perceived difficulty scores, obtained by a questionnaire filled up by participants at the end of each fMRI session, revealed no difference in the perceived general difficulty of the task across groups. Early blind individuals were, overall, slightly slower, at least numerically, in performing the sound analogy task compared to sighted controls, however we controlled for this difference modeling brain activity using a boxcar function with RTs as event duration (See methods). The whole-brain analyses conducted on neuroimaging data gave further support to the hypothesis that both sighted and blind participants were navigating our soundscape. Indeed, adaptation analyses on pitch perception and Euclidean distance computation revealed the activation of the same brain regions in both sighted and early blind individuals with no differences between groups. Specifically, we've investigated BOLD modulation with respect to the difference in pitch between the two sounds constituting each sound pair (see method). We've observed a repetition enhancement effect (i.e., greater BOLD modulation for similar pitches) in the Heschel's gyrus of both sighted and early blind individuals. Increases in BOLD magnitude in response to sounds that have similar pitches is a phenomenon that had already been reported in animals and humans[56,57] and was associated with low-level computation of pitch characteristics.

Furthermore, in literature, is widely reported that computation of Euclidean distances between two spatial locations relies on the activation of frontal, parietal, and medial temporal lobe regions [58–60]. Recently, the engagement of these brain regions has been demonstrated to subtend also the computations of Euclidean distance in conceptual spaces [29,61]. To solve correctly our conceptual navigation tasks, participants needed to navigate the 2D duration-pitch space, going from one sound to the other in order to extract the relation between them. Thus, we've investigated whether we could observe BOLD-adaptation in those brain areas related to the computation of the Euclidean distance when participants navigate the sound space. We've detected a decrease BOLD modulation (adaptation effect) the more the two sounds composing a sound pair (e.g., sound 1 – Sound 2) were closer to each other in the 2D sound space. This effect was evident in frontal and parietal brain regions in sighted and early blind individuals, once again with no difference across groups.

Taken together, the similarity between the two groups in pitch perception and Euclidean distance computations not only rules out differences in perceptual processing but, more importantly, strongly suggests that both sighted and early blind individuals rely on the same fronto-parietal network to compute Euclidean distances in a 2-dimensional sound space. This finding highlights the resilience of this neural mechanism, even in the absence of early visual input. Furthermore, the results exclude the possibility of task-related effects influencing potential differences in the use of cognitive maps.

The second main result of this experiment is that early blindness influences the emergence of a grid-like coding in the entorhinal cortex in conceptual navigation tasks. Indeed, we observed a 60° sinusoidal modulation of the BOLD signal in the EC of sighted control individuals during the conceptual task, replicating previous studies [24,29] as well as results obtained in our pilot experiment. However, we observed no 6-fold symmetry in the EC of early blind individuals while performing the same task. Crucially, the magnitude of the detected grid-like coding in sighted individuals' EC was significantly higher compared to the one observed in early blind participants' EC. These results suggest a possible influence of the absence of visual experience on the emergence of grid-like coding in the EC in conceptual navigation tasks. In humans, at least to our knowledge, only one study investigated the influence of blindness on the emerging of grid-like coding (Chapter 2 of this thesis, [45]) during an imagined spatial navigation task, reporting a similar disruption of the 6-fold symmetry effect, accompanied by an alteration of the neural geometry of cognitive maps expressed in a 4-fold symmetry (90° modulation of the BOLD signal). If the emergence of a 4-fold symmetry in Chapter 2 could be due to some peculiarity of the chosen environment (see General Discussion), it appears clear that early visual deprivation influences the neural geometry of entorhinal maps both in spatial and conceptual navigation, disrupting the typical hexadirectional coding related to canonical grid-cells activity.
On a side note, the 8-fold symmetry (~ 22° modulation of the BOLD signal) detected in early blind individuals' EC during the first relation extraction period, in this experiment, might suggest, at first, the construction of a different representation of the navigated environment by this group of participants. However, this alternative periodicity did not survive multiple comparisons, and it was, therefore, hard to draw a conclusion on it. Further analyses (e.g., RSA) will be needed to better understand reliability of this result.

In this study, we have shown that the neural correlates of Euclidean distance computation are shared between sighted and early blind individuals and thus resilient to early visual deprivation. We, moreover, provided the first, yet preliminary evidence, of the influence of blindness on the development of cognitive maps for conceptual spaces, with a significantly reduced 6-fold symmetry in early blind individuals' EC compared to the one detected in sighted control individuals.

**References:**


1. Bellmund JLS, Gärdenfors P, Moser EI, Doeller CF. Navigating cognition: Spatial codes for human thinking. *Science*. 2018;362(6415):eaat6766. doi:10.1126/science.aat6766

2. Courellis HS, Minxha J, Cardenas AR, et al. Abstract representations emerge in human hippocampal neurons during inference. *Nature*. 2024;632(8026):841-849. doi:10.1038/s41586-024-07799-x

3. Peer M, Brunec IK, Newcombe NS, Epstein RA. Structuring Knowledge with Cognitive Maps and Cognitive Graphs. *Trends in Cognitive Sciences*. 2020;0(0). doi:10.1016/J.TICS.2020.10.004

4. Banino A, Barry C, Uria B, et al. Vector-based navigation using grid-like representations in artificial agents. *Nature*. 2018;557(7705):429-433. doi:10.1038/s41586-018-0102-6

5. George D, Rikhye RV, Gothoskar N, Guntupalli JS, Dedieu A, Lázaro-Gredilla M. Clone-structured graph representations enable flexible learning and vicarious evaluation of cognitive maps. *Nat Commun*. 2021;12(1):2392. doi:10.1038/s41467-021-22559-5

6. Stachenfeld KL, Botvinick MM, Gershman SJ. The hippocampus as a predictive map. *Nat Neurosci*. 2017;20(11):1643-1653. doi:10.1038/nn.4650

7. Zhang K. Representation of spatial orientation by the intrinsic dynamics of the head-direction cell ensemble: a theory. *J Neurosci*. 1996;16(6):2112-2126. doi:10.1523/JNEUROSCI.16-06-02112.1996

8. Dekker R, Otto F, Summerfield C. *Determinants of Human Compositional Generalization*. PsyArXiv; 2022. doi:10.31234/osf.io/qnpw6

9. Epstein RA, Patai EZ, Julian JB, Spiers HJ. The cognitive map in humans: Spatial navigation and beyond. *Nature Neuroscience*. 2017;20(11):1504-1513. doi:10.1038/nn.4656

10. Whittington JCR, Muller TH, Mark S, et al. The Tolman-Eichenbaum Machine: Unifying Space and Relational Memory through Generalization in the Hippocampal Formation. *Cell*. 2020;183(5):1249-1263.e23. doi:10.1016/j.cell.2020.10.024

11. Whittington JCR, McCaffary D, Bakermans JJW, Behrens TEJ. How to build a cognitive map: insights from models of the hippocampal formation. *arXiv:220201682 [cs, q-bio]*. Published online February 3, 2022. Accessed March 4, 2022. http://arxiv.org/abs/2202.01682

12. Behrens TEJ, Muller TH, Whittington JCR, et al. What Is a Cognitive Map? Organizing Knowledge for Flexible Behavior. *Neuron*. 2018;100(2):490-509. doi:10.1016/j.neuron.2018.10.002

13. Tolman EC. Cognitive maps in rats and men. *Psychological Review*. 1948;55(4):189-208. doi:10.1037/h0061626

14. O'Keefe J, Dostrovsky J. The hippocampus as a spatial map. Preliminary evidence from unit activity in the freely-moving rat. *Brain Research*. 1971;34(1):171-175. doi:10.1016/0006-8993(71)90358-1

15. Taube JS, Muller RU, Ranck JB. Head-direction cells recorded from the postsubiculum in freely moving rats. I. Description and quantitative analysis. *J Neurosci*. 1990;10(2):420-435. doi:10.1523/JNEUROSCI.10-02-00420.1990

16. Hafting T, Fyhn M, Molden S, Moser MB, Moser EI. Microstructure of a spatial map in the entorhinal cortex. *Nature*. 2005;436(7052):801-806. doi:10.1038/nature03721

17. Doeller CF, Barry C, Burgess N. Evidence for grid cells in a human memory network. *Nature*. 2010;463(7281):657-661. doi:10.1038/nature08704

18. Giari G, Vignali L, Xu Y, Bottini R. MEG frequency tagging reveals a grid-like code during attentional movements. *Cell Reports*. 2023;42(10):113209. doi:10.1016/j.celrep.2023.113209

19. Horner AJ, Bisby JA, Zotow E, Bush D, Burgess N. Grid-like Processing of Imagined Navigation. *Current Biology*. 2016;26(6):842-847. doi:10.1016/j.cub.2016.01.042

20. Julian JB, Keinath AT, Frazzetta G, Epstein RA. Human entorhinal cortex represents visual space using a boundary-anchored grid. *Nat Neurosci*. 2018;21(2):191-194. doi:10.1038/s41593-017-0049-1

21. Nau M, Navarro Schröder T, Bellmund JLS, Doeller CF. Hexadirectional coding of visual space in human entorhinal cortex. *Nat Neurosci*. 2018;21(2):188-190. doi:10.1038/s41593-017-0050-8

22. Constantinescu AO, OReilly JX, Behrens TEJ. Organizing conceptual knowledge in humans with a gridlike code. *Science*. 2016;352(6292):1464-1468. doi:10.1126/science.aaf0941

23. Bao X, Gjorgieva E, Shanahan LK, Howard JD, Kahnt T, Gottfried JA. Grid-like Neural Representations Support Olfactory Navigation of a Two-Dimensional Odor Space. *Neuron*. 2019;102(5):1066-1075.e5. doi:10.1016/j.neuron.2019.03.034

24. Park SA. Inferences on a multidimensional social hierarchy use a grid-like code. *Nature Neuroscience*. 2021;24:27.

25. Liang Z, Wu S, Wu J, Wang WX, Qin S, Liu C. Distance and grid-like codes support the navigation of abstract social space in the human brain. *eLife*. 2024;12:RP89025. doi:10.7554/eLife.89025

26. Viganò S, Rubino V, Soccio AD, Buiatti M, Piazza M. Grid-like and distance codes for representing word meaning in the human brain. *NeuroImage*. 2021;232:117876. doi:10.1016/j.neuroimage.2021.117876

27. Nitsch A, Garvert MM, Bellmund JLS, Schuck NW, Doeller CF. Grid-like entorhinal representation of an abstract value space during prospective decision making. *Nat Commun*. 2024;15(1):1198. doi:10.1038/s41467-024-45127-z

28. Qasim SE, Reinacher PC, Brandt A, Schulze-Bonhage A, Kunz L. Neurons in the human entorhinal cortex map abstract emotion space. Published online August 12, 2023. doi:10.1101/2023.08.10.552884

29. Viganò S, Bayramova R, Doeller CF, Bottini R. *Mental Search of Concepts Is Supported by Egocentric Vector Representations and Restructured Grid Maps*. Neuroscience; 2023. doi:10.1101/2023.01.19.524704

30. Abrahamse E, van Dijck JP, Majerus S, Fias W. Finding the answer in space: the mental whiteboard hypothesis on serial order in working memory. *Front Hum Neurosci*. 2014;8:932. doi:10.3389/fnhum.2014.00932

31. Cristoforetti G, Majerus S, Sahan MI, van Dijck JP, Fias W. Neural Patterns in Parietal Cortex and Hippocampus Distinguish Retrieval of Start versus End Positions in Working Memory. *Journal of Cognitive Neuroscience*. 2022;34(7):1230-1245. doi:10.1162/jocn_a_01860

32. Fias W. The Importance of Magnitude Information in Numerical Processing: Evidence from the SNARC Effect. *Mathematical Cognition*. 1996;2(1):95-110. doi:10.1080/135467996387552

33. Casasanto D, Bottini R. Mirror reading can reverse the flow of time. *J Exp Psychol Gen*. 2014;143(2):473-479. doi:10.1037/a0033297

34. Casasanto D, Bottini R. Spatial language and abstract concepts. *WIRES Cognitive Science*. 2014;5(2):139-149. doi:10.1002/wcs.1271

35. Becker SL. The ordinal position effect. *Quarterly Journal of Speech*. Published online April 1, 1953. doi:10.1080/00335635309381862

36. Eichenbaum H. Time (and space) in the hippocampus. *Current Opinion in Behavioral Sciences*. 2017;17:65-70. doi:10.1016/j.cobeha.2017.06.010

37. Gevers W, Verguts T, Reynvoet B, Caessens B, Fias W. Numbers and space: a computational model of the SNARC effect. *J Exp Psychol Hum Percept Perform*. 2006;32(1):32-44. doi:10.1037/0096-1523.32.1.32

38. Nau M, Julian JB, Doeller CF. How the Brain's Navigation System Shapes Our Visual Experience. *Trends in Cognitive Sciences*. 2018;22(9):810-825. doi:10.1016/J.TICS.2018.06.008

39. Piccardi L, De Luca M, Nori R, Palermo L, Iachini F, Guariglia C. Navigational Style Influences Eye Movement Pattern during Exploration and Learning of an Environmental Map. *Frontiers in Behavioral Neuroscience*. 2016;10. Accessed May 9, 2023. https://www.frontiersin.org/articles/10.3389/fnbeh.2016.00140

40. Bottini R, Doeller CF. Knowledge Across Reference Frames: Cognitive Maps and Image Spaces. *Trends in Cognitive Sciences*. 2020;24(8):606-619. doi:10.1016/j.tics.2020.05.008

41. Moser EI, Moser MB, McNaughton BL. Spatial representation in the hippocampal formation: a history. *Nat Neurosci*. 2017;20(11):1448-1464. doi:10.1038/nn.4653

42. Rowland DC, Roudi Y, Moser MB, Moser EI. Ten Years of Grid Cells. *Annual Review of Neuroscience*. 2016;39(Volume 39, 2016):19-40. doi:10.1146/annurev-neuro-070815-013824

43. Save E, Cressant A, Thinus-Blanc C, Poucet B. Spatial Firing of Hippocampal Place Cells in Blind Rats. *J Neurosci*. 1998;18(5):1818-1826. doi:10.1523/JNEUROSCI.18-05-01818.1998

44. Asumbisa K, Peyrache A, Trenholm S. *Flexible Cue Anchoring Strategies Enable Stable Head Direction Coding in Both Sighted and Blind Animals*. Neuroscience; 2022. doi:10.1101/2022.01.12.476111

45. Sigismondi F, Xu Y, Silvestri M, Bottini R. Altered grid-like coding in early blind people. *Nat Commun*. 2024;15(1):3476. doi:10.1038/s41467-024-47747-x

46. Schindler A, Bartels A. Parietal Cortex Codes for Egocentric Space beyond the Field of View. *Current Biology*. 2013;23(2):177-182. doi:10.1016/j.cub.2012.11.060

47. Bergmann HC, Rijpkema M, Fernández G, Kessels RPC. Distinct neural correlates of associative working memory and long-term memory encoding in the medial temporal lobe. *NeuroImage*. 2012;63(2):989-997. doi:10.1016/j.neuroimage.2012.03.047

48. Ramezanpour H, Fallah M. The role of temporal cortex in the control of attention. *Current Research in Neurobiology*. 2022;3:100038. doi:10.1016/j.crneur.2022.100038

49. Barron HC, Garvert MM, Behrens TEJ. Repetition suppression: a means to index neural representations using BOLD? *Phil Trans R Soc B*. 2016;371(1705):20150355. doi:10.1098/rstb.2015.0355

50. Allen GL, ed. *Human Spatial Memory: Remembering Where*. Erlbaum; 2004.

51. Röhl M, Uppenkamp S. Neural Coding of Sound Intensity and Loudness in the Human Auditory System. *JARO*. 2012;13(3):369-379. doi:10.1007/s10162-012-0315-6

52. Schirmer A, Fox PM, Grandjean D. On the spatial organization of sound processing in the human temporal lobe: A meta-analysis. *NeuroImage*. 2012;63(1):137-147. doi:10.1016/j.neuroimage.2012.06.025

53. Zündorf IC, Lewald J, Karnath HO. Neural Correlates of Sound Localization in Complex Acoustic Environments. *PLOS ONE*. 2013;8(5):e64259. doi:10.1371/journal.pone.0064259

54. Altmann CF, Nakata H, Noguchi Y, et al. Temporal Dynamics of Adaptation to Natural Sounds in the Human Auditory Cortex. *Cerebral Cortex*. 2008;18(6):1350-1360. doi:10.1093/cercor/bhm166

55. Jääskeläinen IP, Ahveninen J, Bonmassar G, et al. Human posterior auditory cortex gates novel sounds to consciousness. *Proc Natl Acad Sci U S A*. 2004;101(17):6809-6814. doi:10.1073/pnas.0303760101

56. Brosch M, Schulz A, Scheich H. Processing of Sound Sequences in Macaque Auditory Cortex: Response Enhancement. *Journal of Neurophysiology*. 1999;82(3):1542-1559. doi:10.1152/jn.1999.82.3.1542

57. Heinemann LV, Rahm B, Kaiser J, Gaese BH, Altmann CF. Repetition Enhancement for Frequency-Modulated but Not Unmodulated Sounds: A Human MEG Study. *PLOS ONE*. 2010;5(12):e15548. doi:10.1371/journal.pone.0015548

58. Clark BJ, Simmons CM, Berkowitz LE, Wilber AA. The retrosplenial-parietal network and reference frame coordination for spatial navigation. *Behavioral Neuroscience*. 2018;132(5):416-429. doi:10.1037/bne0000260

59. Epstein RA. Parahippocampal and retrosplenial contributions to human spatial navigation. *Trends in Cognitive Sciences*. 2008;12(10):388-396. doi:10.1016/j.tics.2008.07.004

60. Howard LR, Javadi AH, Yu Y, et al. The Hippocampus and Entorhinal Cortex Encode the Path and Euclidean Distances to Goals during Navigation. *Current Biology*. 2014;24(12):1331-1340. doi:10.1016/j.cub.2014.05.001

61. Parkinson C, Liu S, Wheatley T. A Common Cortical Metric for Spatial, Temporal, and Social Distance. *Journal of Neuroscience*. 2014;34(5):1979-1987. doi:10.1523/JNEUROSCI.2159-13.2014

62. Khalid, I. B., Reifenstein, E. T., Auer, N., Kunz, L., & Kempter, R. (2024). Quantitative modeling of the emergence of macroscopic grid-like representations. *Elife*, *13*, e85742.

## Supplementary materials

**Supplementary Table 1. Brain regions modulated by absolute pitch difference (voxel-level: $p < 0.001$; cluster-level: $p_{fwe} < 0.05$)**

| Brain Regions | MNI Coordinates of the Peak Voxel | | | Peak T Value |
|---|---|---|---|---|
| | X | Y | Z | |
| **Sighted** | | | | |
| Right Herschel's gyrus | 50 | -24 | 10 | 6.8 |
| Left Herschel's gyrus | -51 | -14 | 5 | 6.30 |
| **Early Blind** | | | | |
| Right Herschel's gyrus | 50 | -30 | 8 | 7.00 |
| Left Herschel's gyrus | -54 | -17 | 2 | 5.30 |
| **Sighted Controls + Early Blind** | | | | |
| Right Herschel's gyrus | 58 | -24 | 8 | 7.45 |
| Left Herschel's gyrus | -52 | -14 | 2 | 7.59 |

**Supplementary Table 2a. Brain regions modulated by Euclidean Distance (voxel-level: $p < 0.001$)**

| Brain Regions | MNI Coordinates of the Peak Voxel | | | Peak T Value |
|---|---|---|---|---|
| | X | Y | Z | |
| **Sighted** | | | | |
| Right Orbitofrontal Cortex | 16 | 53 | -15 | 4.45 |
| Left Orbitofrontal Cortex | -14 | -53 | -15 | 5.10 |
| Left Angular gyrus | -52 | -52 | 25 | 4.78 |
| **Early Blind** | | | | |
| Right Orbitofrontal Cortex | 20 | 60 | -15 | 5.13 |
| Right Angular gyrus | 40 | -64 | -48 | 4.46 |

**Supplementary Table 2b. Brain regions modulated by Euclidean Distance voxel level: $p < 0.001$; cluster-level: $p_{fwe} < 0.05$)**

| Brain Regions | MNI Coordinates of the Peak Voxel | | | Peak T Value |
|---|---|---|---|---|
| | X | Y | Z | |
| **Sighted Controls + Early Blind** | | | | |
| Right Orbitofrontal Cortex | 23 | 60 | -15 | 5.69 |
| Left Angular gyrus | -47 | -50 | 55 | 4.41 |
| Right Angular gyrus | 43 | -57 | 48 | 4.38 |

**Supplementary Table 3. Demographics of early blind and sighted individuals**

| EB CODE | AGE | GENDER | ONSET OF TOTAL BLINDNESS | ETIOLOGY | SC CODE | AGE | GENDER |
|---|---|---|---|---|---|---|---|
| EB01 | 23 | M | Birth | Optic nerve hypoplasia | SC14 | 29 | M |
| EB02 | 45 | M | Birth | Retinitis pigmentosa | SC11 | 41 | M |
| EB03 | 34 | F | Birth | Retinal burnt in the incubator | SC05 | 29 | F |
| EB04 | 54 | M | Birth | Microphthalmia | SC20 | 58 | M |
| EB05 | 37 | F | Birth | Premature retinopathy | SC03 | 30 | F |
| EB06 | 35 | F | Birth | Bilateral aplasia | SC08 | 29 | F |
| EB07 | 36 | F | Birth | Retrolenticular fibroplasia | SC19 | 38 | F |
| EB08 | 30 | M | Birth | Leber congenital amaurosis | SC07 | 27 | M |
| EB09 | 36 | M | 8 months | Congenital retinitis Pigmentosa | SC15 | 32 | M |
| EB10 | 33 | M | Birth | Bilateral congenital anophthalmos | SC02 | 31 | M |
| EB11 | 39 | M | 2 years | Bilateral retinoblastoma | SC09 | 34 | M |
| EB12 | 43 | F | Birth | Premature retinopathy | SC16 | 43 | F |
| EB13 | 35 | M | Birth | Premature retinopathy | SC06 | 33 | M |
| EB14 | 46 | F | Birth | Optic nerve hypoplasia | SC01 | 51 | F |
| EB15 | 52 | M | Birth | Congenital retinitis pigmentosa | SC12 | 47 | M |
| EB16 | 35 | F | Birth | Premature retinopathy | SC22 | 32 | F |
| EB17 | 40 | M | 3 years | Dominant optic atrophy | SC10 | 37 | M |
| EB18 | 35 | M | Birth | Premature retinopathy | SC04 | 31 | M |
| EB19 | 52 | M | Birth | Bilateral congenital Glaucoma | SC13 | 53 | M |
| EB20 | 54 | M | Birth | Microphthalmia | SC23 | 44 | M |
| EB21 | 36 | F | Birth | Premature retinopathy | SC17 | 26 | F |
| EB22 | 33 | F | Birth | Premature retinopathy | SC24 | 26 | F |

| | | | | | | | |
|---|---|---|---|---|---|---|---|
| EB23 | 37 | F | Birth | Congenital retinitis pigmentosa | SC21 | 30 | F |
| | | | | | SC18 | 26 | M |

# IV

# GENERAL DISCUSSION

Spatial and conceptual knowledge is organized in dynamic flexible representations that take the name of cognitive maps [1–10]. As extensively discussed in the introduction section of this thesis, the creation of cognitive maps relies on the integrated activity of spatially tuned cells situated within the hippocampal-entorhinal system, among which we find grid cells that tessellate the environment in a hexagonal lattice. Grid-like coding has been observed, among other species, in humans' entorhinal cortex during spatial navigation tasks [2,4,11] and tasks that required the navigation of abstract spaces such as social space or word space [12,13]. Although the influence played by spatial experience on the organization of abstract knowledge is well reported in literature, outside the cognitive maps field [14–17], the relation between these two cognitive domains, at the brain level, is far from being understood.

Here, I've tried to provide the first insight into the relation between space and concepts by focusing on grid-like coding. Moreover, I've proposed two complementary hypotheses to try to explain this relation: the scaffolding hypothesis and the independence hypothesis. Briefly, the scaffolding hypothesis assumes that the neural mechanisms developed for navigating in space have been recycled for navigating abstract knowledge. Thus, differences in the way space is navigated will be reflected in the way concepts are navigated. In contrast, the independence hypothesis proposes that the mechanisms underlying spatial and conceptual navigation develop independently; therefore, conceptual navigation will not be affected by differences in how space is encoded and navigated. To provide evidence for one of the two hypotheses, I've implemented one imagined spatial navigation (Chapter 2) and one conceptual navigation (Chapter 3) experiment and performed them, comparing sighted and early blind reliance on entorhinal cortex cognitive maps to solve the tasks. In summary, the critical findings of the two studies were that the typical six-fold symmetry found in the entorhinal cortex during spatial and conceptual navigation, and observed in the sighted participants, was reduced in early blind people. This was the case both during spatial and conceptual navigation, although during spatial navigation we observed an alternative

organization (4-Fold) of the neural geometry in the entorhinal cortex of early blind individuals. Here I integrate the results of the two experiments by interpreting them in the light of the two proposed hypotheses.

Are the predictions of the scaffolding hypothesis upheld? In its most general instantiation, the scaffolding hypothesis will predict that if sighted and early blind individuals showed a different grid structure in spatial navigation, they will also show a difference in conceptual navigation. This is not necessarily predicted by the independence hypothesis, because here the hypothesis is that spatial and conceptual navigation develop, indeed, independently.

At this general level, the scaffolding hypothesis is upheld by our results. In fact, early blind individuals showed a reduced 6-Fold modulation of the BOLD signal during spatial as well as during conceptual navigation, while a significant 6-Fold symmetry was detected in both cases in sighted individuals' EC. Control analyses in both the experiments (Chapter 2 and Chapter 3) strongly suggested that these differences can't be attributed to the fact that early blind individuals were not performing the tasks or were not navigating the environments. On the contrary, our analyses suggest that the involvement of the Human Navigation Network (HNN, Chapter 2), as well as the representations of the Euclidean Distances (ED, Chapter 3) in parietal-frontal regions, were identical in sighted and early blind participants showing strong resiliency of these neural networks in face of early visual deprivation. This makes our results in the entorhinal cortex even more striking because the grid system seems to be the only system, among the ones tested, affected by visual deprivation. Why this should be the case? The reason might emerge if we think about what is the role of grid cells, and more generally, of the entorhinal cortex, in spatial and conceptual navigation. It has been suggested that grid cells encode and store relational information about different landmarks, objects, and concepts in cognitive maps [2,18,19]. Such relational information is the one that allows the extraction of the structure of the environment [1] which, at least in a spatial context, is believed to be allocentric [6,20]. It is this allocentric structural representation that indeed might be distorted and more difficult to extract in early blind individuals compared to sighted individuals. In space, the construction of allocentric cognitive maps benefits largely from vision [21–23], especially when it comes to large environments [24,25]. This is also supported by studies showing allocentric impairments but preserved egocentric representations in early blind individuals [26–29]

The scaffolding hypothesis suggests that such allocentric deficit in spatial representations is extended to conceptual spaces. Indeed, recent evidence in our laboratory shows that also conceptual navigation takes place across complementary allocentric and egocentric frames of reference (respectively in the entorhinal and the parietal cortices)[10,30,31] supporting the possibility that a preference for a reference frame in spatial navigation could correspond to a similar preference during conceptual navigation.

Nevertheless, in our spatial navigation experiment, we detected in early blind individuals' entorhinal cortex an alternative periodicity, a 4-Fold symmetry, which was not present during conceptual navigation. This might constitute a potential issue for the scaffolding hypothesis because, according to this one, if an alternative periodicity emerges in spatial navigation, then we would expect the same alternative periodicity arising during conceptual navigation. However, the emergence of a 4-fold symmetry might be related to the feature of the chosen environment (i.e., a clock), more than to the lack of visual experience itself. The clock environment may have spurred the overuse of the two principal axes, as in previous tasks in which the 4-Fold symmetry emerged (such as a hairpin maze[32]). As discussed in Chapter 2, the main axis of the clock may have provided an important anchor to navigate the environment and represent its overall relational structure, increasing the stability of entorhinal structural representation although with a different grid-cell geometry (4-Fold). The same anchorage, instead, was not available in the conceptual space in which therefore a stable grid geometry, across blind individuals, could not emerge. If this is the case, we would predict that during (imagined) spatial navigation in an environment without major perpendicular axes, early blind individuals would not show a 4-Fold symmetry, and, in turn, if it would be possible to construct a conceptual space with clear perpendicular axes that can be used as anchors, 4-Fold symmetry would emerge also in conceptual navigation.

Despite these considerations, however, one may say that the independence hypothesis would have better predicted these results, given that partially different patterns emerged in spatial and conceptual navigation. We think this is a hard position to hold because, at this point, the independence hypothesis should also explain why blind people did not show the typical Hexadirectional modulation during conceptual navigation as sighted people do. Especially given that blind people offer a behavioral and neural profile that is indistinguishable from the one of

sighted. Explaining this result without considering the role that vision may have in organizing relational information, and therefore falling back on the scaffolding hypothesis, seems quite challenging to us.

In this thesis, the focus was put mainly on grid cells and grid-like coding as the crucial neural mechanisms subtending cognitive maps' development, and, more generally, the humans' ability to encode and navigate throughout relational knowledge. However, one could argue that considering just entorhinal cortex cognitive maps might be reductive, as many more neural correlates participate in, and guarantee, the successful navigation of spatial and abstract knowledge. Indeed, other brain regions such as the medial temporal lobe, particularly the hippocampus, as well as frontal and parietal areas have been observed to encode relational knowledge and support its navigation [3,10,12,33]. It is important to stress that, the works presented here aimed to unveil the relationship between spatial and abstract navigation by testing the scaffolding hypothesis, and that studying grid cells, relying on early blindness as a model, offered an easy way to reach our goal. However, it should also be acknowledged that considering the global picture, rather than a specific neural correlate, could offer a valid alternative which might explain the observed absence of differences in behavioral performance, throughout the experiments, across sighted and early blind participants. Indeed, in both the spatial navigation study (Chapter 2) and conceptual navigation study (Chapter 3), the two groups performed equally well at the behavioral level, despite the differences detected in the entorhinal cortex activity. In the conceptual navigation task, moreover, grid-like coding was absent and no other regular periodicity was detected without any apparent effect on the navigation abilities of early blind people. How is it possible that the difference in grid-like coding recruitment between sighted and early blind individuals results in the same behavioral pattern? The answer may lie in the fact that grid cells might support navigation through relational knowledge but are not essential for it. This idea is supported by two main considerations. First, cognitive map representations are sustained not only by grid cells but also by the activity of other spatially tuned cells, such as place cells, which provide information about the navigator's position in the environment[34]; head direction cells, which encode the navigator's heading direction[35]; and boundaries vector cells[36], which account for the proximity of the agent to boundaries in the environment. Secondly, when grid-like coding is altered (e.g., deviations from the typically reported 60° sinusoidal modulation) or reduced, as observed in our experiments

(Chapters 2 and 3), compensatory mechanisms may occur that involve the engagement of other cognitive areas (see above). Greater reliance on these complementary brain regions, while possibly resulting in different navigation behaviors, might mitigate the impact of changes in grid cell activity (or grid-like coding). With these two considerations in mind, we can predict that alterations in the entorhinal cortex activity, particularly in grid-like coding, may not lead to complete impairments in spatial navigation. Indeed, animal lesion studies [37–4041] observed that, although in a less precise way, rodents with lesions to the entorhinal cortex were still able to perform spatial navigation tasks, such as the Morris water maze. Although there is no evidence about how lesions in the entorhinal cortex would impact human navigation behavior, studies on patients, together with the results of our experiments (Chapters 2 and 3) could provide a first insight on that. As already cited and described in the introduction, in 2015, Kunz and colleagues[42] performed an experiment to investigate grid-like coding in the entorhinal cortex of APOE-ε4 carriers individuals. In this study, it was reported a reduction of grid-like coding in APOE-ε4 carries compared to controls during a spatial navigation task, which could not be deputy to any structural difference of the entorhinal cortex in the two groups. Interestingly, the authors found a negative correlation, more pronounced in the APOE-ε4 carriers than control, between hippocampal activity during the task and grid-like coding. Moreover, the increased hippocampal activity during the task in APOE-ε4 carriers individuals, positively correlates with behavioral performance during the experiment. Thus, the absence of performance differences in the task across groups could be related to the APOE-ε4 carriers' higher reliance on the hippocampus which serves as a compensatory mechanism to solve task [42]. In similar terms, in our spatial navigation task [43] (Chapter 2) we observed a higher activity of the inferior parietal cortex in early blind compared to sighted individuals during the navigation task (Nav-Math experiment), which positively correlates, in early blind, but not in sighted participants, with the behavioral performance in the clock-navigation experiment (see Chapter 2 for details). Similar to what was observed by Kunz and colleagues [42], also in this case, we could hypothesize that the detected higher parietal cortex activity in blind individuals served as a compensatory mechanism to account for the reduced grid-like coding observed in the entorhinal cortex. However, both animal and human evidence referred only to spatial navigation tasks [37–39,41–43], therefore, it is still unclear whether compensatory mechanisms would take place in the brain during conceptual navigation in a population that showed reduced grid-like coding. Notwithstanding further experiments in this direction will be needed, further

analyses on our sound-navigation experiment (Chapter 3) could offer a valid starting point to address this question. For instance, following the same rationale as in Kunz 2015 [42], we could investigate whether during the navigation of the sound space early blind individuals recruit more hippocampal or parietal areas and whether this correlates with the performance throughout the experiment.

Another possibility is that blind individuals do not rely on cognitive maps representations but rather on other, non-Euclidean or non-metric, representations[44–47]. This latter possibility could be applied to humans in general, not only blind individuals. Indeed, there is evidence supporting the hypothesis that heuristic knowledge may facilitate navigation through spatial information more effectively than metric spatial knowledge does[48,49]. For instance, in studies where participants were asked whether a spatial landmark (such as a city) was more northern or southern relative to another landmark, incorrect responses often indicated reliance on heuristic rather than metric spatial knowledge[48,49]. More in general, it could be that, to solve navigation tasks, humans rely on a combination of heuristics and spatial metrics rather than only spatial metrics[47,50]. Interestingly, it has been observed that early blind individuals generally prefer to rely on a verbal encoding of spatial information, which is also reflected in a higher volume of their hippocampal tail compared to sighted individuals[51].

Further evidence challenging the idea that cognitive maps are necessary for spatial navigation, comes from studies in which participants have demonstrated the ability to navigate non-Euclidean spaces[52,53] or to find novel paths or shortcuts in environments where they were partially unaware of the spatial metrics[54,55]. Graph-like structure, in which the different nodes are constituted by different spatial landmarks, might better explain this pattern of behaviors than map-like structure[56]. Cognitive graphs might offer more flexible representations of space, because they are not constrained by Euclidean principles, and have lower computational costs, as only a limited number of spatial landmarks are encoded within them ( differently from cognitive maps, which arguably provide a more fine-grained representation of the surrounding environment)[56]. Neuroimaging studies support the hypothesis of the existence of cognitive graphs and demonstrate that a network of brain regions, including the hippocampus, medial prefrontal cortex, and orbitofrontal cortex, activates while performing tasks that require the extraction of a graph-like structure. However, the

involvement of the different brain regions in this network seems to vary according to the specific requirements of the experimental task [56–59].

Testing the hypothesis of the recruitment of other types of non-Euclidean representations to navigate through spatial and abstract knowledge goes beyond the scope of this thesis. The results obtained in the spatial navigation experiment (Chapter 2) seem to suggest that both sighted individuals, in whom we detected a 60° modulation of the BOLD signal (typically associated to grid cells activity), and early blind individuals rely on entorhinal cortex recruitment, albeit this recruitment is expressed with a different sinusoidal modulation (90° modulation) in this latter population. However, the non-significant modulation of the BOLD signal in the entorhinal cortex observed in early blind individuals during the conceptual navigation task (Chapter 3) might suggest that, rather than relying on allocentric representations, typically supported by entorhinal cortex recruitment, for computing abstract relationships, this population relies on other, possibly more egocentric, representations, which may lead to greater recruitment of parietal brain regions The preference for adopting egocentric rather than allocentric representations in early blind individuals has already been reported in the field of spatial navigation[25,29,60]; however, whether this applies to conceptual navigation is unclear, and further studies will be needed to investigate the use of different representations in the early blind population for processing abstract knowledge.

In sum, the results of our two experiments, taken together, support the scaffolding hypothesis. As the analyses of the experiment in Chapter 3 progress, they may add new important information and better qualify our findings and interpretations. For the time being, we can conclude that people who learn to navigate space differently also navigate conceptual spaces differently.

**References:**


1. Behrens TEJ, Muller TH, Whittington JCR, et al. What Is a Cognitive Map? Organizing Knowledge for Flexible Behavior. *Neuron*. 2018;100(2):490-509. doi:10.1016/j.neuron.2018.10.002

2. Bellmund JLS, Gärdenfors P, Moser EI, Doeller CF. Navigating cognition: Spatial codes for human thinking. *Science*. 2018;362(6415):eaat6766. doi:10.1126/science.aat6766

3. Constantinescu AO, OReilly JX, Behrens TEJ. Organizing conceptual knowledge in humans with a gridlike code. *Science*. 2016;352(6292):1464-1468. doi:10.1126/science.aaf0941

4. Doeller CF, Barry C, Burgess N. Evidence for grid cells in a human memory network. *Nature*. 2010;463(7281):657-661. doi:10.1038/nature08704

5. Julian JB, Keinath AT, Frazzetta G, Epstein RA. Human entorhinal cortex represents visual space using a boundary-anchored grid. *Nat Neurosci*. 2018;21(2):191-194. doi:10.1038/s41593-017-0049-1

6. Nadel L. Cognitive maps. In: *Handbook of Spatial Cognition*. American Psychological Association; 2013:155-171. doi:10.1037/13936-009

7. Nau M, Navarro Schröder T, Bellmund JLS, Doeller CF. Hexadirectional coding of visual space in human entorhinal cortex. *Nat Neurosci*. 2018;21(2):188-190. doi:10.1038/s41593-017-0050-8

8. Qasim SE, Reinacher PC, Brandt A, Schulze-Bonhage A, Kunz L. Neurons in the human entorhinal cortex map abstract emotion space. Published online August 12, 2023. doi:10.1101/2023.08.10.552884

9. Tolman EC. Cognitive maps in rats and men. *Psychological Review*. 1948;55(4):189-208. doi:10.1037/h0061626

10. Viganò S, Bayramova R, Doeller CF, Bottini R. *Mental Search of Concepts Is Supported by Egocentric Vector Representations and Restructured Grid Maps*. Neuroscience; 2023. doi:10.1101/2023.01.19.524704

11. Horner AJ, Bisby JA, Zotow E, Bush D, Burgess N. Grid-like Processing of Imagined Navigation. *Current Biology*. 2016;26(6):842-847. doi:10.1016/j.cub.2016.01.042

12. Park SA. Inferences on a multidimensional social hierarchy use a grid-like code. *Nature Neuroscience*. 2021;24:27.

13. Viganò S, Rubino V, Soccio AD, Buiatti M, Piazza M. Grid-like and distance codes for representing word meaning in the human brain. *NeuroImage*. 2021;232:117876. doi:10.1016/j.neuroimage.2021.117876

14. Casasanto D. Embodiment of abstract concepts: good and bad in right- and left-handers. *J Exp Psychol Gen*. 2009;138(3):351-367. doi:10.1037/a0015854

15. Casasanto D, Bottini R. Mirror reading can reverse the flow of time. *J Exp Psychol Gen*. 2014;143(2):473-479. doi:10.1037/a0033297

16. Bottini R, Mattioni S, Collignon O. Early blindness alters the spatial organization of verbal working memory. *Cortex*. 2016;83:271-279. doi:10.1016/j.cortex.2016.08.007

17. Pitt B, Ferrigno S, Cantlon JF, Casasanto D, Gibson E, Piantadosi ST. Spatial concepts of number, size, and time in an indigenous culture. *Science Advances*. 2021;7(33):eabg4141. doi:10.1126/sciadv.abg4141

18. Moser EI, Moser MB, McNaughton BL. Spatial representation in the hippocampal formation: a history. *Nat Neurosci*. 2017;20(11):1448-1464. doi:10.1038/nn.4653

19. Rowland DC, Roudi Y, Moser MB, Moser EI. Ten Years of Grid Cells. *Annu Rev Neurosci*. 2016;39(1):19-40. doi:10.1146/annurev-neuro-070815-013824

20. O'Keefe J. An allocentric spatial model for the hippocampal cognitive map. *Hippocampus*. 1991;1(3):230-235. doi:10.1002/hipo.450010303

21. Nau M, Julian JB, Doeller CF. How the Brain's Navigation System Shapes Our Visual Experience. *Trends in Cognitive Sciences*. 2018;22(9):810-825. doi:10.1016/J.TICS.2018.06.008

22. Piccardi L, De Luca M, Nori R, Palermo L, Iachini F, Guariglia C. Navigational Style Influences Eye Movement Pattern during Exploration and Learning of an Environmental Map. *Frontiers in Behavioral Neuroscience*. 2016;10. Accessed May 9, 2023. https://www.frontiersin.org/articles/10.3389/fnbeh.2016.00140

23. Thinus-Blanc C, Gaunet F. Representation of Space in Blind Persons: Vision as a Spatial Sense?

24. Gori M, Cappagli G, Baud-Bovy G, Finocchietti S. Shape Perception and Navigation in Blind Adults. *Frontiers in Psychology*. 2017;8. Accessed May 4, 2023. https://www.frontiersin.org/articles/10.3389/fpsyg.2017.00010

25. Iachini T, Ruggiero G, Ruotolo F. Does blindness affect egocentric and allocentric frames of reference in small and large scale spaces? *Behavioural Brain Research*. 2014;273:73-81. doi:10.1016/j.bbr.2014.07.032

26. Noordzij ML, Zuidhoek S, Postma A. The influence of visual experience on the ability to form spatial mental models based on route and survey descriptions. *Cognition*. 2006;100(2):321-342. doi:10.1016/j.cognition.2005.05.006

27. Ottink L, van Raalte B, Doeller CF, Van der Geest TM, Van Wezel RJA. Cognitive map formation through tactile map navigation in visually impaired and sighted persons. *Sci Rep*. 2022;12(1):11567. doi:10.1038/s41598-022-15858-4

28. Pasqualotto A, Proulx MJ. The role of visual experience for the neural basis of spatial cognition. *Neuroscience and Biobehavioral Reviews*. 2012;36:1179-1187. doi:10.1016/j.neubiorev.2012.01.008

29. Ruggiero G, Ruotolo F, Iachini T. Congenital blindness limits allocentric to egocentric switching ability. *Exp Brain Res*. 2018;236(3):813-820. doi:10.1007/s00221-018-5176-8

30. Bottini R, Doeller CF. Knowledge Across Reference Frames: Cognitive Maps and Image Spaces. *Trends in Cognitive Sciences*. 2020;24(8):606-619. doi:10.1016/j.tics.2020.05.008

31. Dutriaux L, Xu Y, Sartorato N, Lhuillier S, Bottini R. Disentangling reference frames in the neural compass. Published online May 21, 2023:2023.05.21.541641. doi:10.1101/2023.05.21.541641

32. He Q, Brown TI. Environmental Barriers Disrupt Grid-like Representations in Humans during Navigation. *Curr Biol*. 2019;29(16):2718-2722.e3. doi:10.1016/j.cub.2019.06.072

33. Parkinson C, Liu S, Wheatley T. A Common Cortical Metric for Spatial, Temporal, and Social Distance. *Journal of Neuroscience*. 2014;34(5):1979-1987. doi:10.1523/JNEUROSCI.2159-13.2014

34. O'Keefe J, Dostrovsky J. The hippocampus as a spatial map. Preliminary evidence from unit activity in the freely-moving rat. *Brain Research*. 1971;34(1):171-175. doi:10.1016/0006-8993(71)90358-1

35. Taube JS, Muller RU, Ranck JB. Head-direction cells recorded from the postsubiculum in freely moving rats. I. Description and quantitative analysis. *J Neurosci*. 1990;10(2):420-435. doi:10.1523/JNEUROSCI.10-02-00420.1990

36. C. Barry, C. Lever, R. Hayman, et al. The Boundary Vector Cell Model of Place Cell Firing and Spatial Memory. *Reviews in the Neurosciences*. 2006;17(1-2):71-98. doi:10.1515/REVNEURO.2006.17.1-2.71

37. Parron C, Poucet B, Save E. Entorhinal cortex lesions impair the use of distal but not proximal landmarks during place navigation in the rat. *Behavioural Brain Research*. 2004;154(2):345-352. doi:10.1016/j.bbr.2004.03.006

38. Van Cauter T, Camon J, Alvernhe A, Elduayen C, Sargolini F, Save E. Distinct Roles of Medial and Lateral Entorhinal Cortex in Spatial Cognition. *Cerebral Cortex*. 2013;23(2):451-459. doi:10.1093/cercor/bhs033

39. Poitreau J, Buttet M, Manrique C, Poucet B, Sargolini F, Save E. Navigation using global or local reference frames in rats with medial and lateral entorhinal cortex lesions. *Behavioural Brain Research*. 2021;413:113448. doi:10.1016/j.bbr.2021.113448

40. Save E, Sargolini F. Disentangling the Role of the MEC and LEC in the Processing of Spatial and Non-Spatial Information: Contribution of Lesion Studies. *Front Syst Neurosci*. 2017;11. doi:10.3389/fnsys.2017.00081

41. Kanter BR, Lykken CM, Avesar D, et al. A Novel Mechanism for the Grid-to-Place Cell Transformation Revealed by Transgenic Depolarization of Medial Entorhinal Cortex Layer II. *Neuron*. 2017;93(6):1480-1492.e6. doi:10.1016/j.neuron.2017.03.001

42. Kunz L, Schroder TN, Lee H, et al. Reduced grid-cell-like representations in adults at genetic risk for Alzheimer's disease. *Science*. 2015;350(6259):430-433. doi:10.1126/science.aac8128

43. Sigismondi F, Xu Y, Silvestri M, Bottini R. Altered grid-like coding in early blind people. *Nat Commun*. 2024;15(1):3476. doi:10.1038/s41467-024-47747-x

44. Mcnamara TP, Diwadkar VA. Symmetry and Asymmetry of Human Spatial Memory. *Cognitive Psychology*. 1997;34(2):160-190. doi:10.1006/cogp.1997.0669

45. Moar I, Bower GH. Inconsistency in spatial knowledge. *Mem Cogn*. 1983;11(2):107-113. doi:10.3758/BF03213464

46. Huttenlocher J, Hedges LV, Corrigan B, Crawford LE. Spatial categories and the estimation of location. *Cognition*. 2004;93(2):75-97. doi:10.1016/j.cognition.2003.10.006

47. Warren WH. Non-Euclidean navigation. el Jundi B, Kelber A, Webb B, eds. *Journal of Experimental Biology*. 2019;222(Suppl_1):jeb187971. doi:10.1242/jeb.187971

48. Okabayashi H, Glynn SM. Spatial Cognition: Systematic Distortions in Cognitive Maps. *The Journal of General Psychology*. 1984;111(2):271-279. doi:10.1080/00221309.1984.9921116

49. Stevens A, Coupe P. Distortions in judged spatial relations. *Cognitive Psychology*. 1978;10(4):422-437. doi:10.1016/0010-0285(78)90006-3

50. Ekstrom AD, Harootonian SK, Huffman DJ. Grid coding, spatial representation, and navigation: Should we assume an isomorphism? *Hippocampus*. 2020;30(4):422-432. doi:10.1002/hipo.23175

51. Fortin M, Voss P, Lord C, et al. Wayfinding in the blind: Larger hippocampal volume and supranormal spatial navigation. *Brain*. 2008;131(11):2995-3005. doi:10.1093/brain/awn250

52. Muryy A, Glennerster A. Route selection in non-Euclidean virtual environments. *PLOS ONE*. 2021;16(4):e0247818. doi:10.1371/journal.pone.0247818

53. Warren WH, Rothman DB, Schnapp BH, Ericson JD. Wormholes in virtual space: From cognitive maps to cognitive graphs. *Cognition*. 2017;166:152-163. doi:10.1016/j.cognition.2017.05.020

54. Hölscher C, Meilinger T, Vrachliotis G, Brösamle M, Knauff M. Up the down staircase: Wayfinding strategies in multi-level buildings. *Journal of Environmental Psychology*. 2006;26(4):284-299. doi:10.1016/j.jenvp.2006.09.002

55. Passini R. Spatial representations, a wayfinding perspective. *Journal of Environmental Psychology*. 1984;4(2):153-164. doi:10.1016/S0272-4944(84)80031-6

56. Peer M, Brunec IK, Newcombe NS, Epstein RA. Structuring Knowledge with Cognitive Maps and Cognitive Graphs. *Trends in Cognitive Sciences*. 2020;0(0). doi:10.1016/J.TICS.2020.10.004

57. Schapiro AC, Rogers TT, Cordova NI, Turk-Browne NB, Botvinick MM. Neural representations of events arise from temporal community structure. *Nat Neurosci*. 2013;16(4):486-492. doi:10.1038/nn.3331

58. Schapiro AC, Turk-Browne NB, Norman KA, Botvinick MM. Statistical learning of temporal community structure in the hippocampus. *Hippocampus*. 2016;26(1):3-8. doi:10.1002/hipo.22523

59. Schuck NW, Cai MB, Wilson RC, Niv Y. Human Orbitofrontal Cortex Represents a Cognitive Map of State Space. *Neuron*. 2016;91(6):1402-1412. doi:10.1016/j.neuron.2016.08.019

60. Ruggiero G, Ruotolo F, Iachini T. The role of vision in egocentric and allocentric spatial frames of reference. *Cogn Process*. 2009;10(S2):283-285. doi:10.1007/s10339-009-0320-9

# Appendix A

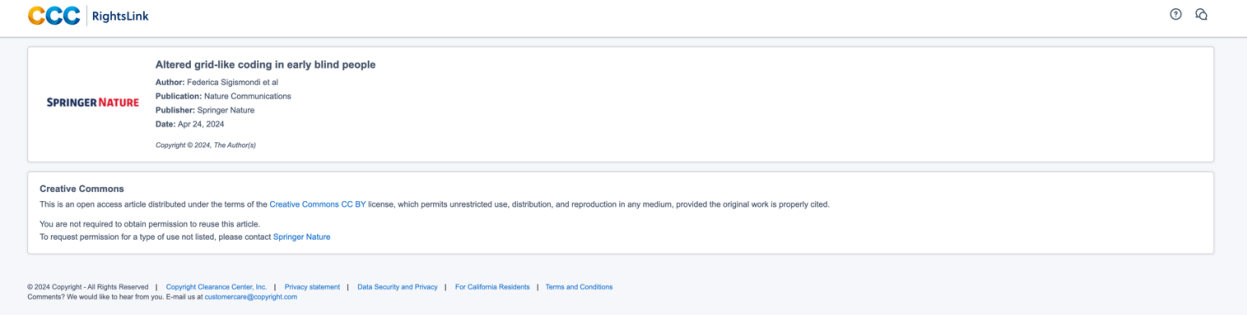

CCC | RightsLink

**Altered grid-like coding in early blind people**

**Author:** Federica Sigismondi et al
**Publication:** Nature Communications
**Publisher:** Springer Nature
**Date:** Apr 24, 2024

*Copyright © 2024, The Author(s)*

**Creative Commons**

This is an open access article distributed under the terms of the Creative Commons CC BY license, which permits unrestricted use, distribution, and reproduction in any medium, provided the original work is properly cited.

You are not required to obtain permission to reuse this article.
To request permission for a type of use not listed, please contact Springer Nature



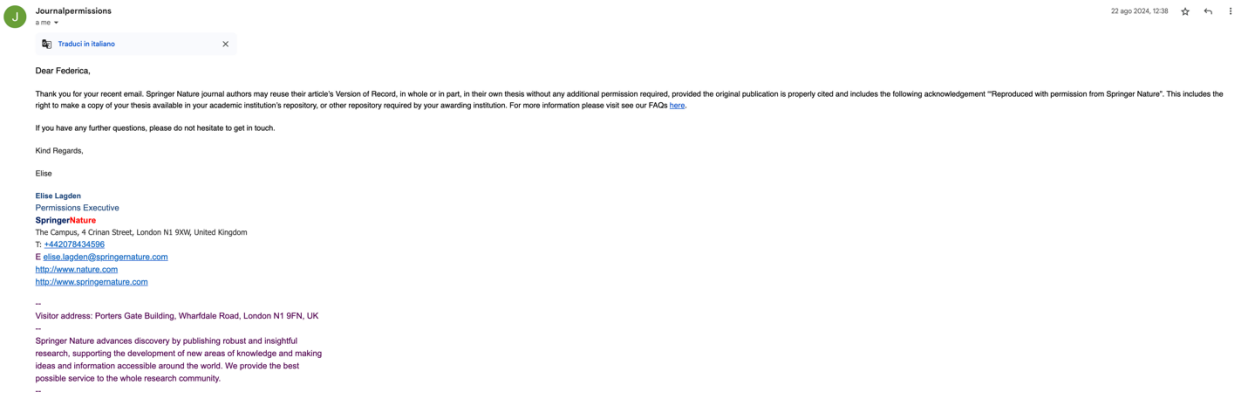

**Journalpermissions**
a me

22 ago 2024, 12:38

Traduci in italiano

Dear Federica,

Thank you for your recent email. Springer Nature journal authors may reuse their article's Version of Record, in whole or in part, in their own thesis without any additional permission required, provided the original publication is properly cited and includes the following acknowledgement "Reproduced with permission from Springer Nature". This includes the right to make a copy of your thesis available in your academic institution's repository, or other repository required by your awarding institution. For more information please visit see our FAQs here.

If you have any further questions, please do not hesitate to get in touch.

Kind Regards,

Elise

**Elise Lagden**
Permissions Executive
**SpringerNature**
The Campus, 4 Crinan Street, London N1 9XW, United Kingdom
T: +442078434596
E elise.lagden@springernature.com
http://www.nature.com
http://www.springernature.com

--
Visitor address: Porters Gate Building, Wharfdale Road, London N1 9FN, UK
--
Springer Nature advances discovery by publishing robust and insightful research, supporting the development of new areas of knowledge and making ideas and information accessible around the world. We provide the best possible service to the whole research community.
--